Computational and Analytical Approaches Towards Epidemic Spread Containment of Temporal Animal Trade Networks

vorgelegt von

M.Sc.
George Jason Bassett
geb. in Melbourne

von der Fakultät II – Mathematik und Naturwissenschaften
der Technischen Universität Berlin
zur Erlangung des akademischen Grades
Doktor der Naturwissenschaften
-Dr. rer. nat.-
genehmigte Dissertation

Promotionsausschuss:

Vorsitzender: Prof. Dr. Michael Lehmann
Gutachter: Dr. habil. Philipp Hövel
Gutachter: Prof. Dr. Dr.h.c. Eckehard Schöll, Ph.D.

Tag der wissenschaftlichen Aussprache: 18. Dezember 2018

Berlin 2019

Abstract

In this thesis a threefold approach to assess the risk of epidemic spread on animal trade networks and pinpoint strategies to contain it is presented. Firstly, an exhaustive description of a stochastic, event-driven, hierarchical agent-based model designed to reproduce the infectious state of the cattle disease called *Bovine Viral Diarrhea* (BVD) on the German trade network is outlined. It takes into account a vast number of breeding, infectious and animal movement mechanisms as provided by expert opinion with *Susceptible-Infected-Recovered* type of dynamics with an additional permanently infectious class for the farm-node dynamics and a supply-demand farm manager mechanism governing the network structure and dynamics. A sensitivity analysis on several key parameters of the model is also presented, and the resulting disease and breeding dynamics are ultimately studied from many aspects including numerous mitigation strategies of present and past government regulations, and of corresponding future, financial interest. Next a mean field model for the spread of BVD is formulated to compare with the agent based model and provide an analytical means towards the description of the farm level dynamics including birth-death processes. A numerical stability analysis is presented as well as the derivation of the epidemiological quantity of the *basic reproduction number* stemming from bifurcation arguments. Moreover, numerical integrations are performed and a benchmark is provided for the farm infectious and population dynamics of large farms within the agent based model context. Lastly, a number of network analysis tools are presented and applied on a dataset of cattle movements for the German trade network. Each one tackles connectivity questions from a static, a temporal, an embedded-geographical (spatial) and a topological point of view, culminating in a worst-case assessment of a susceptible-infected, one-way process.

Deutsche Zusammenfassung

In dieser Arbeit wird ein dreifacher Ansatz zur Beurteilung des Risikos der Ausbreitung einer Epidemie in Tierhandelsnetzen und zur Ermittlung von Strategien zu ihrer Eindämmung vorgestellt. Zunächst erfolgt eine ausführliche Beschreibung eines stochastischen, ereignisgesteuerten, hierarchischen, agentenbasierten Modells zur Reproduktion des Infektionszustandes der Rinderkrankheit namens *Bovine Virusdiarrhoe* (BVD) auf das deutschen Handelsnetz. Es berücksichtigt eine Vielzahl von Zucht-, Infektions- und Tierbewegungsmechanismen, die durch ein Expertengut- achten über das *Susceptible Infected-Recovered* Modell bereitgestellt werden. Das Modell wird zusätzlich durch eine permanente Infektionsklasse für die Betriebsknotendynamik und einen Angebots-Nachfrage-Betriebsverwaltungs- mechanismus erweitert, welcher die Netzwerkstruktur und -dynamik vorgibt. Des Weiteren wird eine Sensitivitätsanalyse zu mehreren Schlüsselparametern des Modells vorgestellt. Die daraus resultierende Krankheits- und Zuchtdynamik wird letztendlich unter vielen Aspekten untersucht, einschließlich zahlreicher Eindämmungsstrategien aktueller und vergangener staatlicher Vorschriften und entsprechender zukünftiger finanzieller Interessen. Anschließend wird ein Mean Field Modell für die Ausbreitung von BVD formuliert, um es mit dem agentenbasierten Modell zu vergleichen und ein analytisches Mittel zur Beschreibung der Dynamik des landwirtschaftlichen Niveaus einschließlich der Geburts- und Sterbeprozesse bereitzustellen. Es wird eine numerische Stabilitätsanalyse vorgestellt, sowie die Ableitung der epidemiologischen Größe der *basic reproduction number* aus Bifurkationsargumenten. Darüber hinaus werden numerische Berechnungen durchgeführt und mit der Infektions- und Populationsdynamik von Großbetrieben im Rahmen des agentenbasierten Modellkontextes verglichen. Schließlich werden eine Reihe von Netzwerkanalyse-Tools vorgestellt und auf einen Datensatz von Rinderbewegungen im deutschen Handelsnetz angewendet. Jedes von ihnen befasst sich mit Fragen der Konnektivität aus statischer, temporärer, geografischer (räumlicher) und topologischer Sicht und endet schließlich mit einer Worst-Case-Analyse eines susceptible-infected Einwegprozesses.

- Ack ja. Hur man vänder sig har man rumpan bak, det är en stor sanning.
- Rumpan bak, rumpan bak, det är en stor sanning.
Det Sjunde Inseglet av Ingmar Bergman

- Ah, me. No matter which way you turn, you have your rump behind you. That's the truth.
- The rump behind you, the rump behind you there's a profound truth.
The Seventh Seal by Ingmar Bergman

Acknowledgments

First and foremost I would like to thank my advisor Dr. habil. Philipp Hövel for putting his trust in me and making me reconsider my meager notions of efficiency and organisation with his ever encouraging example and guidance throughout the course of my doctoral studies. Secondly, my friends and close colleagues Andreas Koher, for his patience, thoroughness and insight in addressing details of problems of even the most irritatingly simple nature, and Philipp Lorenz for keeping the communication channels and ideas flowing, contrary to my introvert nature. The task would probably have been achieved, but with much more turmoil and dullness without them. Furthermore, it would be remiss of me to neglect mentioning my students', Inia Steinbach and Pascal Blunk, contributions with their master's theses on the network analysis and the agent-based model presented in this thesis respectively. Especially the latter kept supporting me with programming issues even long after his master's thesis and obligations to our group had ended. Furthermore, I thank Stefan Ruschel for his criticising, relentless spirit in formulating the mean field epidemic model presented in this thesis and for encouraging me not to abandon the project despite the many challenges presented, which at times seemed insurmountable. Moreover, I would like to dearly thank our collaborators Dr. Jörn Gethmann and Dr. Hartmut H. K. Lentz for providing constantly expert opinion, guidance and advice on the development of the agent-based model of this thesis. On that matter, I would like to also thank my friend and ex-colleague Dr. Thomas Isele for initiating and supporting the project at its first stages and whenever help was asked for, Dr. Bryan Iotti for his expert advice and for spending more than two intense weeks with me over a screen on debugging and code development, Denis Nikhitin and Liudmila Tumash for their friendship and expert programming support at the last stages of the project, as well as professor Vitaly Belik for the fruitful discussions and encouragement towards an analytical description at its first stages. In addition, I would like to thank Dr. Fakhteh Ghanbarnejad and Leon Merfort for sharing an office with me and cheerfully helping me out whenever needed in various topics. I would also like to acknowledge and thank my old advisor, Dr. Astero Provata, without whose guidance and support throughout the years back from my bachelor studies I would most likely never have been brought to

Philipp Hövel's group. In addition, I am grateful for having the opportunity of academic exchanges with Dr. Vittoria Colizza's team in Paris. I further kindly thank the members of the scientific committee of this thesis apart from Philipp Hövel, namely professor Dr. Dr.h.c. Eckehard Schöll for accepting my request to assess it, as well as professor Dr. Michael Lehmann for accepting the invitation to moderate its defence. Lastly, I would like to thank my mother Kalliopi Kapsomera and Nadiya Shupyk for supporting me in their own way throughout my doctoral studies and teaching me important lessons in life.

The doctoral studies culminating to the writing of this thesis were committed with the support of the German research association (DFG) within the framework of the collaborative research centre 910 (SFB 910) and the German academic exchange agency (DAAD).

Jason Bassett,

Berlin, October 23$^{\mathrm{d}}$, 2018.

Contents

CHAPTER 1

Introduction

1.1 Purpose and State of the Art

The topic of epidemic spread and its control in a theoretical manner has been the topic of numerous studies ranging from the times of Daniel Bernoulli to nowadays [Murray, 2002]. However it was the 20$^{\text{th}}$ century that witnessed an unprecedented growth in the field after a series of works in its first half, culminating in the seminal *Susceptible-Infected-Recovered* (SIR) system formulated by Kermack and McKendrick [Kermack and McKendrick, 1927]. The authors assumed a population of individuals in the three aforementioned states and arrived from first principles (by enumeration) to the ubiquitous SIR model, which arguably has formed the starting point of every epidemic study, distinguishing the population in aggregates called *compartments* [Allen et al., 2008; Anderson and May, 1992; Brauer and Castillo-Chavez, 2012; Diekmann et al., 2013; Kiss et al., 2017]. Despite the fact that epidemic spread studies thereon into the 20$^{\text{th}}$ century have often been rather detached from observations [Anderson and May, 1992], the simplicity and predictive power of the SIR model was exhibited on historical data, as well as on an ongoing outbreak of malaria in India at the time of its formulation [Kermack and McKendrick, 1927; Murray, 2002].

Notwithstanding, the original SIR model had underlying assumptions of homogeneity of the population in age, susceptibility, infectiousness and spatial distribution which soon became a topic of rigorous study per se and added enormously to the literature and to the complexity of the field [Anderson and May, 1992; Diekmann et al., 2013; Murray, 2002]. In particular and in regard to the spatial structure of the population, apart from methods of diffusion borrowed directly from physics [Murray, 2002; Postnikov and

Sokolov, 2007], the capabilities that graph and network theory have offered to epidemic spread studies has been phenomenal. Analyses on infectious connectivity revolving around rigid structures (so-called *static* approaches) [Ganesh et al., 2005; Holme et al., 2002; Pastor-Satorras and Vespignani, 2001] or assuming a dynamic regard in potential connections (time evolving approaches) [Holme and Saramäki, 2012] have tremendously added to epidemiological understanding, forecasting and to epidemiology's value as a consultancy tool. In particular, introducing a network structure to an epidemic model can extend immensurably the basic SIR-type approaches by introducing such dynamics at the node level (so-called *metapopulation models*), by introducing age structure in the population, hierarchy in infections, or even indicate the conditions leading to an outbreak through a *percolation* threshold [Colizza and Vespignani, 2007; Kiss et al., 2017; Sander et al., 2002].

In the last quarter of the 20^{th} century and continuing onwards to the 21^{st} an additional powerful tool, with an ever increasing potential in time, was added to the arsenal of theoretical epidemiology: the advent of computer simulations [Epstein, 2006]. Work on simulating epidemic spread can mainly be classified in two approaches: that concerning aggregates of populations and an agent-based one. While the former is based, as the name suggests, in groups of infectious individuals within a population, the latter is a *microscopic* approach focusing on each individual and to his interaction with the rest under well-defined rules as the system evolves. Either of the two provides insight and results under conditions and assumptions which are cumbersome and vastly complicated to model and calculate analytically. The initial focus of such simulations was agent-based and centered on obtaining results of transitioning from one infectious state to another via sampling methods (e.g. Monte-Carlo) [Elveback et al., 1971]. Lately, although studies are incessant in the agent-based paradigm [Burke et al., 2006; Vestergaard and Génois, 2015], there has been considerable predictive success in aggregated models introducing network structure to account for migration and connectivity of population groups [Bisset et al., 2009; Van den Broeck et al., 2011], demonstrating the manifold potential and value of computational studies in epidemiology.

With recurring epidemic outbreaks in human and animal populations the interest in such models keeps attracting attention from theoreticians to policy makers. Naturally, all the aforementioned tools and methods can be applied to human as well as to animal populations, making in each case the necessary adjustments pertinent to the case at hand. For the latter populations, there has been increasing interest in the late 20^{th} century onwards on epidemiological modelling motivated by domesticated animals' outbreaks, such as that of *bovine spongiform encephalopathy* or the *foot-and-mouth* disease, which can have dire effects on both the economy and public health [Green et al., 2006; Murray, 2002; Ortiz-Pelaez et al., 2006]. In addition, the focus

has been more and more orientated towards the combination of predictive, comprehensive epidemiological results and intervention or control of the animal systems under study, as the demand for intuitive, risk assessment and data-oriented results has been on the rise [Hoscheit et al., 2016; Natale et al., 2009; Sun et al., 2013; Widgren et al., 2016]. To that end, all three topics broached above come combined into play to provide epidemiological insight and risk assessment, namely mathematical modelling, network theory and computer simulations under the restrictive scope of observations manifested in datasets.

It is exactly this last point on which we aim to contribute with the work presented in this thesis. Having attained from the Friedrich-Loeffler institute a movements' dataset concerning the cattle trade network of Germany and expert opinion on a particular cattle disease called *Bovine Viral Diarrhea* (BVD) we aim to bring all three components, computer simulations, standard, analytical mathematical modelling and dynamical network theory to the service of epidemiologically significant questions from a theoretical physics perspective.

1.2 Thesis Organisation

Having introduced the topic to the reader we now proceed to briefly outline the structure of this thesis which is divided into three chapters following the above mentioned points: one treating the BVD epidemic spread computationally, one from a dynamical system perspective and one from a network analysis viewpoint.

In chapter 2 we treat the problem of BVD spread in the German cattle trade network in a computational fashion. We start by introducing some related biological background to the reader, as well as some information related to the structure of the agricultural system, the corresponding policies for the containment of BVD in Germany, as well as the current status of BVD on the network. We then proceed to thoroughly describe a stochastic, event-driven, agent-based model that we will use for the analysis. We also perform a sensitivity analysis on some key parameters of the system and lastly present results of the simulation investigating different scenarios of intervention strategies on a global and local (farm-node) level for the parametric setup as dictated by the literature and expert opinion. We finally summarise and conclude with potential future work.

In chapter 3 we formulate a deterministic, delayed, mean field model as a first approximation to analytically compare the results of the agent-based model presented in the previous chapter. We first prove some basic theoretical properties of interest and then go on to numerically investigate the stability of the system while listing several theoretical prerequisites. Finally, we follow a formulation to derive an important epidemiological quantity

called the *basic reproduction number* and numerically integrate the system to benchmark with the results of the agent-based model from the previous chapter. We finally summarise and provide an outlook of this work.

The last chapter 4 presents a network epidemic risk assessment of the five-year German cattle movement dataset based on a selection of four complementary network analysis scopes. The first consists of a static treatment of the dataset including statistics, component and degree distribution analysis. The second involves a temporal treatment based on activity and similarity (what we will call *memory*) distributions. The third is about a spatial treatment embedding the network in a geographical framework and performing Fourier analysis on the movement time-scales, as well as examining distance distributions. The fourth presents a temporal accessibility treatment leading to a worst-case epidemic scenario assessment on the dataset given an initial infectious seed. Similarly to the previous chapters we summarise and consider future research directions.

CHAPTER 2

BVD Agent-Based Model

2.1 Preliminaries

To set the stage we introduce some biological aspects of *Bovine Viral Diarrhea* (BVD), how it is identified, its current status and the related containment policies in Germany. All this information will act as a driving force to develop and set the parameters with a biological justification of an agent-based model, with which we aim to reproduce the existing BVD conditions and policies in Germany. We shall thoroughly describe this model following a particular format from the literature. Lastly, once we have achieved the goal of emulating the current status of BVD in Germany we will proceed to simulate counter strategies of financial interest in order to assess their benefits towards the eradication of the disease in Germany.

2.1.1 BVD Description, Identification and General Policies

Disease Description and Transmission Mechanisms

BVD is a disease caused by a virus of the genus *Pestivirus* affecting bovines with a high worldwide prevalence [Kelling, 2004; Lindberg and Alenius, 1999; Pinior et al., 2017; Sørensen et al., 1995]. Specifically for the case of cattle its prevalence in livestock has a significant economical impact [Greiser-Wilke et al., 2003; Ståhl and Alenius, 2012] as it affects mainly the milk yield of cattle and the population itself [Gethmann et al., 2015]. BVD is not a human transferable disease (zoonotic in the veterinary terminology), and as such the main concern about its consequences is financial [Pinior et al., 2017].

BVD appears in three distinct identified virus strains, of which the two (BVDV-1 and BVDV-2) have been well understood, account for the vast

majority of the worldwide cases and are the main concern in the related containment strategies [Santman-Berends et al., 2015; Ståhl and Alenius, 2012]. In addition, BVD is a virus which can be spread both horizontally and vertically, i.e. through contact mechanisms in an existing population and via breeding across generations respectively. Horizontally, the virus can spread to individual animals via pathways such as direct contact (through droplet spreading by e.g. sneezing), feces, all sorts of bodily fluids, contaminated farm tools or workers' garments and more rarely from external wildlife reservoirs. Vertically, a carrying animal which is transiently infected can either (except for the case of abortions) give birth to an immunosuppressed animal which will be carrying and spreading the virus to the end of its life or to an animal which has attained immunity during its mother's infection [Lanyon et al., 2014; Lindberg, 2003; Viet et al., 2007].

Animals suffering from BVD can be roughly classified into acutely, transiently infected and persistently infected ones [Lindberg, 2003], with the latter being the main source of direct transmissions. Furthermore, an infection can have dire consequences for a carrying animal's fetus.

- *Transiently Infected (TI) Animals*

  A healthy animal infected by BVD undergoes an incubation period of 2-4 days before it exhibits the first symptoms. These include respiratory and gastrointestinal disorders such as coughing and diarrhea, mucosal lesions, general fatigue, lack of appetite, and reduced milk yield for the females. Additionally, BVD can affect the cows' reproductive system leading to probable future malformations, abortions, sterility and frail births. In most cases the infection is not lethal and the animal recovers within one to two weeks.

  Except for the danger of disease spread, this stage is particularly dangerous for pregnant cows, as persistently infected animals can be produced from such infections (*in utero*) and appear upon birth. In particular, the early stage of the first trimester is the most critical when the fetus' immune system has not yet developed and can be infiltrated by the virus causing permanent immunosuppression and far more pronounced symptoms than the ones appearing in transiently infected animals. In later stages of the pregnancy the probability of the offspring being persistently infected drops drastically. The infection upon pregnancy though can still have averse effects on the newborn even at later stages. Such effects include but are not limited to lifelong weaknesses of the offspring, an abortion or general degeneracies which would be more probable than normal [Gethmann, 2018; Gethmann et al., 2015; Kelling, 2004; Lanyon et al., 2014; Lindberg, 2003].

- *Persistently Infected (PI) Animals*

> If a carrying, otherwise healthy cow is infected during its first trimester of pregnancy and the embryo survives, in the vast majority of cases it will be born into a persistently infected state as explained above. Such pregnant cows are called 'trojan' cows in the veterinary community, exactly because they do not give any signs that would give rise to suspicion for the PI animal to be brought to life and they themselves can be perfectly healthy. The newborn in this case will be frail and weak throughout its (reduced) lifetime, it will be immunosuppressed (low antibody level protection) and prone to other diseases due to the virus establishing itself in an embryonic state prior to the embryo's immunological development and will of course have a very low milk yield. Most importantly these animals shed huge amounts of the virus, up to ten times more than their TI counterparts [Sarrazin et al., 2014], constituting a severe hazard to the whole herd where they belong as well as to neighbouring herds with which they may come into contact, especially if the herds are naive (i.e. have not had prior exposure to BVD) [Rodning et al., 2012]. Albeit their shorter lifespan and reduced reproductive abilities compared to the rest of the cattle, if such animals do get pregnant and produce offspring, then the offspring will be PI in virtually all cases, as the virus will have been introduced to the embryo since its conception [Gethmann, 2018; Gethmann et al., 2015; Lanyon et al., 2014; Lindberg, 2003].

A well known complication of BVD is the mucosal disease, which is the result of a mutation of the BVD virus [Gethmann, 2018; Lanyon et al., 2014; Lindberg, 2003]. This condition is lethal and mostly concerns animals of 6 months to 2 years of age. Essentially it exhibits all the reported symptoms of a BVD acute infection in far more severe forms particularly regarding dermatological symptoms such as erosive lesions and bloats. The duration of the infection lasts from 2 days to 3 weeks, in which the animal wastes away from high loss of fluids (from the aforementioned dermatological symptoms and diarrhea), high fever and anorexia.

Lastly, regarding maternal antibody protection mechanisms they come from two sources: either from colostrum administration with the first meal or from a mother cow which had been immune to BVD prior to carriage. The protection is transient and lasts between 6-9 months [Gethmann, 2018; Lindberg, 2003; Tratalos et al., 2017].

Policy Orientation and Goals

From the short previous description it follows that from a policy maker's point of view the points of focus for first the containment and then the eradication of BVD would revolve around the following [Lindberg and Alenius, 1999]:

1. Develop a sound biosecurity (i.e. surveillance and action) programme.
2. Identify and eliminate the PI animals as soon as possible.
3. Label compromised premises as such according to some criteria (e.g. PI identification).
4. Define restriction periods in animal movements for compromised premises.
5. Closely monitor newborns at the beginning of their lives, especially in previously compromised premises.

Since the early 2000's many northern European countries have introduced regional or national containment programmes, which in time tend to evolve to eradication programmes of BVD depending on the assessed severity on the economy and political factors [Brülisauer et al., 2010; Gethmann et al., 2015; Greiser-Wilke et al., 2003; Höfig, 2014; Houe, 1999; Marschik et al., 2018; Pinior et al., 2017; Sørensen et al., 1995; Ståhl and Alenius, 2012; Thomann et al., 2017; Thulke et al., 2017]. Two have been the models mostly followed in European BVD counter programmes, namely the *Scandinavian* and the *Swiss* [Ståhl and Alenius, 2012] with their main differences lying in the testing of animals either through a combined antibody (serological) and antigen (virus) course of testing or in a direct virus test respectively.

BVD Tests and Statistical Identification

As already explained the identification of BVD relies mainly on two test categories: the *antibody* test and the *antigen* test.

Antibody Test This type of test (usually ELISA) consists of testing a blood sample (typically the serum), for the presence of antibodies, which would imply that the animal has been exposed to the virus in the past and has therefore developed resistance mechanisms (antibodies). If the animal is infected or suspicious for infection at the time of the test and its BVD virus antibody levels are low or non existent, with a repeated test after 2-3 weeks (typical recovery time of the animal) the test can verify whether the animal was a TI or is a PI by examining the post infection concentration of antibodies. Furthermore, except for individual-based such a test can be an indicator of the BVD herd immunity level by testing pools of collected blood (serum) or the bulk tank milk of a herd [Gethmann, 2018; Lanyon et al., 2014]. Regarding the 'trojan' cows carrying a PI in their uterus, it has been reported by [Lanyon et al., 2014] that their antibody concentration levels can be significantly higher in the mid to later stages of the pregnancy due to the immunological reaction of the cow to its PI embryo shedding internally the virus. This test however is not considered to be a good

proxy for BVD herd-immunity due to the logistics involved in gathering sufficiently large specimen pools, selecting representative animals and to the compromised time frame in which such tests are performed against possible movement of calves [Tratalos et al., 2017].

Antigen Test This type of test (usually RT-PCR due to its cost-efficiency compared to other such tests, and excellent sensitivity and specificity performance) may come either from a collected tissue or blood of the animal and aims at detecting the virus directly at the individual animal level. Consequently, this test matches policies' focus on identifying and removing PI animals as soon as possible. It does not however make any guarantees for herd immunity as the antibody test, since an animal can be infected directly after the test [Gethmann, 2018; Lanyon et al., 2014].

Combining all the previously outlined information about the antibody, the antigen test and the description of BVD one can draw four points of complementary interpretations and conclusions of the results:

Antibody Negative and Antigen Negative No evidence of past or present BVD virus infection. Possible early stages of the infection (before symptoms and immunological reaction). Quarantine for three weeks and retest animals in case of any animal movement to account for the latter case.

Antibody Positive and Antigen Negative Antibody presence from three possible sources: a) Colostrum administration to younglings in effect, b) prior vaccination in effect, c) previous infection. From the third case there arises the danger of a PI offspring.

Antibody Negative and Antigen Positive The animal is infected with the virus. To discern a PI from a TI infection a retesting after 3 weeks would be required.

Antibody Positive and Antigen Positive A rare case of a test assertion of BVD virus infection. Retest the animal after 3 weeks to conclude whether it was a TI or a PI.

Moreover, the veterinarian community mostly qualifies the success of the two aforementioned tests by measuring their sensitivity and specificity according to a predefined sample group of animals [Brülisauer et al., 2010; Gethmann, 2018; Lanyon et al., 2014; Lindberg, 2003; Thulke et al., 2017]. In both these and all the related statistical measures of a binary result's veracity there is always an interplay between the four possible outcomes of the tested binary characteristic as can be seen in table 2.1: Truly Positive (TP), Truly Negative (TN), Falsely Positive (FP) and Falsely Negative (FN). We follow [Skiena, 2017] for a brief overview of these two quantities.

	Result (Positive, Negative)	
Veracity (True, False)	TP	FP
	TN	FN

Table 2.1: Truth table for a binary (positive-negative) test.

Sensitivity It quantifies the test's capacity to correctly identify truly positive results over the universally true cases (i.e. TP and FN) in a population $\mathrm{Se} = \frac{\mathrm{TP}}{\mathrm{TP+FN}}$ with the marginal values being in $[0, 1]$ for absolute failure of the goal or success respectively. In the context of BVD, a high sensitivity for the antibody test means that most of the animals which have had some infectious history with BVD, are under the protection of a vaccination's effect or of maternal antibodies (colostrum) are identified by the test as immune, while for the antigen test it means that most of the animals which are infected by the BVD virus at the time of the test are correctly identified as such.

Specificity It quantifies the test's capacity to correctly reject truly negative results over the universally false cases (i.e. TN and FP) in a population $\mathrm{S}p = \frac{\mathrm{TN}}{\mathrm{TN+FP}}$ with the marginal values in $[0, 1]$ for absolute failure of the goal or success respectively. In the context of BVD, a high specificity for both the antibody and the antigen test means that most of the animals at the time of the test are correctly identified as susceptible (or perhaps at a very early stage of infection).

In Germany the current level of both the sensitivity and specificity (ear tag and ELISA) of all tests (antigen only implemented) is at 99% [Gethmann, 2015], a value exceeding those reported for Scotland in 2010 and for Ireland in 2017 [Thulke et al., 2017].

2.1.2 Legal Status and Regulations in Germany

The E.U.'s communal concerns on agricultural policies dealing with diseases such as BVD in the early 2000s were not the first attempts on that matter. In Germany in particular regulations and legislation at the federal or regional level were already existent at the time [Gethmann, 2018; Wernike et al., 2017]. However, due to the effect of BVD on the economy, the need for a systematic understanding and containment of BVD, as well as due to political progress made at the E.U. level, Germany has enforced a nationwide surveillance programme since the 1$^{\mathrm{st}}$ of January 2011 [Ministry of Food and Agriculture, 2008; Wernike et al., 2017]. This testing scheme envisions antigen, ELISA ear tag tests.

The details of this programme can be found in the corresponding mandate (from here on 'old regulation'), but in a nutshell contain of the following essential points:

- All newborn animals should be tested within two weeks from their birth.
- Traded animals have to be tested before their movement if they have no test status. Positively tested animals cannot be moved from their farm.
- An identified infected animal should be removed within two weeks from its verified status. The farm can still trade in that time.
- Should a farmer be convinced that a positive test is questionable, he can ask for a second test within 60 days. In case of a repeated positive result the animal should be removed within one week from its confirmed status. This option is advisable only for exceptionally precious animals.
- A farm is declared to be BVD-free if all tests for any of its animals over six months of age have always resulted to a negative result for at least twelve months.

As there were several liabilities with the old regulation, especially concerning the freedom to move animals after their confirmed positive status and before their elimination, amendments to the first mandate have been put into effect since 2016 [Ministry of Food and Agriculture, 2016]. The main differences from the old regulation are summarised in the following points

- Should an animal be tested positive, the farm is quarantined for 40 days. No animal movements to or from the farm is allowed.
- In the case of a requested second test from a farmer the test should be performed within 40 days.

In figure 2.1 the various stages of the possible two rounds of ear tag testing are presented in detail. In practice and for modelling purposes though the most important piece of information in case of a positive test is the total elapsed time between the first test and the removal of the animal in days.

2.1.3 Towards an Agent-Based Model

If one bears in mind the combined factors of the current German agricultural system, the past and present national legislation and practices against BVD as well as the PI animals' statistics since the adoption of a national intervention programme in 2011 one realises that there is a wide range of details to be taken into account towards a model of BVD spread with demographics and migration from node to node (farm). To that end, a microscopic agent-based approach (i.e. a system of 'agents' interacting with a predefined set of

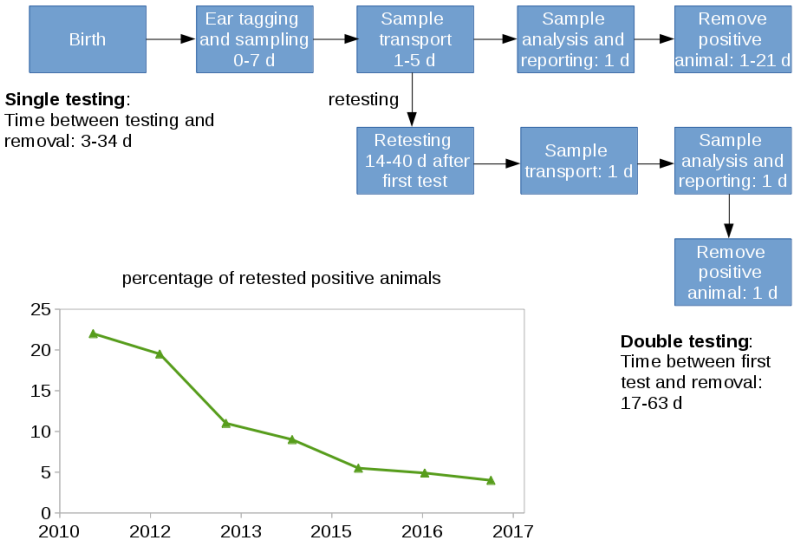

Figure 2.1: Retesting regulations and practices according to the old (2011-2016) and new (2016 onwards) mandate ('d' stands for days). The inset displays the actual percentage of positively tested animals since 2011. Courtesy of J. Gethmann. Data extracted from the HIT database (see section 2.1.3).

rules) would provide the sufficient level of detail to capture in a model all the aforementioned factors and to serve towards the disease's eradication, which is the present goal of the relevant German policy makers [Macal and North, 2010]. Additionally, to circumvent the conundrum of the agents' nature definition we set hierarchical levels for them. By that we mean that except for the obvious selection of the animals being the agents in the model, hierarchically higher entities such as the farm and the global system should play a role in the model through their individual behaviour and set of actions.

Regarding the specifics of the design and structure of the model, except for the reasoning we already mentioned, our decisions were largely dictated by field studies compiled by expert opinion [Gethmann, 2015] as well as similar work on the matter [Damman et al., 2015; Iotti et al., 2017; Thulke et al., 2017; Tinsley et al., 2012].

There is a vast variety of ways from which one can choose and classify agent-based models in the literature [Albrecht and Stone, 2017; Grimm et al., 2010; Shoham and Leyton-Brown, 2008]. In our case we choose the model to be stochastic, event-driven and to some extent data-driven. Firstly, the stochasticity reflects the complexity of real-world fluctuations in the breeding and infectious dynamics, as well as in their interplay in a causally evolving system and in line with previous work [Damman et al., 2015; Iotti et al., 2017; Thulke et al., 2017; Viet et al., 2004]. Especially for the infection dynamics, we set them to be realised as a *Markov* process's events (i.e. all the variables pertaining to the infection are dependent only on the corresponding ones of the previous time step [van Kampen, 2003]) implemented with a variant of the Gillespie algorithm [Gillespie, 1976; Vestergaard and Génois, 2015]. Secondly,the event-driven paradigm is an appealing choice for the model as the breeding and infectious dynamics of BVD on cattle can be modelled as a chain of discrete events triggered from one another and of whose next series of events can be scheduled and calculated upon the formers' execution in a causal manner [Fishman, 2013; Kiss et al., 2017]. This is also similar to the model used on the assessment of the BVD current policies on the Irish cattle trade network[Thulke et al., 2017]. Lastly, we aim to initialise the model and introduce the node heterogeneities of the real cattle trade network of Germany by using the farm size distribution extracted from the Herkunftssicherungs und Informationssystem für Tiere (HIT) database provided from our collaborators from the Friedrich-Loeffler Institute (FLI). Notwithstanding, we do not design the model so as to allow cattle movement data to drive the trading events or distinguish between farm types (e.g. beef, dairy or mixed) as in [Courcoul and Ezanno, 2010; Tinsley et al., 2012] and [Iotti et al., 2017]. Our goal is to design a simple supply and demand system, which we achieve by defining a farm manager entity for every farm (the network's node unit). This farm manager submits demands and offers of animals according to its needs to a central entity called 'the market', which in turns distributes and regulates the posted demands and offers. We will

describe these entities and mechanisms in detail in the following section 2.2. Regarding the farm types, as demonstrated in [Iotti et al., 2017] the dairy farms account for the vast majority of the spreading events of BVD for the agricultural system of Italy. In Germany this effect is even more pronounced as animals reaching fattening (beef) farms virtually in all cases are destined for the slaughterhouse, thus narrowing the analysis and our simulation's design attention to dairy farms [Gethmann, 2018].

Available Data

As explained in [Wernike et al., 2017] the current German nationwide control programme has brought the PI prevalence of BVD to 0.02% in animals and 0.16% in holdings for the whole country, which makes Germany one of the leading countries in the related biosecurity measures. The progressional improvement of the BVD situation since the adoption of the old regulation (01.01.2011) can be clearly seen per federal state and nationwide in the statistics of figure 2.2. Nevertheless, due to the regional and federal level BVD intervention programmes adopted prior to the old regulation we can only speculate as to the exact PI prevalence level at the beginning of the old regulation (01.01.2011) countrywide. In figure 2.3 we can see the trend of the annual BVD prevalence per federal state since 2000 when the records begin. It becomes immediately evident that before 2011 there were great variations among the federal states in annual PI prevalence. This led us to calibrate the model speculatively and according to expert opinion on that matter as we will see in the description of the model that is to follow in section 2.2.8 [Bioglio et al., 2016; Ezanno et al., 2007; Gethmann, 2018; Viet et al., 2004].

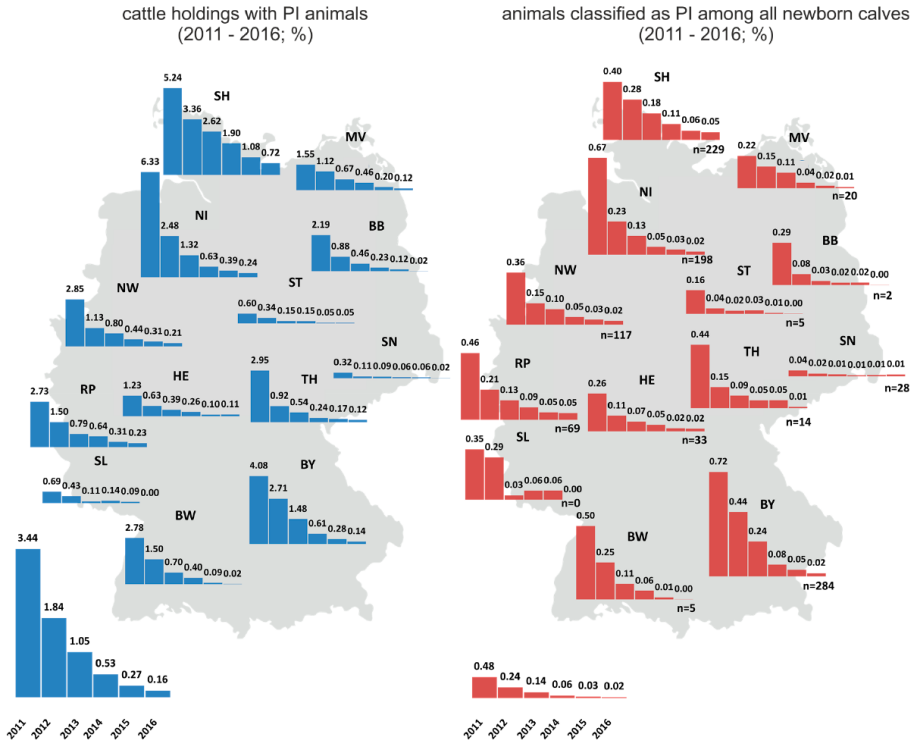

Figure 2.2: Bar charts for PI-infected holdings (left) and PI population (right) per German federal state (centered around the state prefixes) for the years 2011 to 2016. The bottom bar charts refer to the country as a whole for the same years. The 'n' to the right refers to PI animal count. Taken from [Wernike et al., 2017].

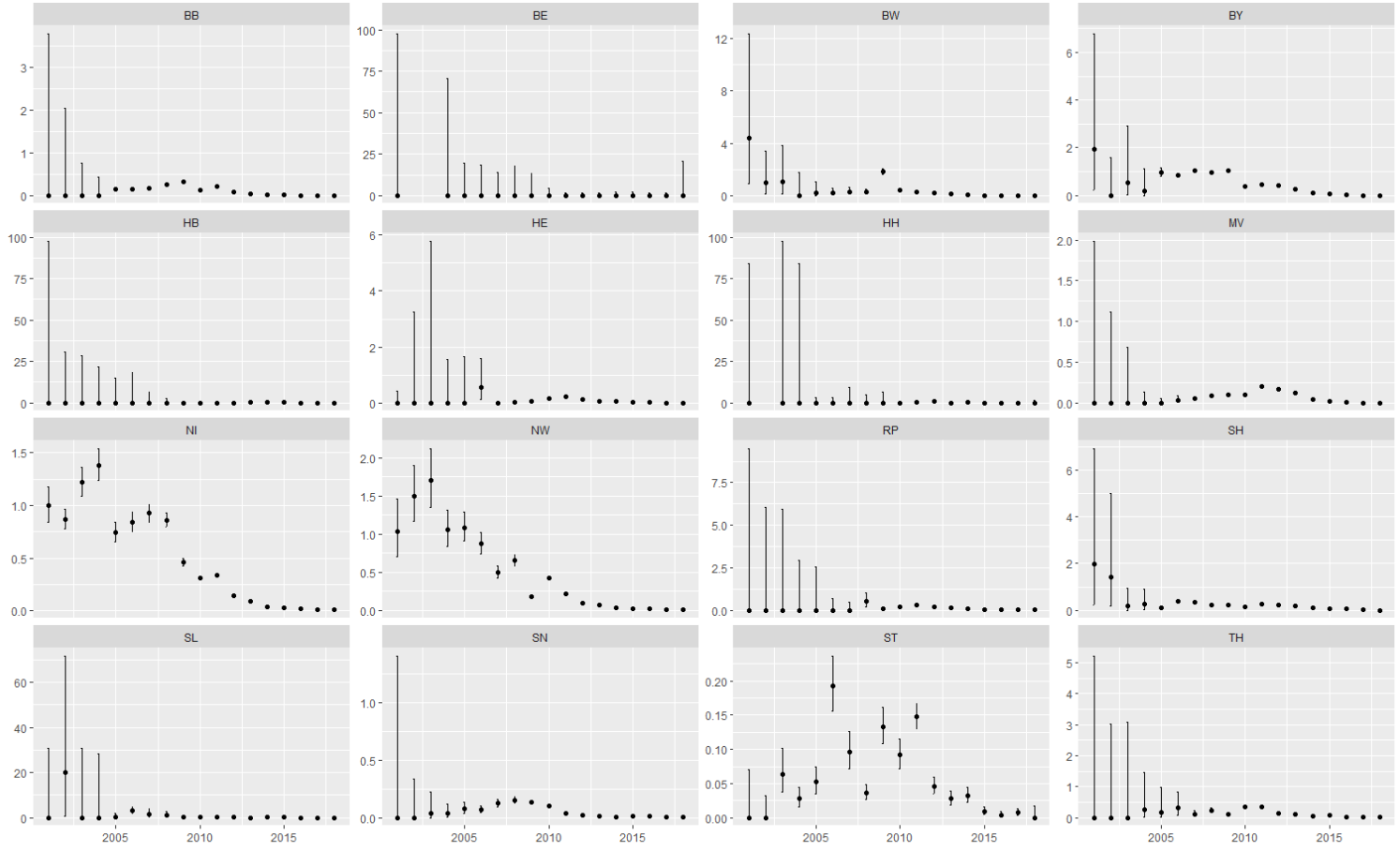

Figure 2.3: Persistently infected annual prevalence percentage (on the vertical axis) as points for each federal state since 2000 (year on the horizontal axis). The huge confidence intervals (vertical lines) mostly correspond to the beginning of the data records when there were still many inconsistencies in the reporting and recording process [Gethmann, 2018]. Courtesy of J. Gethmann. Data extracted from the HIT database. See table 2.2 for the correspondence between state names and the title codes.

In regard to the model's breeding calibration we use animal demographics extracted from the HIT database in the period 01.01.2010–31.12.2014, the living age and age of death distributions of which can be seen in figure 2.4. We shall refer to the calibration procedure in section 2.2.8. A last remark concerning the subplots of figure 2.4 is the notable lower male life expectancy than the female one. Although expert opinion confirms that the birth ratio of female to male animals is approximately $1:1$ leaning slightly on the female side [Gethmann, 2018], the needs of the agricultural system, the fact that cow inseminations takes place artificially and the fact that dairy farms consist predominantly of female animals lead us to expect a longer life expectancy of female animals as indicated by the relevant data of the subplots of figure 2.4.

Finally, as will be explained in section 2.2.6 the simulation we will be presenting is based on the farm size distribution of the state of Thuringia (our model system), which includes 4,054 farms containing 342,211 animals in total. Furthermore, we will use for scaling purposes the corresponding farm size distribution of Germany, which includes 156,620 farms containing 12,642,530 animals in total. Both these distributions were provided by the FLI (extracted from the HIT database) in two-column CSV format, where the first column's entries referenced the number of animals and the second the number of farms corresponding to that number of animals on the same line. Both of the distributions reflected the recorded farm numbers in Germany for the year 2014. For the latter distribution this count can be seen in the trend of figure 2.5 displaying the registered farms in Germany per year from 2008 to 2016. To end with, the aforementioned farm size distributions, as well as those of the states of Bavaria and Rhineland-Palatinate (also for 2014 and provided by the FLI from the HIT database), are displayed in figure 2.6 on a semi-log scale for a countrywide comparison.

2.2 BVD Agent-Based Model Description

In this section we present and describe thoroughly the agent-based model following the *Overview, Design concepts and Details* (ODD) protocol after its last revision in [Grimm et al., 2010] and after the example of [Thulke et al., 2017]. The source code of the model can be found in the repository https://github.com/Yperidis/bvd_agent_based_model.

2.2.1 Overview

The ODD protocol is followed to describe a hierarchical event-driven, stochastic agent-based model written in C++ for single-thread execution, which models the spread of *Bovine Viral Diarrhea* (BVD) between animals in the herd, the farm (through contact) and the in between farm level (through animal movements).

Federal State	Code Name
BB	Brandenburg
BE	Berlin
BW	Baden-Württemberg
BY	Bavaria
HB	Bremen
HE	Hesse
HH	Hamburg
MV	Mecklenburg-Vorpommern
NI	Lower Saxony
NW	North Rhine-Westphalia
RP	Rhineland-Palatinate
SH	Schleswig-Holstein
SL	Saarland
SN	Saxony
ST	Saxony-Anhalt
TH	Thuringia

Table 2.2: Code names of the 16 German federal states according to the ISO 3166-2:DE part of the ISO 3166 standard for country prefixes.

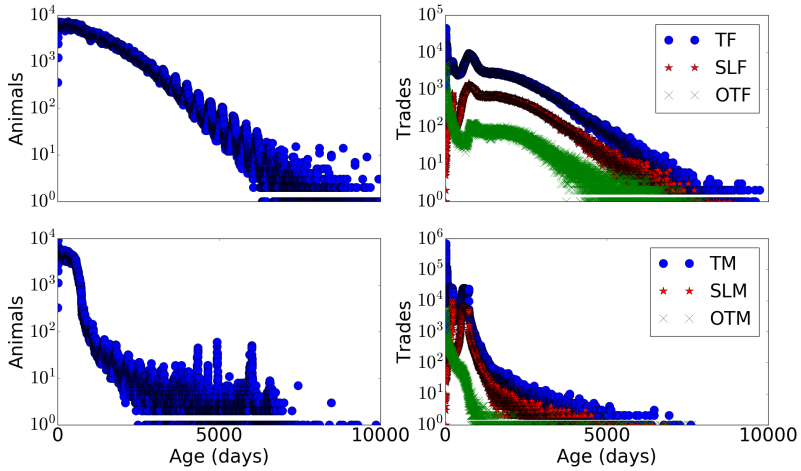

Figure 2.4: Age distribution of female and male animals (top and lower left column respectively) and age distribution of female and male animals (top and lower right column respectively) at trade, slaughter and other causes of death as provided by [Gethmann, 2018] from the HIT database. The label shorthands 'T', 'SL' and 'OT' stand for trade, slaughter and other deaths respectively, while the 'M' and 'F' refer to male and female animals. Semi-log plots.

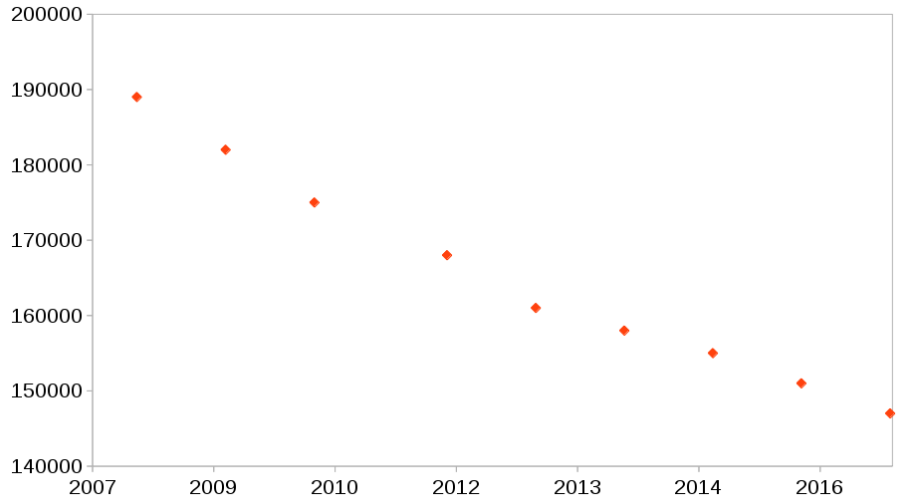

Figure 2.5: Trend of Germany's farm count for the years 2008-2016. The farm count is on the vertical axis. Courtesy of J. Gethmann. Source data from the federal statistical bureau of Germany ('GENESIS-Online Datenbank', Statistisches Bundesamt).

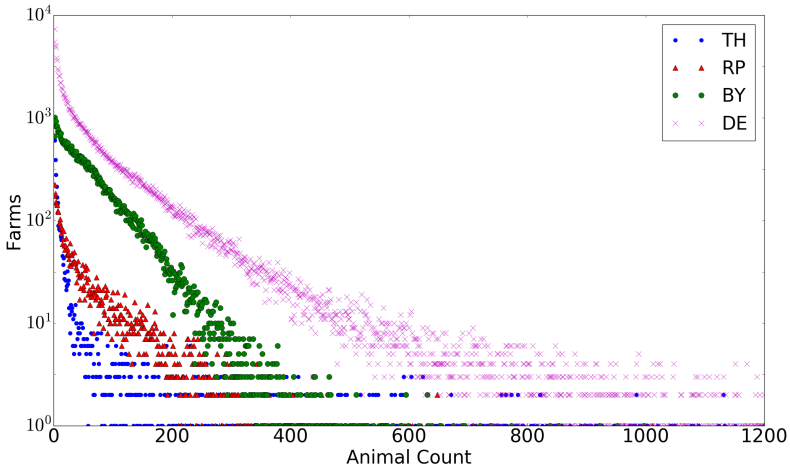

Figure 2.6: Comparative farm size distributions of the German states of Thuringia (TH in blue small dots), Rhineland-Palatinate (RP in red triangles), Bavaria (BY, in green big dots) and of all of Germany (DE in magenta 'X's) in semi-log plot.

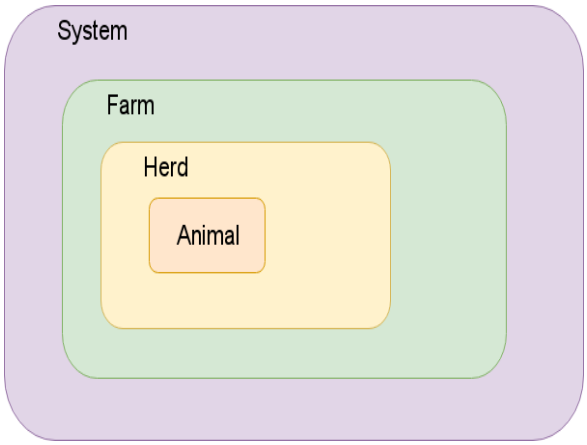

Figure 2.7: The simulation's four hierarchical levels in descending order: System, Farm, Herd, Animal.

2.2.2 Purpose

The whole simulation was designed in a way to accommodate the particularities pertinent to the agricultural cattle system of Germany. In addition, all the results and the related sensitivity analysis performed were generated using farm size distributions of federal German states as extracted from the HIT database. The simulation is to serve as a tool for approximating the current status of the BVD dynamics within the German agricultural system and most importantly for assessing the effect of various considered strategies implemented as policies by the administration in a cost effective manner to promote the eradication of BVD.

2.2.3 Entities, State Variables and Scales

There are four hierarchical levels of the simulation, *the System*, *the Farm*, *the Herd* and *the Animal*, with the *System* being the superset of all and the *Animal* being the smallest unit as shown in figure 2.7. As will be apparent in the upcoming lists the animal agent entity is by far the most complex of all the levels, as it contains events and variables to model breeding, infectious, movement and trading, testing and vaccinating features.

1. **Pregnancy Related Cow Events**

   Note that breeding and health related states are intertwined in this category.

   - *No calf*, i.e. a non pregnant cow.
   - *Susceptible* mother.
   - *Persistently infected* mother.

- *Immune*, i.e. mother with life-long immunity.
- *Cripple*, i.e. a cow which gives birth to a malformed calf, which is to be put down immediately.
- *Abort*, i.e. a cow which is going to have an abortion.
- *Infertile*, i.e. a cow which has met the criteria to be classified as such.

2. **Infectious States**

   - *Susceptible*
   - *Transiently Infected*
   - *Immune*
   - *Persistently Infected*

3. **Test Related States**

   - *No status*, i.e. the animal has not been tested.
   - *Negative* test
   - *Positive* test
   - *Positive once*, i.e. an animal which has been tested positive once.
   - *Positive twice*, i.e. an animal which has been tested positive twice.
   - *Positive mother*, i.e. an animal which has been tested positive and has had offspring prior to testing.

4. **Animal Trade Related Criteria**

   - *Calf* (female).
   - *Heifer pre breeding*, i.e. a heifer which is not ready to be inseminated.
   - *Heifer ready for breeding*
   - *Infertile*
   - *Pregnant*
   - *Dairy cow*
   - *Old cow*
   - *Male calf*
   - *Young bull*
   - *Old bull*
   - *Number of types.* Accounting for future extensions (additional criteria).

5. **Events**

   Given in descending priority. Each one refers to a single hierarchical level of the system, i.e. to the system level, to the herd level, to the farm level or to the animal level.

   - *Change containment strategy*. System level.
   - *Jungtier small group*. Farm level. *Jungtier* refers to the young calf window strategy.
   - *Jungtier exec*. System level (triggers *Jungtier small group*).
   - *Quarantine end*. Farm level.
   - *Virus test*. Refers to a blood, antigen (virus) test initiated from the young calf window strategy. Animal level.
   - *Antibody test*. Animal level. Refers to a serological test (blood).
   - *Test*, accounting for the virus test through tissue testing (ear tag). Initiated via birth. Animal level.
   - *Manage*, calls the farm manager. System level.
   - *Stop*, halts the simulation. System level.
   - *Write output*, writes the specified output to a file. System level.
   - *Log output*, writes the specified output to the memory. System level.
   - *Abortion*. Animal level.
   - *Insemination*. Animal level.
   - *Conception*. Animal level.
   - *Birth*. Animal level.
   - *Death*. System level.
   - *End of MA*, signifies the expiry of the maternal antibody effect for a calf. Animal level.
   - *Infection*. Animal level.
   - *Recovery*. Animal level.
   - *Slaughter*. System event.
   - *Culling*, accounting for extensions of *Slaughter*. System event.
   - *Vaccinate*. Animal level.
   - *End of vaccination*, signifies the expiry of a vaccination's effect. Animal level.
   - *Trade*. Farm level.
   - *Remove cow*, which is an action for a positive test. Animal level.

6. **Time-Scales**

   A direct consequence of the events' definition, the time-scales refer again to a single hierarchical level of the system.

   - BVD transiently infectious period (recovery). Animal level.
   - Maternal antibody protection period. Animal level.
   - Pregnancy period. Animal level.
   - Animal movement event's period. Farm level.

7. **Farm Types**

   - Simple One Herd Farm
   - Small One Herd Farm
   - Slaughterhouse
   - Well

8. **Network Entities**

   - Farm manager
   - Market

2.2.4 Process Overview and Scheduling

As an overview of the code's processes and scheduling flows we distinguish three intertwined modules as seen in figures 2.8, 2.9 and 2.10: one for the breeding mechanism, one for the infectious mechanism and one for the management protocol respectively. We further present a short set of serial instructions, which illustrates the flow of the model as a whole according to a *priority queue* containing all the scheduled events. We finally illustrate in figure 2.11 the vertical and horizontal (i.e. by birth or contact respectively) infectious transmission flow as modelled in the simulation. Everything takes place in (floating point) continuous time, in which events take place in discrete points in time. The events in turns trigger one another in the spirit of the event-driven paradigm [Fishman, 2013].

1. START
2. Initialise system (farm and animal variables)
3. Schedule future events for initialised animals
4. Log the system's (initial) state
5. Execute the queue's events of any of the 4 system levels (system, farm, herd or animal) until either the queue is empty or the *stop* event (equivalent to the specified end time) is reached

6. Log every event after its execution
7. STOP

To give a brief explanation of the various actions and objects in figures 2.8, 2.9 and 2.10, the green triangles represent the initiation of an event, the rhombuses a binary query, the rectangles operations within the scope of an event, the red ovals the scheduling of an event and the yellow parallelograms a frozen state awaiting to be initiated by an event. Further, for each of the modules and across them in the various figures 2.8, 2.9 and 2.10, we can discern distinct submodules which feed each other to form the module of the corresponding figure. To clarify this interdependence, we give just one example for each figure to initiate the reader into the logic of the underlying event-driven mechanisms. The corresponding details to interpret the flow charts of all figures 2.8, 2.9, 2.10 and 2.11 in depth can be found in section 2.2.7 where we scrutinise through all the steps of the simulation's submodels.

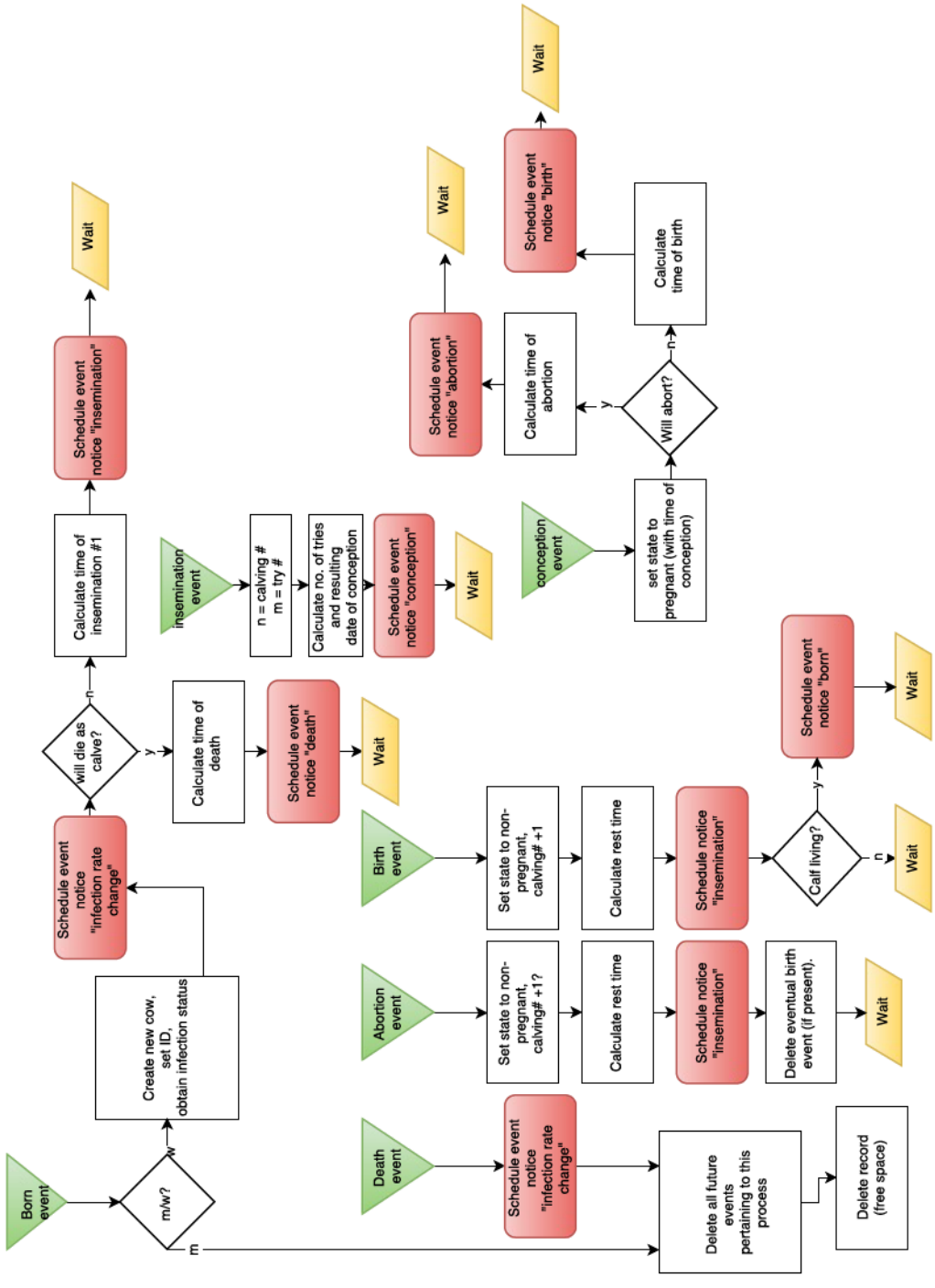

Figure 2.8: The simulation's breeding module in a reduced, flow chart version. All instructions refer to the animal level.

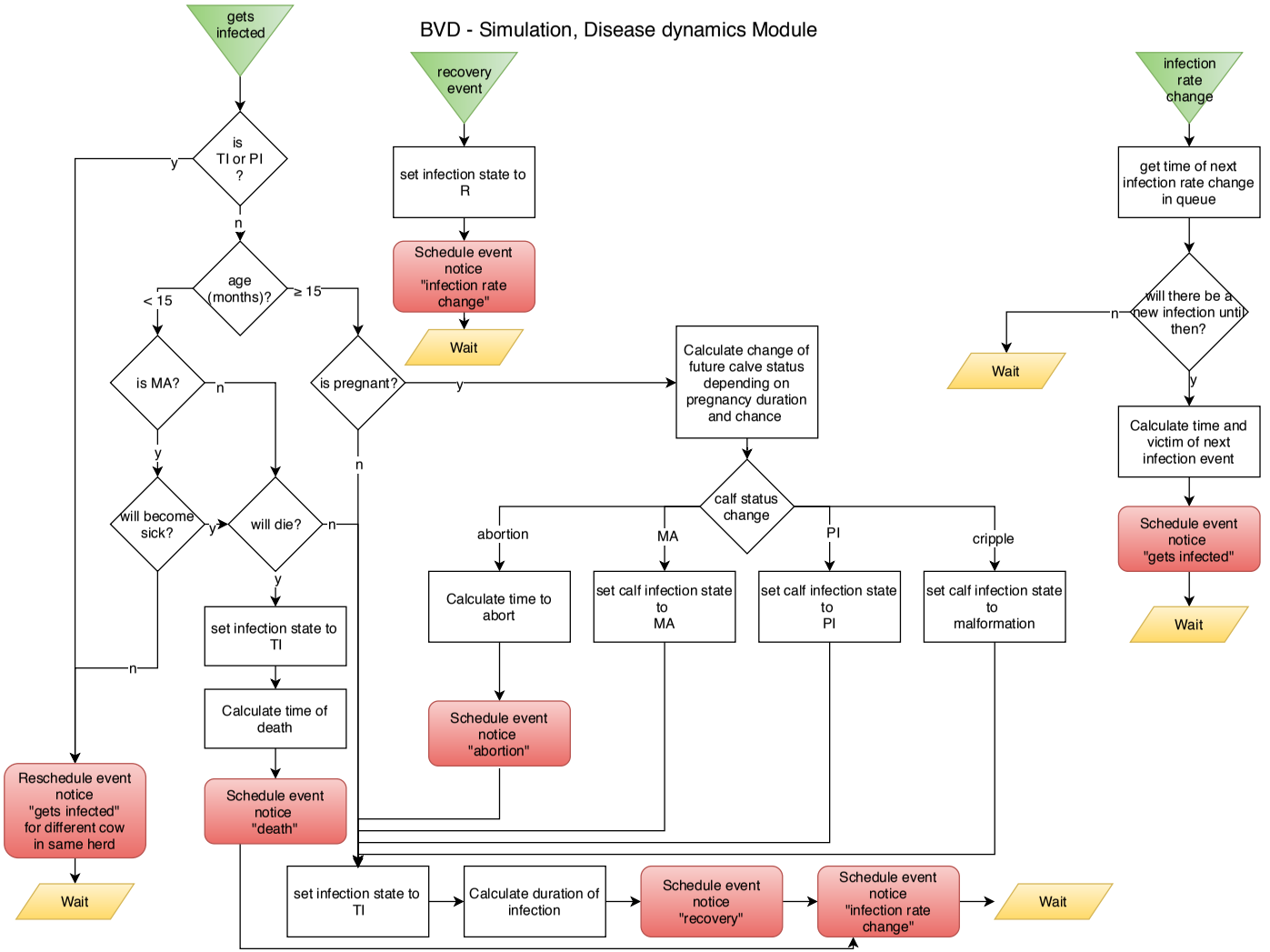

Figure 2.9: The simulation's infectious module in a reduced, flow chart version. All instructions refer to the animal level.

In figure 2.8 we take the example of a birth event. Such an event will eventually lead to the scheduling of an insemination for the newborn in its adult life. Until that age is reached the event is put on hold. In turns, once the insemination is executed it leads to the scheduling of a conception event within a number of tries (stochastically determined). If some try is going to be successful the conception event is scheduled, which is again put on hold until the system time reaches its execution time counting from the time of the insemination event's execution. Similarly and serially, the execution of the conception event at the appropriate system time will lead to the scheduling of either a birth or an abortion event (within some stochastically determined gestation period from the conception event's execution time) and then be put on hold. Finally, when the time for a new birth event has been reached, the circle between two birth events will have been completed.

In figure 2.9 we present an example for an infection event. It is initiated in a farm and, depending on the age group of an animal, after several operations and queries on the animal's state will eventually lead to the scheduling of a recovery event and to the scheduling of a change of the infection rate (farm level event), which we are going to see in section 2.2.7 in equation (2.1). Both are then put on hold. The former, once executed will in turns lead to the scheduling of the change of the infection rate of the farm again and then be put on hold. Eventually, the animal will die by the execution of a death event, scheduled from the module of figure 2.8. Once this latter event is executed one more infection rate changing event will be scheduled. Meanwhile, depending on the availability of susceptible animals in a farm, the existence of an infected animal (TI or PI) in a farm will trigger a new infection event to be scheduled according to the value of the infection rate for the farm in question at the time when the infected animal appears in it.

In figure 2.10 the only initiated event is the managing one. For a certain farm, the managing event will go through the demands of the farm in animals (so as to keep its population constant), calculate them and depending on the farm's status of being quarantined or not might schedule a direct trade to the slaughterhouse in the former case (the only possible trade for a farm in case it has been quarantined). Then it is put on hold until the predefined time of its execution. Then the farm will be managed in its next period according to its determined value from the system parameters.

Regarding figure 2.11 the horizontal (contact) mechanism consists of the straightforward infectious transmissions of susceptible animals within a farm, owing to their (random) contact with either of the infectious animals TI or PI with corresponding infectious transmission rates λ_{TI} and λ_{PI}. Eventually, the infection will spontaneously lead to a recovery within a recovery period τ_{rec}. Furthermore, animals with a temporary immunity acquired from their parent (maternal antibodies) lose this immunity spontaneously within a period τ_{mat}. Lastly, animals that have been vaccinated retain their immunity for a period τ_{vac}.

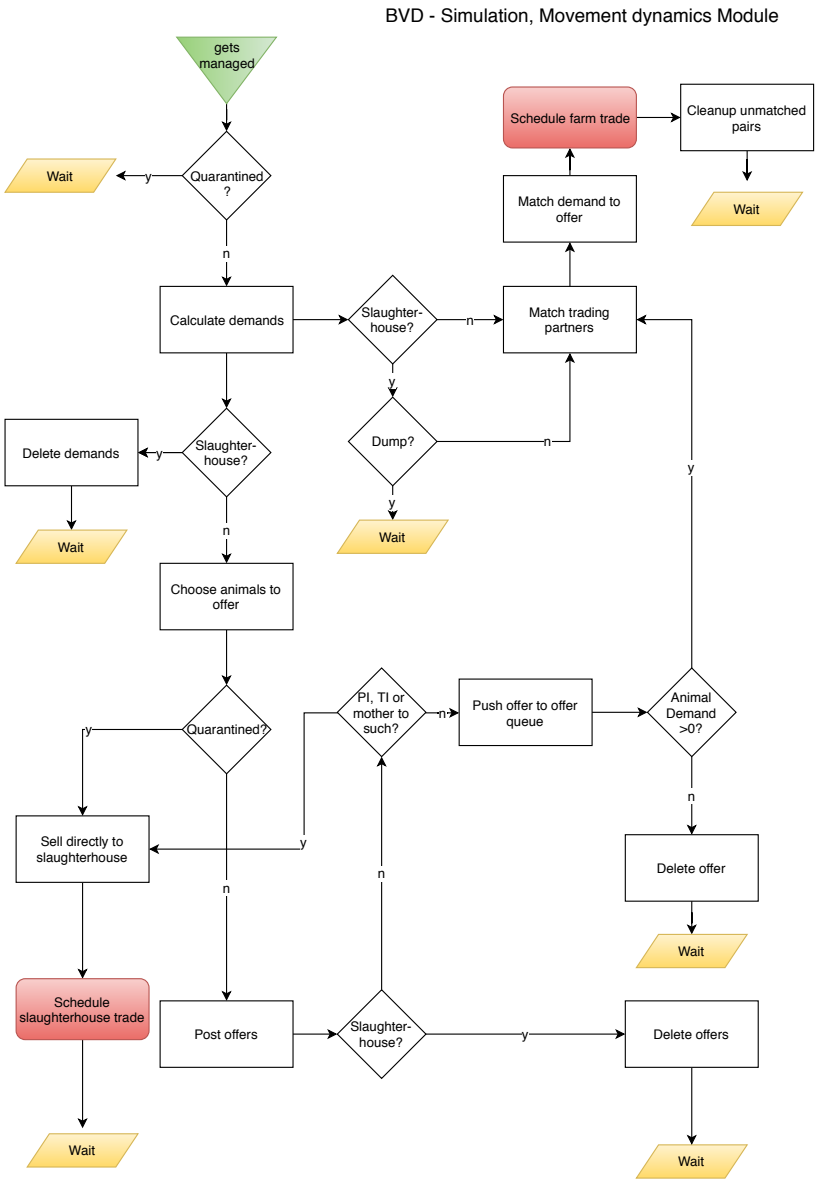

Figure 2.10: The simulation's movements' module in a reduced, flow chart version. All instructions refer to the farm level.

Vertically (i.e. through breeding) a susceptible carrying cow throughout its gestation period τ_{gest} will give birth to a susceptible animal. A carrying cow which has recovered prior to its conception, will give birth to an animal with temporary (maternal antibody) immunity after her gestation period τ_{gest} has elapsed. The same holds for a carrying cow that has been under the effect of a vaccination upon her conception. A PI carrying cow will always give birth to a PI after her gestation period τ_{gest}. Finally, a carrying cow that will become temporarily infected during its early pregnancy stages will give birth to a PI animal. Conversely, if it will get infected in its later pregnancy stages it will give birth to a recovered animal after time τ_{gest}. Moreover, there is a chance that the embryo will be aborted within some stochastically determined abortion period τ_{abort}.

2.2.5 Design Concepts

In this section we summarise the concepts permeating the design of the simulation.

Basic Principles

After initialisation the simulation flow is executed according to a *priority queue* of the simulation's scheduled events. This is a LIFO ('last in, first out') container (i.e. a data structure with specific access rules) essentially representing a queue with its elements being sorted pairwise first according to some criteria and then according to its LIFO principle [Skiena, 1998; Thulke et al., 2017]. The priority criteria are

1. Causality priority. This means that given two events scheduled for execution at times t_1 and t_2 with $t_1 < t_2$, the event corresponding to t_1 would be sorted to be executed before that corresponding to t_2, even if the one of t_2 was stored in the queue structure before that of t_1.

2. Event priority. This sorting follows the list sorting presented for the events in section 2.2.3, which has a basis relevant to the BVD disease biology and to the agricultural system's structure. Events with a higher priority are sorted to be executed before ones with a lower priority.

Due to the sequential triggering of events in an event-driven simulation a priority queue container is the natural data structure to employ for such computations [Fishman, 2013; Skiena, 1998]. Such a structure has also been implemented in a patch-based scheme [Allen et al., 2008; Brauer and Castillo-Chavez, 2012] simulation for evaluating BVD within the Irish agricultural system [Thulke et al., 2017].

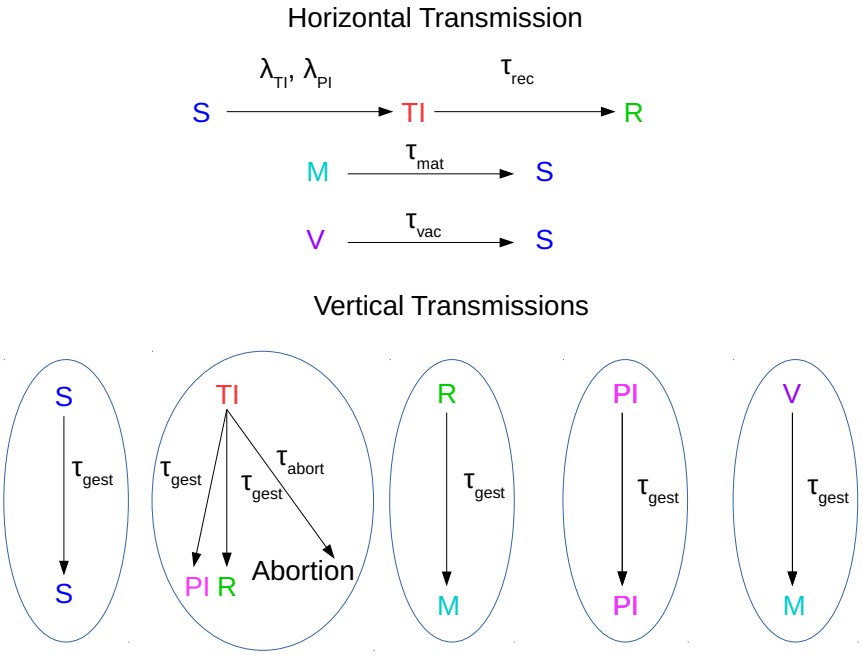

Figure 2.11: The modelled horizontal and vertical transmission schemes of BVD within the simulation. τ_{gest}, τ_{abort}, τ_{rec}, τ_{mat} and τ_{vac} stand for the gestation period, the time elapsed between the infection and an abortion, the average recovery time, the maternal antibody effect period and a vaccination's effect duration respectively. The symbols λ_{TI} and λ_{PI} correspond to the transmission rates of S to TI from a contact between a susceptible animal and a TI or a PI animal respectively. M refers to animals with temporary immunity being born from immune cows (of either active or passive immunity) prior to their conception. Compare also with the nomenclature in [Viet et al., 2004].

Stochasticity

All events pertaining to breeding, infections, recoveries, testing, vaccinations and animals selected to be classified in a certain group are executed at times and have outcomes drawn from either a uniform or a triangular distribution (float or integer depending on the application). Naturally, the stochastic times are drawn in a way which respects causality. For the choice of either one of the two aforementioned random number distributions made, the expert opinion of [Gethmann, 2015, 2018] was utlilised. All the random generator calls employ the Mersenne-Twister algorithm as implemented in the GNU Scientific Library [Galassi et al., 2018]. For the infectious waiting times an exponential random distribution was employed due to the *Markovian* nature of the infection events.

Sensing

Overall, the dynamics of the animal movement network are governed by three intertwined factors: the farm manager, the market and the independent mechanisms (testing and end of life cycle) that dispatch an animal to the slaughterhouse.

Each farm of the network has a farm manager which posts its demands and offers in animals to a central entity called 'the market', which in turns decides how the trading partners (farms) are going to be distributed based on the posted demands and offers. The offer and demand of cows (described in section 2.2.7 by equation (2.4)) therefore implicitly dictates largely the connectivity evolution of the movements' network in time. Furthermore, animals that are identified as PI or that end their life cycle and are scheduled for removal also dictate a farm's connection to the slaughterhouse.

Given the aforementioned ways with which the agents in the network evolve, their movements can provide information about an epidemic both through 'infection tracing' (i.e. tracing an infection of nodes back to a source node) or through 'contact tracing' (i.e. identifying all the possible contacts of nodes for control strategies) [Eames, 2005].

Collectives

The 3 higher-level entities out of the 4 of the system presented in section 2.2.3 are regarded as *collective entities*. This is a direct consequence of the model's hierarchical structure: animals are part of a herd, herds belongs to a farm (although not considered in this study, there can be more than one in a farm) and farms belong to the system.

Apart from the intrinsic hierarchy of the system, when selected for demands and offers the animals can be classified into collective sex and age classes, which constitute trade criteria groups. The different classes of animal trading groups have been exhibited in section 2.2.3 and are specified in

detail in table 2.6.

2.2.6 Initialisation

The system is initialised with all links being inactive, i.e. at the snapshot corresponding to $t = 0$ the cattle movements' network has no edges.

1. *Setting up the farm size distribution*

   A farm list is read from an input csv file with two columns of integers and the total number of animals and farms (including wells and slaughterhouses separately from the rest of the farms) is counted at this stage. The farm distribution is created.

2. *Setting up the farm infectious levels, the animal count and the respective age distribution*

   From the total number of farms the amount of those which are going to be PI-infected and PI-free is determined stochastically with a threshold provided by the ini file. Subsequently the animal count and the age distribution (triangular) for every animal of the farm are determined.

3. *Setting up the types of farms*

   All the types of farms are initialised iterating through the farm size distribution. This effectively determines which of the non well or slaughterhouse farms are going to be of the small or simple one-herd type. The former does not include annual replacement on the herd, while the latter does. The threshold of animals which determines the type of the farm is defined from an ini file.

4. *Farm initialisation*

   For every accessed farm its corresponding number of animals is initialised.

5. *Animal initialisation*

   For every initialised animal multiple parameters including its age, sex, health status (S, I, R, P) and future events are determined. The future events are discerned into those for male and those for female animals separately.

   - For male animals their transfer to the slaughterhouse is scheduled at a time equal to their life expectancy. This life expectancy is determined by assigning different probability margins for three age cohorts of the animals. The greatest weight lies in the second and third, which also contain larger maximal life expectancies than the first cohort (up to around 2 years). More details at the birth event.

- For female animals their first insemination age is determined and the time for calving as well. If they are not of the right age to calve (i.e. produce offspring), then their insemination is scheduled within a time from when they will come of age to calve plus a uniform number between 0 and the minimum pregnancy duration. If they are of the right age to calve, their labour is scheduled within a time ranging from the current time and the minimum pregnancy duration. Subsequently to the right calving age, the health status of the calves to be born is determined based on the health status of their mothers.
  (a) If the mother at this stage is TI then the calf can only be PI or an an abortion will occur. This is a stochastic outcome of the parameter settings for the infection during the first period of pregnancy. See tables 2.12 and 2.14
  (b) If the mother at this stage is PI then the calf will be a PI.
  (c) If the mother is S or R at this stage the calf is set to be S (potential MA protection is provided upon the call of the birth event if the mother is R).

2.2.7 Submodels

In this section the functionality of the different modules of the simulation is described in detail. In spite of the fact that effort was made to set clear borderlines among the different modules there is occasionally considerable overlap as will be apparent in what is to come. The specific choice of distributions and parameters used follow [Gethmann, 2015].

Breeding Cycle

Naturally, this mechanism concerns only female animals (cows). It is assumed that cows will always give birth to a single animal.

1. *Insemination*

   Specified in time upon initialisation for non-calf females, the insemination is the event which can trigger a conception, and in turns a birth, and a vaccination for an animal already in the system.

   Apart from the initialised cows the first insemination is scheduled upon the birth of surviving female calves between one and a half and two years (see table 2.17).

   For cows remaining in the system and taking part in the calving process (i.e. regardless of whether they gave a birth or had an abortion, their carriage was counted as a calving) the next insemination is scheduled during their resting time after they gave birth or had an abortion.

This resting time is determined by drawing random numbers from a triangular distribution with an upper limit of roughly a month and a lower of four months (see table 2.17).

Regarding the triggering of a conception, an insemination will determine whether and when a conception would be scheduled depending on the animal's age. In any case each animal gets up to four chances to get inseminated, each with increasing probability of success. The waiting times between successive inseminations are determined by drawing randomly from a triangular distribution with an upper limit of 18 days and a lower of 24. The setup of the model is such that heifers will always be impregnated within the four insemination attempts, while a 0.08% chance of infertility exists for the rest of the cows. In this last case the cow is declared to be infertile after the four attempts' time has passed plus a uniformly drawn random number between 0 and 14 days, and then the registering of it for sale to the slaughterhouse takes place instead of a conception event within a day from that time.

Regarding the case of an active vaccination strategy, provided that the effect of a potential previous vaccination has worn out, in the case that this effect's expiry took place before a minimum time which must elapse between the insemination and the vaccination (set to a month by default), then a vaccination event is scheduled by the insemination upon the insemination's scheduling.

2. *Conception*

   This event can only be triggered from an insemination and its outcome is either the scheduling of a birth or the scheduling of an abortion. In any case the survival and state of the embryo are determined by the state of the mother at this stage (tables 2.12 and 2.14). In particular:

   - If the mother is transiently infected at this stage the embryo will either become a persistently infected animal or it will even more likely be aborted, in which case its abortion is scheduled within the next two days.
   - If the mother is persistently infected at this stage the embryo will definitely reach birth and will be a persistently infected animal as well.
   - If the mother is susceptible the embryo will be susceptible if a birth is scheduled for it.
   - If the mother has any sort of immunity (i.e. temporary from a vaccination or permanent from an infection), the embryo will acquire maternal antibody protection upon its birth, if the birth is realised.

At this point the realisation of a birth or an abortion (if the latter has not already been scheduled due to the mother being transiently infected) is determined by drawing randomly from uniform distributions within different time windows of the gestation period. These windows were defined as follows with a probability up to 12% and are biologically motivated:

- The first two months (abortion).
- The second to the third month (abortion).
- The third to the fourth month (abortion).
- The remaining time up to the 210^{th} day of the pregnancy (abortion).
- The time from the 280^{th} to the 292^{nd} day of the pregnancy (birth).

For the exact parametrisation of the abortion probabilities at a particular pregnancy stage see table 2.14.

3. *Birth*

   This event is either triggered for the initialised cows at the beginning of the simulation or through a conception event, as long as a cow has not been declared infertile as previously explained.

   The history of births a cow has had is the indicator of how many times it will continue being inseminated and therefore possibly reach a birth event, a feature which was already anticipated at the insemination's description. In the model this history is defined through a calving number at the creation of an animal. This number is determined by drawing randomly from a triangular distribution with an upper limit of 3 and a lower of 5. Therefore, the maximum number of calvings a cow can have is 5 and in every birth event a unit is subtracted from its calving number (table 2.17). Once its calving number has been spent, i.e. becomes zero, the cow is sent to the slaughterhouse within one day of its last labor instead of having its rest time scheduled after calving (see the insemination cycle regarding the rest times). At this stage the cow's labour is being recorded in its birth history.

   Having dealt with the birth history of the cow in labor, the first thing that is specified upon birth is whether the embryo is a stillbirth. All further actions in respect to a birth event assume that the birth is not a stillbirth.

   At first, the health statuses of the newborn calf and the mother are determined, the birth of the calf is noted in time and the mother is declared to be non-pregnant. The possible outcomes read thus:

- If the mother is susceptible then the newborn will also be susceptible.
- If the mother has any sort of immunity (i.e. permanent or temporary) acquired prior to the conception, then the newborn will acquire a temporary immunity inspired biologically by maternal antibody protection. The duration of this immunity is determined in days by drawing random numbers from a triangular distribution with an upper limit of 180 and a lower of 270, corresponding roughly to 6 to 9 months (table 2.17).
- If the mother has acquired permanent immunity during the pregnancy and this stage (of birth) has been reached, then this means that the calf will either be permanently infected (early pregnancy stages) or will have acquired permanent immunity (later pregnancy stages). See table 2.12.
- If the mother gives birth to a malformed calf, regardless of her status the model assumes that this is equivalent to the death of the calf (it is being directly put down).

Next and depending on the specified health status of the calf, its survival or not as a calf is determined.

- If it is a persistently infected calf then its theoretical absolute lifetime maximum is set to 10 years according to field observations. For approximately the three quarters of the observed cases, four cohorts are defined for the lifetime of such calves corresponding to their four first years of life. A fifth cohort accounts for the rest of the cases. Finally, the lifetime of the persistently infected calf is determined by drawing randomly from uniform distributions respective to each cohort, after the animal has been assigned to a particular cohort by drawing randomly from a uniform percentage distribution in the following manner (see also table 2.15):
  (a) A lifetime of up to a year with a 50% probability.
  (b) A lifetime of a year up to two years with a 17% probability.
  (c) A lifetime of two years up to three years with a 5% probability.
  (d) A lifetime of three years up to four years with a 1.5% probability.
  (e) A lifetime of four years up to ten years with a 26.5% probability.
- In all the rest of the cases the calves are distributed in three mortality age cohorts of their category by drawing randomly from a uniform percentage distribution. Each cohort has a corresponding

lifetime probability, being drawn randomly from uniform distributions once more, defined in the following:

(a) $[0, 2.5)$ days with a 2.5% probability.
(b) $[2.5, 182.5)$ days with a 10% probability.
(c) $[182.5, 365)$ days with a 1.5% probability.

Afterwards the sex of the newborn is determined (see table 2.16). If the newborn is female and it has been determined to survive its first insemination age, then its first insemination age is scheduled by drawing randomly from a triangular distribution with an upper limit of 480 days and a lower of 600.

If the newborn is a male, additionally to its survival conditions set before, its life expectancy is scheduled as outlined for the male animals at initialisation. The male newborns are distributed in the cohorts by drawing randomly from a uniform percentage distribution. These three cohorts have a corresponding lifetime probability, each of which is defined by drawing randomly from a triangular distribution. At the end of its lifetime each male animal is sent to the slaughterhouse. The probabilities to be distributed in each cohort and the two limits of the corresponding triangular distributions (2.17) are as follows:

(a) Upper limit 0 and lower 30 days with a 30% probability.
(b) Upper limit 170 and lower 250 days with a 35% probability.
(c) Upper limit 450 and lower 750 days with a 35% probability.

If the newborn is a female and it survives at least until its first insemination age, then an insemination is scheduled for it at that time.

Lastly, in case an ear tag strategy is in effect the testing time of the newborn is scheduled for a time being drawn randomly from a triangular distribution with an upper limit of 4 days and a lower of 30 (first month of life).

4. *Abortion*

   This event essentially checks that the animal in question is indeed female, cancels a possible scheduled future birth or abortion (see explanation in the infection scheme), counts the abortion as a calving if the time elapsed since the last conception event is larger than 240 days and schedules the resting time of the animal until its next insemination (if applicable –see insemination's description).

5. *Death*

   Any of the *death, culling* or *slaughter* events encountered are treated similarly and signify the removal of the animal in question (and its associated scheduled events) from the system.

6. *Rest time after abortion*

   This event has a dual role. Apart from scheduling the rest time of the animal in question as described in the insemination, it also sets the criterion which signifies the end of the breeding cycle of the animal. This criterion is that the calving number of the animal has reached to zero. In this case its selling to the slaughterhouse is scheduled within half a day.

Infection Cycle

1. *Infection*

   An infection happens at the animal level for susceptible animals and is dependent on the number of its infected neighbours, i.e. the number of TI and PI animals. The neighbourhood of an animal is defined to be any member of the herd with an equal contact probability and infections in a specific time t take place with a certain instantaneous, stochastic infection rate, of the form found in [Viet et al., 2004]:

$$\lambda_l(t) = \beta_{\mathrm{PI}} \frac{\mathrm{PI}_l(t)}{N_l(t)} + \beta_{\mathrm{TI}} \frac{TI_l(t)}{N_l(t)} + \sum_{m \neq l} \beta_{\mathrm{m,l}} \frac{\mathrm{PI}_m(t)}{N_l(t) N_m(t)} \tag{2.1}$$

   where β_{PI} and β_{TI} are the BVD transmission coefficients with inverse time units, $\mathrm{PI_l(t)}$, $\mathrm{TI_l(t)}$ and $\mathrm{N_l(t)}$ the PI, TI and total animal number in the herd l at time t, $\beta_{\mathrm{m,l}}$ the BVD transmission rate from the PI animals of any other herd m to l and $\mathrm{PI_m(t)}$ and $N_m(t)$ the number of PI animals in herd m. While the β coefficients are fixed throughout the simulation, the TI, PI and total herd numbers are generally stochastically changing for every time t, thus the characterisation of the rate $\lambda_l(t)$ as stochastic. If the rate $\lambda_l(t)$ is multiplied with the population of S of the herd (number of infection candidates) for time t then the resulting rate represents the *total infections per time unit* $a(t) = \lambda_l(t) \times S(t)$.

   It is clear from the summation term in equation (2.1) that infections can also occur across herds as well (as only one herd per farm is simulated in the scope of this study, this is of no concern), but only due to the infectiousness of the PI animals as in [Viet et al., 2004]. This introduces subnetwork dynamics within the node, where each herd is a node and can influence its neighbouring (i.e. within the farm node) herd nodes' infectious states. The TI contribution is negligent in this case of infection in-between herds.

   Regarding the infectious process, we define it to be a random, Markovian event within the herd l. Due to the fact that the average waiting time for such events from one arbitrary time point t_1 to the next t_2 is

exponentially distributed [van Kampen, 2003], the total infections per time unit a are constant in that time window (and thus its factors S and λ_l) and serves as the rate parameter of the exponential distribution from which the probability to observe a waiting time τ_w in the said time frame is drawn. Said differently, the average waiting time between two successive infection events at t_1 and t_2 ($t_1 < t_2$) for a constant and positive, non-zero infection rate coefficient a in this time interval is

$$\langle \tau_w \rangle = a \int_0^\infty e^{-at} t dt = \frac{1}{a}, \tag{2.2}$$

with the integral's limits being so because of the domain on which time is defined.

Let it be stressed succinctly again that the average waiting time from one infection to another is defined for constant total infections per time unit a in the time window $[t_1, t_2]$. This a is in turns calculated after the susceptible population in the herd in question and equation (2.1) for every time an infection rate changing event takes place, i.e. for any event of priority equal or lower to that of *birth* as ordered in the event list in section 2.2.3. Thus the average waiting time $\langle \tau_w \rangle$ changes with every change of the instantaneous infection rate $\lambda_l(t)$. By examining the two marginal cases of the total infections per time unit a between two successive infection events at t_1 and t_2 the necessity of the definition of a becomes evident.

- For $a \gg 1$ or $t_1 \to t_2$ then $\langle \tau_w \rangle \to 0$, which means that the waiting time is negligible if the distinct infection events are very close to each other, if the pool of susceptible candidate victims is enormous in that time window ($S \gg 1$) or conversely if the instantaneous infection rate of (2.1) assumes a high value in $[t_1, t_2]$, $\lambda_l \gg 1$.
- For $a \to 0$ then $\langle \tau_w \rangle \to \infty$. This means that if the pool of the susceptible population is zero and the instantaneous infection rate is not zero (e.g. if the S portion of the population has been depleted and only R, TI and PI remain), then the waiting time between two successive infection events will be infinite as (for all else remaining constant) there will be no available candidates to infect.

It follows that, although the infection event refers to the animal level, the *infection rate changing* event refers to the herd level and therefore its change will correspond to a herd, not an animal. Note that if the infection rate is scheduled to change before a potential scheduled infection, the infection will not be scheduled as the conditions for its

realisation change exactly due to the rate's variation. Consequently, an infection event's *transition probability* is only dependent on the state variables corresponding to the time step directly prior to its execution, therefore qualifying it to be termed a *Markov process* [van Kampen, 2003].

As already mentioned, for the particular case of this model, the inter-herd transmission coefficients do not play a role as they refer to herds within the same unit (e.g. farm) and a single farm has been modeled to contain only one herd.

Once an animal from a certain herd has been chosen for an infection its age plays a role in the decision on whether it should recover or die from the disease. Furthermore, if the animal is a carrying cow a stochastic decision is made on the effect of the disease on its pregnancy. The exact aforementioned cases read as follows:

(a) *Calf Animal*: A decision is made on its survival from BVD (see table 2.11):
   - If it survives, its recovery is scheduled after its infection duration.
   - If it does not survive, its death is scheduled after its infection duration.

(b) *Non-Calf Animal*: Its sex is determined. If the animal is a cow the outcomes of BVD on the embryo are the following depending on the stage of the pregnancy:
   - It will be persistently infected (early stages).
   - It will be aborted (early to mid stages).
   - It will be malformed, which in this model is killed immediately (mid to later stages).
   - It will have lifelong immunity (mid and mostly later stages).

   Note that the pregnancy stages were only qualitatively described here and correspond to four successive cohorts in time. Each cohort has its own probability definition for the possible embryo outcome. For details see table 2.12. Furthermore, an important assumption made for carrying cows during the infection is that should an infection-caused abortion be defined to occur sooner than an already scheduled abortion originating from a conception event, then the conception-caused abortion will be invalidated and the infection-caused abortion will take its place in the event schedule. Moreover, three marginal cases of the abortion in respect to the birth scheduling are distinguished so as to avoid conflicts. Specifically:

- If an infection-induced abortion is to take place after a scheduled birth, then the abortion is executed immediately.
- If an infection-induced abortion is to take place before a scheduled birth, then the abortion is scheduled as planned with all the considerations so far outlined.
- If an infection-induced abortion is to take place simultaneously with a birth, then the birth prevails.

Regardless, the non-calf animal is not modeled to die from the infection, thus its recovery is scheduled after the duration of the infection.

2. *Infection rate change*

   Any of the events *birth, death, end of MA, infection, recovery, trade, remove cow, slaughter, culling, vaccinate* or *end of vaccination* change either the herd population, the TI or the PI population, or change the neighbors of any animal within the herd. This means that these events would change the infection rate (2.1) directly or its effect on the population of susceptible animals.

   The trade and the rest of the infection rate changing events are handled separately. This is because in the former case the scheduled events are transferred along with the animal to the destination herd/farm, while in the latter all the scheduled events for the animal pertain to its herd (also the farm in the modelling so far).

3. *Recovery*

   This event simply depopulates the TI group and transfers the output to the R group at the scheduled times of recovery for the corresponding animal.

4. *End of maternal antibody protection*

   This event signifies the end of the maternal antibody protection from BVD for calves drawing random numbers from a triangular distribution ranging up to three quarters of a year (see table 2.17).

5. *Vaccination scheduling, duration and expiry*

   If a vaccination strategy is in effect, the first vaccination of a surviving calf is determined upon its birth for its 186^{th} day of age. The effect of this vaccination for a susceptible animal, (i.e. a transition in the R group with a note that the immunity is temporary), provided it is successful, is set for a year (365 days) from the ini file, upon which time a compensation between the R and S groups will take place for the particular animal. If the animal is not susceptible, the vaccination will simply have no effect on the health status of the animal, but its

Test correct?	Status	Result
True	TI, PI	Positive
False	S, R	Negative
False	TI, PI	Negative
True	S, R	Negative

Table 2.3: The conditions for the four different possible outcomes of an antigen test result pertaining to a single animal.

Test correct?	Status	Result
True	R	Positive
False	S, TI, PI	Negative
False	R	Negative
True	S, TI, PI	Negative

Table 2.4: The conditions for the four different possible outcomes of an antibody test result pertaining to a single animal.

next vaccination will be scheduled in one year from the current time. The only reason for a vaccination not to take place in precisely these scheduled time frames, provided the animal in question is alive, is that the vaccination scheduling overlaps with the minimum distance from the insemination (see 2.2.7).

Testing Schemes

In the code both testing an animal for BVD through an antigen test (the so called *virus test*) or by an antibody test are in effect, depending on the implemented testing strategy. Taking that into account, the settings in the code for an antigen test to be declared positive are shown in table 2.3 and are determined by the accuracy of the test. Similarly for the antibody test see table 2.4. In essence, the *Result* column of table 2.3 is a *logical conjunction* result between the test correctness truth value and whether the animal in question is indeed sick (i.e. TI, PI being *True*) or not (S, R being *False*) for the antigen test, and whether the animal in question is indeed immune (i.e. R being *True*) or not (S, TI, PI being *False*) for the antibody test. In other words, the result asserts if the test identified a positive animal, which is identical to the test's sensitivity as defined in section 2.1.1.

The following distinctions of tests are in terms of periodicity and scope, i.e. either once in their lifetime for all animals or periodically for a sample of animals from each farm.

- *Ear Tag*

If the *ear tag* strategy is in effect, then a test is scheduled for the animal in question depending on its age and scheduled only by the birth scheme. This test concerns the antigen test (virus test) by a tissue sample (ear tag), is non periodical in the lifetime of the animal and can lead to a second round of antigen test testing (blood testing) as will be clear in the following (see also figure 2.1).

Before anything else, what is determined is whether the test is positive. This can naturally be either a true or a false positive depending on the set sensitivity threshold value from the ini file (i.e. the probability to detect a truly sick animal) and the health status of the animal, as seen in table 2.3. The specificity (i.e. the probability to successfully identify a non-infected animal) has been assumed to be unity (certainty) for the aims of the simulation [Gethmann, 2018].

1. If the test is positive, then firstly the default values are being read on whether the farm will be quarantined and for how long. This depends on the strategy implemented, but for the baseline scenario (no strategy) no quarantine is enforced. Next the animal is being registered to have been tested once with a 92% probability and with the remaining 8% for a second test. If the animal is to be tested only once, then it is registered for removal within a time drawn randomly from a uniform distribution between 3 and 34 days. In the case of a second scheduled test, the next test is scheduled by drawing again randomly from a uniform distribution between the same day and a maximum time for retesting the animal set from the ini file. By default this is set to two months (60 days). See also figure 2.1. The second round of test is a different event than the first ('virus test' instead of 'test') accounting for a blood test instead of a tissue one. If the animal is specified to be positive again, this time its removal is scheduled by drawing randomly from a uniform distribution between 3 and 23 days. Lastly, if the animal is a cow and has had offspring, all of them are declared to have had a positive mother. This is significant to determine whether the offspring of a cow corresponding to a farm should automatically also be sent to the slaughterhouse without further testing if their mother's test results is positive.
2. If the test is negative the animal is simply declared to be such and in case it is not one of the initialised cows it is declared negative in the event that its mother had been positive.

- *Young Calf Window*

  If the *young calf window* (YCW) strategy is in effect, then a sample of animals is scheduled to be selected for testing for every farm of the

system periodically. The period is defined in the ini file and is set by default to be 186 days (approximately half a year). The methodology of this approach follows [Conraths and Gethmann, 2015] and asserts that given a herd of a certain size only a random sample of its animals older than six months and younger than two years of age suffices to determine the existence of infectious animals in it up to a certain limit with a confidence of 95% through testing. That is because animals over six months of age will have, on average, lost any potential maternal antibody immunity that they may have acquired upon birth by the time of the test (especially in an agricultural system where the calves are being massively administered colostrum with their first meal) and if they are younger than two years of age they will not have, on average, started to produce offspring. Therefore, any positive tests from such a specimen would suggest that there has been some source of infection in the farm exceeding the set limit at the 95% confidence interval. In the model's case the upper limit of 20% prevalence of infected animals in the herd (of size N) given a random sample size n of negatively tested animals was set, as displayed in table 2.5. The table (the simulation's sample size is within the population limits of table 2.5) was derived with reasoning starting from the hypergeomteric distribution (formula (2.3)). That means that given a finite population of animals N, from which n are randomly drawn (tested) *without replacement* and K are indeed positive in the population, then k from the drawn ones will be positive. Formulated symbolically, this translates to the probability mass function

$$p\left(X = k\right) = \frac{\left(\begin{array}{c} K \\ k \end{array} \right) \left(\begin{array}{c} N-K \\ n-k \end{array} \right)}{\left(\begin{array}{c} N \\ n \end{array} \right)}, \tag{2.3}$$

where with $\left(\begin{array}{c} a \\ b \end{array} \right)$ the binomial coefficient is meant [Krishnamoorthy, 2006].

Since what is being sought with this strategy is herd immunity the antibody test is used on the sampled animals (see table 2.4 for the correspondence of the test outcomes to the animals' infectious states).

In case even one animal is identified as positive during the YCW protocol, then all the animals of the herd (and thus of the farm in the scope of the model) are scheduled within half a day to be tested according to the virus test (blood test) of the *ear tag* protocol previously described.

N	≤ 10	≤ 20	≤ 40	≤ 80	≤ 160	> 180
n	8	10	12	13	13	14

Table 2.5: Population sizes (N) and the corresponding samples (n) needed to be tested negative so that the prevalence of the infected animals in the population will not exceed 20% with a confidence of 95%.

Animal Movements

This is the module that builds the network and allows it to evolve. The terms *trade* and *movement* shall be used indiscriminately here, regardless of whether the movement is defined in the system to be an actual trade or a removal of the animal i.e. a dispatch to a slaughterhouse.

1. *The Manage Action*

   This is the first stage a farm has to go through in order to have some contact with the rest of the system. The *manage action* consists of a series of actions, which assess whether a farm can have any interactions with the rest of the system in the first place, whether it needs input, if it is eligible for output and of what kind should the input or output (animals) in question be. To that end, each farm has its own managing protocol called the *farm manager*.

   To start with, for the running time of the system a daily management period is set by default, but this can be changed from the ini file and for the results we have assumed a weekly management period. That means that each and every farm runs its management protocol (the farm manager) in every management period of 7 days.

   The management protocol is comprised of a number of steps.

   (a) Check if the farm is under quarantine for selling and for buying animals. If yes, that is the end of the current management action.

   (b) The demand of animals is calculated. This is realised by firstly ensuring that the animals to be purchased will only be pregnant cows and above a purchasing margin set at the input ini file (by default this is zero). Next, the actual demand calculation takes place, which depends on the type of farm taken into account. Currently this would mean either a *simple one herd farm* or a *small one herd farm*, the difference of the two lying in the inclusion of herd rejuvenation or not respectively (see section 2.2.7). Regardless, a quota of pregnant cows demanded by the farm in question for a specific herd is set upon its creation and is equal to its herd size per herd (remember that the farms in this scope

include only one herd each). Thus, the number of requested cows is calculated as the difference between the fixed quota and the herd size in question at the time of demand, for the case that this difference is above zero. Naturally, if the farm type is of the simple one herd, the fixed quota number is reduced by the farm's replacement percentage (again, see section 2.2.7).

(c) The farm's demand is registered to the market (see further below in the same section), which decides on which two farms (of any farm type) will be the exchanging partners.

(d) Next the supply of animals is calculated for the farm at hand. For that a similar methodology is followed to that for the demanded animals, with the difference being that the momentary herd size should be larger than the fixed quota of animals for any number of animals to be registered for selling.

The farm manager goes through ten available animal trading criteria for each herd and groups the herd's animals to each one of them according to their sex and age status. Then it attempts to sell as many of the herd's animals as possible from groups with a higher priority and disproportionately many animals when compared to the rest of the groups. These criteria were already outlined in section 2.2.3 and are summarised in their corresponding sex, age and fertility groups in table 2.6. The reasoning of categorising the animals to such trading groups is that, should the animals to be traded be prioritised, then animals with decreased financial benefit against others (mainly older or infertile cows) should be traded first if possible. As implied though, it is possible to set the selling sorting criteria to be evenly distributed among the different groups through a setting in the ini file or by leaving the related field empty.

Regarding priority trading criteria, at this stage it is possible to define the trading criterion for the animals to be following the numbering of table 2.6[1] in descending order for each farm. Animals from groups with the same priority numbering are drawn for filling the selling group with a weight proportional to the group size they belong to. This last point is also the distribution rule for the offered group for sale when there is no prioritising of the trade). The way to activate this priority in animal selling is to fill the related field of the ini file with the value 'OldCowsFirst' (see table 2.7).

(e) Provided the farm is not under quarantine, similarly to the farm's demand, its animal supply is registered to the market, which de-

[1] A month is assumed to have 30 days.

cides on which any two farms will be once again the exchanging partners.

(f) If the farm is under quarantine its animal supply is met by the slaughterhouse's demand.

(g) Before the management cycle for the farm ends the farm's registered demands and offers (in the form of queues) which were not directed to a trade by the market are fulfilled. This is achieved in two different ways depending on the related setting from the ini file.

The first (called 'dump') consists of matching all of the farms' demands from the well farms and conversely, all of the farms' offers from the slaughterhouse. It follows logically that the demands and offers in question cannot come from the slaughterhouses or the wells as they serve as drains and sources of the system respectively. Furthermore, self-trade is inhibited as well as direct trade from the wells to the slaughterhouses.

The second (called 'demand') treats the slaughterhouses and the wells as the rest of the farms, with the logical restriction that the first cannot post offers to the market while the latter cannot post requests (demands). In case of unfulfilled trade offers the animals offered remain in their farms.

2. *The Market*

If the market is to be distinguished from the management cycle, then it is simply to make clear that it performs the matching between the trading partners (i.e. different farms) and the demands and offers posted to it by the farm manager with queue containers. It is therefore an integral part of the management cycle, but a separate entity from the farm manager protocol.

Effectively it uses a similar mechanism for both registering demands and offers of animals to match them in pairs. The criterion for the matching is defined by four factors:

- The trading partners (farm types) cannot be the same (self-trade).
- The trading partners cannot be the pair well-slaughterhouse (source to drain case).
- If the behavior of the well and the slaughterhouse is set to fulfill the offers and requests of the unfulfilled trades at the end of a management cycle ('dump' setting in the ini file) the farm registering a demand cannot be a slaughterhouse (see the last step of the *manage* protocol).

Group Type	Status
1) Male calf	Male of age < 6 months
1) Young bull	Male of age < 17 months
1) Old bull	Male not calf and not young
1) Infertile	Female > 15 months with > 3 inseminations
2) Old cow	Female of age > 4 years
3) Heifer pre breeding	Female animal of age 6-15 months
4) Heifer ready for breeding	Female of age > 15 months with no offspring
5) Calf	Female up to 6 months of age
6) Pregnant	Female of age > 25 months with offspring
6) Dairy cow	Non pregnant cow able to breed

Table 2.6: The various categories the animals of a herd can be grouped in to be sold according to some global selling strategy. The numbering corresponds to the ascending diminishing of prioritisation for the various selling groups assuming the OLD_COWS_FIRST selling strategy. Groups of the same number have the same level of priority. In case of an evenly distributed selling strategy the group numbering is rendered irrelevant.

- If the previous point is the opposite ('demand' setting in the ini file), all the remaining offers and requests are annulled.

Farm Types

In this section we describe the differences of the four different farm types presented as system entities in section 2.2.3. The threshold for farms to be either of the simple one herd or of the small one herd type can be set in the ini file according to the number of animals corresponding to a farm. The field is called 'smallFarmSizeMax'and indicates the limit of animals that a farm should have to be specified as a small one herd farm.

- *Simple One Herd Farm*

  This is a farm containing only one herd of animals. It both offers and demands animals according to its needs, which are to preserve its population constant in every management period by comparing some quota set upon initialisation randomly from the given farm size distribution, reduced by a replacement percentage corresponding to a rejuvenation strategy of such farms, with the instantaneous population of the farm. Symbolically those needs are expressed in equation (2.4) rounded to the closest integer value. The surplus sees to the term $N_{quota} \times (1 - replacement)$ being greater than $N_{instant.}$, while the opposite holds for the deficit.

The replacement percentage for the one herd farm type is set by default to be $27.9\% \times 7/365$ [Gethmann, 2018], which roughly translates to a quarter of the herd being rejuvenated every year for a weekly management period (numerator) and can be altered in the given ini file. Rejuvenation means that a said percentage of animals is subtracted from the herd population's quota and is requested once per year through trades in pregnant heifers. Given the default values, it becomes evident from equation (2.4) that this rejuvenation effect has an effect only for farms with an animal population above 100.

$$\text{surplus/deficit} = |N_{\text{quota}} \times (1 - \text{replacement}) - N_{\text{instant}}| \tag{2.4}$$

- *Small One Herd Farm* This farm type is similar to the simple one herd farm with the sole difference being that it does not include rejuvenation for its animals via trades. The rationale behind this is that small unit farmers will keep in general their domestic animal population constant and not renew it throughout the animals' lifetime.

- *Slaughterhouse*

  This farm type has a dual function as a sink and as a demand farm which can be alternated in the ini file. On the one hand it can act as a sink for the simulation (slaughterhouse type demand set to 'dump' in the ini file), i.e. if after all the demands in a management period have been met the market still has unmatched offered animals, those animals will be channeled to the slaughterhouse. On the other hand, the slaughterhouse can act as a small one herd farm, but only with demands (slaughterhouse type demand set to 'demand' in the ini file), therefore contributing to the supply-demand mechanism of the market. Thus, it will always ascertain that all the offers that it can accommodate ('dumping capacity per type' setting in the ini file) will be met. The rest will remain in their original farms.

- *Well*

  This farm type acts inversely to the slaughterhouse dually as a source and an offering farm depending on the settings of the ini file (same as for the slaughterhouse). On the one hand, if there are not enough offers of animals to keep the population constant it will provide them (slaughterhouse type demand set to 'dump' in the ini file). On the other hand, it can also act as a small one herd farm which only offers animals, making sure that no demand is left unmet at the end of a management period, provided the well has enough animals to offer ('number of cows in well' setting in the ini file).

Note that either one of the functions of the well or the slaughterhouse are mutually activated as per the description. Therefore they can either

simultaneously function as a sink and source only entity of the simulation or as small one herd farms which either only demand or only offer animals, fulfilling the unmatched offers and demands in the market to their given capacity respectively. Assuming the latter setting in effect ('demand') it is possible to include more than one well or slaughterhouse in the simulation.

2.2.8 Parameters and Sensitivity Studies

First the calibration according to demographic data from the HIT database is presented and then all the simulation's parameters and random distributions are listed. Finally, a sensitivity analysis based on previous work and expert opinion is performed. Guidelines from field observations and expert opinion were provided by [Gethmann, 2015].

Calibration

For tuning the breeding and network behaviour of the system the work of [Blunk, 2017] in section 4.3 was followed closely as the treatment there is exhaustive. The idea was to follow common practice [Tinsley et al., 2012] and compare age and sex distributions (see figure 2.4 in section 2.1.3) with different simulation outcomes. For that purpose, the eight possible permutations of three binary parameters controlled from the ini file were examined. Those were the selling strategy (see the first column of table 2.6), the slaughterhouse behaviour (dump or demand, see section's 2.2.7 explanation) and whether the market is set to ignore the type of demands that the farms post to it (true or false for any specific group demanded from table 2.6) as exhibited in table 2.7. The result was that combination 7 of the three parameters fitted the data of figures 2.4 most closely and was thus adopted for the simulations. In words, the seventh combination of table 2.7 envisions the selling strategy to be evenly distributed among the different groups of animals classified in table 2.6, the slaughterhouse to act as a small one herd farm that only posts demands to the market and the market to ignore the specific demands of the farms in groups of animals.

Parameter Selection

For all the parameters not concerning calibration expert opinion was used [Bioglio et al., 2016; Ezanno et al., 2007; Gethmann, 2018; Gethmann et al., 2015; Viet et al., 2004]. All the simulations ran for a simulation runtime of T_{sim} = 20,000 steps with a resolution of 5 steps. As a result of the global parameters' selection (tables 2.8 and 2.10), those time steps correspond to calendar days. The tests' specificity success probability was assumed to be 100% for the needs of the simulation following expert opinion [Gethmann, 2018].

#	selling strategy	slaughterhouse behaviour	ignore type of demand
1	OldCowsFirst	dump	true
2	OldCowsFirst	dump	false
3	OldCowsFirst	demand	true
4	OldCowsFirst	demand	false
5	evenlyDistributed	dump	true
6	evenlyDistributed	dump	false
7	evenlyDistributed	demand	true
8	evenlyDistributed	demand	false

Table 2.7: The 8 different trading scenarios based on the existent binary values of the 3 dominant, relevant parameters.

To start with, table 2.8 contains all the parameters in regard to all the dynamics within the farm and the scope of the strategies presented in table 2.22 of section 2.3. The farms' population infectious states were initialised randomly from the given farm size distribution CSV file. Their infectious states were also randomly allocated between the PI and PI-free farms (see table 2.9) with a 98% bias towards PI-free farms, as explained in table 2.10. Furthermore, table 2.10 contains all the relevant details permeating the type of farms, their number and their animal movement capabilities through the market.

In tables 2.11, 2.12, 2.13, 2.14 and 2.15 all the probabilities concerning hard-coded infectious and breeding parameters as well as their interplay during the simulation and upon initialisation are presented. Moreover, in tables 2.16 and 2.17 the usage of uniform and triangular random distributions for number generation in the simulation's different processes (breeding and infectious in the former, and breeding, infectious and testing in the latter) is displayed. The latter implicates lack of homogeneity and detailed information about the interval over which the process in question takes place and its 'mode' defines an 'educated guess' bias [Krishnamoorthy, 2006]. The application details and necessity of the aforementioned tables become apparent as one inspects the various submodels listed and unravelled in section 2.2.7. Lastly, for all the statistical results the pseudo random number generator environment was setup as the *GNU Scientific Library* dictates [Galassi et al., 2018] was seeded with the number 2,333,600,960.

Sensitivity Analysis

According to what has been explained up to this point and previous work [Ezanno et al., 2007], the system parameters whose diverse effect if changed should be checked are dominantly four: the transmission coefficients of (2.1), the vaccination success probability, the ear tag test sensitivity and the gen-

Parameter	Value	Description
β_{TI}	0.03 per time unit	TI infectious coefficient in equation (2.1) [Viet et al., 2004]
β_{PI}	0.5 per time unit	PI infectious coefficient in equation (2.1) [Viet et al., 2004]
$\Delta t_{\text{TI-Ab.}}$	2 days	Time between infection and abortion for a TI, pregnant cow
$\Delta t_{\text{Infert., Fin. insem.-Remov.}}$	14 days	Time elapsed between last insemination attempt and removal for an infertile cow
Calf age threshold	180 days	Beyond this age the animal is not a calf anymore
Abortion as calving	240 days	Beyond this pregnancy stage the abortion is counted as a calving
TI calf death prob.	2%	Probability for a TI calf to die from the infection
1^{st} vacc. age	186 days	First vaccination age for the animal
Vacc. work prob.	98.5 %	Vaccination working probability
Vacc. effect Δt	365 days	Effect duration of a successful vaccination
$\Delta t_{\text{Vacc.-Insem.}}$	42 days	Time interval required for a vaccination to take place before an insemination [Damman et al., 2015]
Sensitiv. success prob.	99%	Test's sensitivity success probability
Test again prob.	2%	Probability for positively tested animals to be retested
Δt_{tests}	60 days	Time elapsed between two tests in the old regulation (strategy 2 in table 2.22) [Ministry of Food and Agriculture, 2008]
Δt_{tests}	40 days	Time elapsed between two tests in the new regulation (strategy 3 in table 2.22) [Ministry of Food and Agriculture, 2016]
$\Delta t_{\text{quarant.}}$	40 days	Quarantine period for a farm after the new regulation [Ministry of Food and Agriculture, 2016]
$\text{T}_{\text{ycw,1}}$	186 days	Periodicity of the YCW test (strategies 5a, 6a, 7, 9 as in table 2.22)
$\text{T}_{\text{ycw,2}}$	356 days	Periodicity of the YCW test (strategies 5b, 6b as in table 2.22)

Table 2.8: Global infectious, breeding, testing, quarantine and vaccination parameters set in the simulation per strategy (see table 2.22) where applicable. The programme follows the outline of [Gethmann, 2015] unless explicitly stated otherwise in the table. All the testing and vaccination parameters can be controlled from the input ini file. The rest are hard-coded.

Tuple of Infectious States' Fractions	Value
$(S, I, R, P)_{\text{PI}}$	$(0.46, 0.06, 0.46, 0.02)$
$(S, I, R, P)_{\text{PI-free}}$	$(0.79, 0.005, 0.205, 0)$

Table 2.9: The various infectious states for the populations of every farm upon initialisation. The fraction with the underscript 'PI' denotes farms destined to have a non-zero PI percentage, while that with 'PI-free' farms free from any PI animals. The PI population tuple fractions were randomly allocated to 2% of the input farms upon initialisation [Gethmann, 2018].

Parameter	Value	Description
Small Farm Margin	10	Population of a farm below which a farm is classified as of small farm type
Farm Size_{min}	10	Farm population above which farms are retained in the input
Farm Size_{max}	10,000	Farm population below which (inclusive) farms are retained in the input
Slaughterhouses	1	Number of additional farms of the slaughterhouse type in the simulation
Wells	1	Number of additional farms of the well type in the simulation
Slaught. capacity	10,000	Number of animals a slaughterhouse can accept in a single call from a farm
Well yield	10,000	Number of animals a well can introduce in a single call to a farm
Well yield in TI	2%	The percentage of TI animals in every farm call from the well
Well yield in PI	2%	The percentage of PI animals in every call from the well
Threshold buy	0	The global threshold above which farms can buy animals
Threshold sell	0	The global threshold above which farms can sell animals
Replacement	0.0054	Relevant term in equation (2.4) (on a herd's annual rejuvenation)
Infectious margin prob.	2%	Selection threshold below which the population of a randomly initialised farm has a PI fraction

Table 2.10: Farm related parameters according to [Gethmann, 2015] and [Gethmann, 2018]. All the parameters can be controlled from the input ini file.

Death	Survival
2%	98%

Table 2.11: Effect probabilities (complementary) of BVD on a calf in case of infection. After [Gethmann, 2015].

Pregnancy periods	PI	Aborted	Cripple	R
1^{st}: [0-70) days	90 %	100%	0%	0%
2^{nd}: [70-120) days	45%	60%	75%	100%
3^{d}: [120-180) days	0%	20%	45%	100%
4^{th}: [180-max) days	0%	5%	20%	100%

Table 2.12: Calf outcome mass (cumulative) probabilities in case of the carrying cow's infection (horizontally) during pregnancy, max=[280-292). After [Gethmann et al., 2015].

Insemination No	Heifers	Dams
1	90.48%	67.03%
2	99.53%	93.84%
3	99.98%	99.2%
4	100%	99.92%

Table 2.13: Mass (cumulative) probabilities for a successful insemination of heifers and dams-cows out of four total inseminations. Note that only cows have a 0.08% probability to be declared infertile. After [Gethmann, 2015].

Stage	Probability
1st [0-60) days	7%
2nd [60-90) days	9%
3d [90-120) days	10%
4th [120-210) days	12%

Table 2.14: Abortion mass (cumulative) probabilities dependent on the stage of pregnancy. After [Gethmann, 2015].

Age	Probability
1st year [0-365) days	50%
2nd year [365-730) days	67%
3d year [730-1095) days	72%
4th year [1,095-1,460) days	73,5%
Further years [1,460-3,650) days	100%

Table 2.15: PI death mass (cumulative) probabilities dependent on age. After [Gethmann, 2015].

Random process	Max	Min
PD	292	280
TI Δt CD	7 days	0 days
Female	50	0

Table 2.16: Uniform distributions used in the simulation: Pregnancy duration (PD), calf time of death by infection (TI Δt CD), sex determination (female). After [Gethmann, 2015].

Random process	Min	Max	Mode
IAAD	0	3,000	200
TFT	4 days	30 days	11 days
IIT	18 days	24 days	21 days
FIA	480 days	600 days	540 days
CA No	3	5	4
DI	4 days	8 days	7 days
TR	42 days	115 days	90 days
MAD	180 days	270 days	210 days
MLE^{1st}	0 days	30 days	10 days
MLE^{2nd}	170 days	250 days	200 days
MLE^{3d}	450 days	750 days	640 days

Table 2.17: Triangular distributions used in the simulation: Initial Animals' Age Distribution (IAAD), time of first test (TFT), inter-insemination time (IIT), first insemination age (FIA), number of calvings (CA No), duration of infection (DI), time of rest (TR), maternal antibody duration (MAD), male life expectancy (MLE). After [Gethmann, 2015].

eral variance of the system (i.e. different seeds).

1. Transmission Rates

   Some preliminary work concerning sensitivity of the transmission coefficients of (2.1) for the baseline scenario was done by Inia Steinbach in 2016 [Steinbach, 2016]. Here this work is extended by testing the final state of the PI animals in numbers as a function of the transmission coefficient for the TI animals β_{TI} and the PI animals β_{PI} of equation (2.1). Once more the catalytic factor affecting the final state of the PI animals is shown to be the PI transmission coefficient β_{PI} as demonstrated in table 2.18. This result is somewhat contrary to that of [Ezanno et al., 2007] mainly because the between-herd (animal group in the authors' case) dynamics were non-existent in this simulation as opposed in that work. To be precise, despite the form of the infectious dynamics being nearly identical in the two works (equation (2.1)) the authors of [Ezanno et al., 2007] considered only a five animal group herd. In the simulation of this work, due to the effect of vertical transmissions, i.e. PI animals latently appearing in the system after a pregnant cow's infection, the effect of the PI transmission coefficient β_{PI} dominates over β_{TI}. Furthermore, the sensitivity analysis of [Ezanno et al., 2007] on the PI animals' death rates is not directly comparable to this work as a uniform random distribution is employed for that purpose.

P_{final} No	β_{TI}	β_{PI}
11	0.01	0.1
210	0.01	0.5
278	0.01	0.8
12	0.03	0.1
305	0.03	0.5
12	0.05	0.1
317	0.05	0.8
21	0.1	0.1

Table 2.18: Final number of persistently infected animals as a function of β_{TI} and β_{PI} from formula (2.1).

Probability	Style (Position)
0	Solid, blue (left)
0.1	Dashed, red (left)
0.2	Dotted-dashed, green (left)
0.3	Dashed, dotted, magenta (left)
0.8	Solid, blue (right)
0.98	Dashed, red (right)
0.99	Dotted-dashed, green (right)
0.998	Dashed, dotted, magenta (right)
1	Dotted, black (right)

Table 2.19: Probabilities of the test's sensitivity for scenario 3 (i.e. old and new regulation implementation, see table 2.22 in section 2.3).

2. Ear Tag and Retesting Laps

   For the tests' effect on the PI prevalence their sensitivity was examined[2] by varying the test's accuracy probability as seen in figure 2.12. Not surprisingly, as the sensitivity probability tends to certainty the PI prevalence tends to eradication as all the infected animals are identified (see the corresponding sensitivity relation in section 2.1.1).

3. Vaccination Success Probability

   For the vaccination's effect on the PI prevalence the vaccination's working probability was varied from zero to one as demonstrated in figure 2.13. As with the tests' sensitivity success probability, the increase of certainty for the vaccine's working probability leads to eventual extinction of the PI population. However, the vaccination's effect on

[2]Do not confuse the statistical quantity of sensitivity with the sensitivity analysis of various parameters in a model.

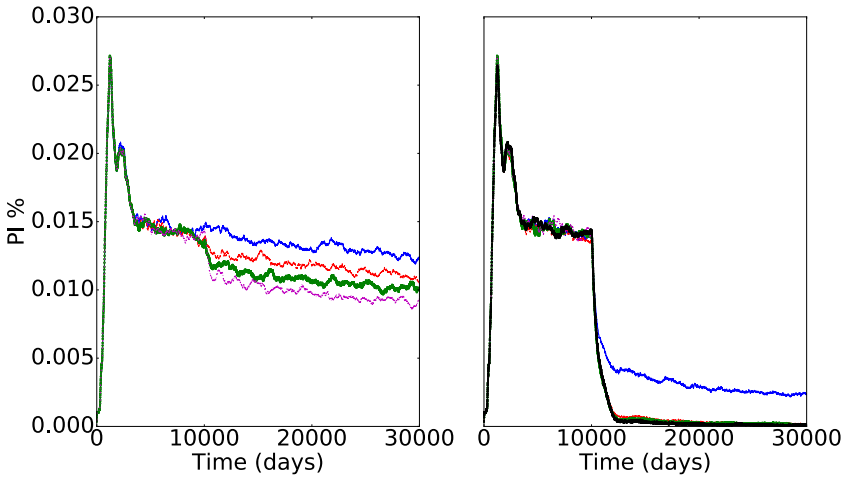

Figure 2.12: Scenario 3 (i.e. old and new regulation implementation with ear tag and blood tests, see table 2.22 in section 2.3) for different test accuracy probabilities ranging from 0 to 1, as outlined in table 2.19. The effect of the ear tag test protocol is enforced from day 10,000 onwards.

the PI population is slower than that of the tests' sensitivity success and requires near certainty values to lead to extinction. This could be attributed to the fact that indiscriminate vaccination of animals regardless of their infectious status reaches its intended targets slower than tests of all animals, which aim to identify and remove the infected ones.

4. Variance

   For completeness and reliability of the stochastic nature of the simulation a sensitivity analysis was performed on the PI prevalence percentage as a function of the seeds of the random number generator as displayed in figure 2.14. The differences proved to be of the order of 0.001% implying that the results have to be robust to stochastic fluctuations.

2.3 Simulation Plan

To emulate the network's behaviour and to predict the effect of different counter measures on the PI prevalence we formulated a simulation plan of intervention strategies according to expert opinion [Gethmann, 2018], precedent and the literature [Conraths and Gethmann, 2015; Damman et al., 2015; Iotti et al., 2017; Thulke et al., 2017; Tinsley et al., 2012; Wernike

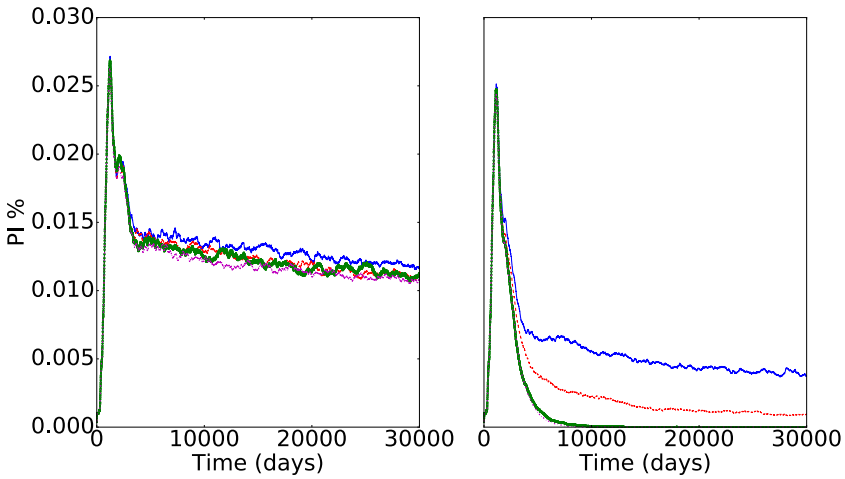

Figure 2.13: Strategy 8 (i.e. only vaccination as explained in table 2.22 of section 2.3) for different vaccination working probabilities ranging from 0 to 1 as outlined in table 2.20.

Probability	Style (Position)
0	Solid, blue (left)
0.1	Dashed, red (left)
0.2	Dotted-dashed, green (left)
0.3	Dashed, dotted, magenta (left)
0.8	Solid, blue (right)
0.9	Red, dashed (right)
0.985 (default)	Dotted-dashed, green (right)
1	Dashed-dotted, magenta (right)

Table 2.20: Vaccination working probabilities for the sensitivity of strategy 8 (only vaccination as intervention strategy -see table 2.22 in section 2.3).

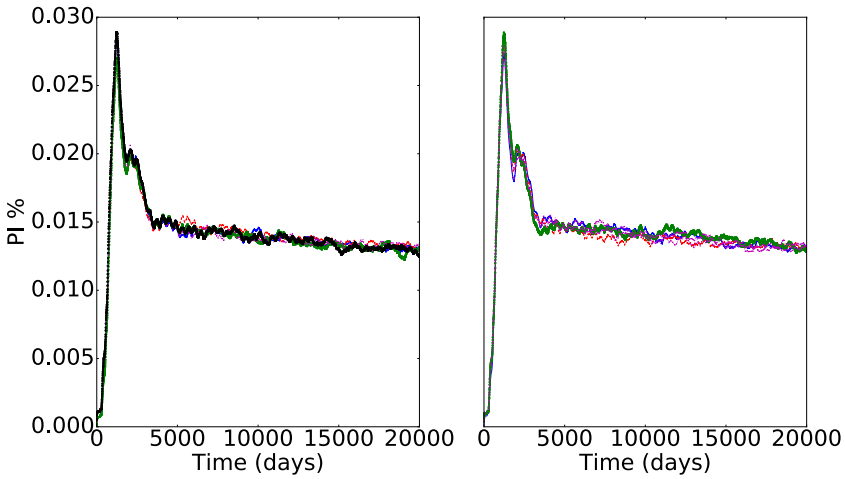

Figure 2.14: Scenario 1 (baseline to all, see table 2.22 in section 2.3) for different seeds as outlined in table 2.21.

Seed No	Style (Position)
2,333,600,960	Solid, blue (left)
2,333,600,970	Dashed, red (left)
2,333,601,960	Dotted-dashed, green (left)
2,333,620,963	Dashed, dotted, magenta (left)
2,333,710,962	Dotted, black (left)
2,333,970,967	Solid, blue (right)
2,333,650,932	Dashed, red (right)
4,333,600,860	Dotted-dashed, green (right)
3,323,601,969	Dashed, dotted, magenta (right)

Table 2.21: Seeds for the variance of scenario 1 (baseline).

Strategy	Description
1	No control (baseline)
2	Old regulation
3	New regulation
4	New regulation and vaccination
5a	New regulation and YCW with a semesterly frequency
5b	New regulation and YCW with an annual frequency
6a	New regulation, vaccination and YCW with a semesterly frequency
6b	New regulation, vaccination and YCW with an annual frequency
7	YCW with a semesterly frequency
8	Vaccination
9	Vaccination and YCW with a semesterly frequency

Table 2.22: The different strategies comprising the scenarios presented in table 2.23. YCW is the young calf window protocol. See the testing description in section 2.2.7.

et al., 2017]. This plan consists of 13 different scenarios, one baseline where the system is allowed to evolve freely without any intervention strategy and 12, each of which contains some sort of mitigation strategy for BVD, applied at different times, after the free system's dynamics (baseline) have settled to an equilibrium. The particular ordering of the strategies in each scenario and consequently the number of scenarios were dictated by the needs of a cost-benefit analysis performed by collaborators of the FLI [Gethmann, 2018] and similar to a recent work done for the federal state of Styria in Austria [Marschik et al., 2018].
We first list the different control strategies and then their application protocol manifested in the distinct scenarios in table 2.22. Similarly we summarise the scenarios with the strategies being applied at targeted times in table 2.23. Following the unit definition, which as we saw arose naturally in the parameter selection section 2.2.8, one time step should correspond to a day. The total running time of our simulations spanned 20,000 days or roughly 55 years, in which we distributed the different strategies. The reasoning has been always to start from a 'no control' state in equilibrium and apply some control strategy on the system once its dynamics have settled on a fixed point or have reached a state of slow variation.

According to table 2.23, the $10{,}000^{\text{th}}$ step of any of the mitigation strategies signifies the start of the old regulation's effect (2011). As explained in section 2.1.3 though, the nationwide PI prevalence before 2011 is not known due to lack of unified records. Hence, we restrict ourselves to the $10{,}000^{\text{th}}$ time step to mark the initiations of the intervention strategies, as a large enough time where the population dynamics appear to have stochastically

Scenarios	Timeline (in days)					
	0	10,000	12,006	12,373	12,738	20,000
1	STR 1					
2		STR 2				
3			STR 3			
4					STR 1	
5				STR 4		
6				STR 5a		
7				STR 5b		
8				STR 6a		
9				STR 6b		
10				STR 7		
11				STR 8		
12				STR4	STR8	
13				STR4	STR9	

Table 2.23: The scenario scheduling plan. STR stands for 'strategy' as outlined in table 2.22. A colour block denotes the effect of the same strategy throughout the different starting days.

settled to a fixed point and the infectious dynamics of the system seem to be changing very slowly as seen in figures 2.15 and 2.16 (upper left) respectively. In other words, our mapping of the 10,000$^{\text{th}}$ time step with the commencement of the year 2011 (enforcement of the old regulation) is only speculative and cannot be precisely determined exactly due to the prior non-nationwide, but regional intervention strategy programmes (compare the fractions of figure 2.17 with figures 2.2 and 2.3).

2.4 Results

2.4.1 The Thuringian Cattle Network

For the results that we present here all the global parameters listed in the previous section (2.3) and in section 2.2.8 are assumed. We have omitted small farms (with a population of less than 10 animals) from the simulation with the assumption that they are in practice family farms, which rarely (if ever) trade their animals and thus their contributions to the connectivity of the network are negligible. This leaves us with a total of 1,657 'simple one herd farms' (see again the global settings of table 2.10 for the 'small one herd farm' threshold) plus one slaughterhouse and one well (drain and source respectively) set at the global parameters' table 2.10. The total animal count for the 1,657 farms from the given farm list of Thuringia is 333,350 animals.

The population remains statistically unchanged for the different scenarios

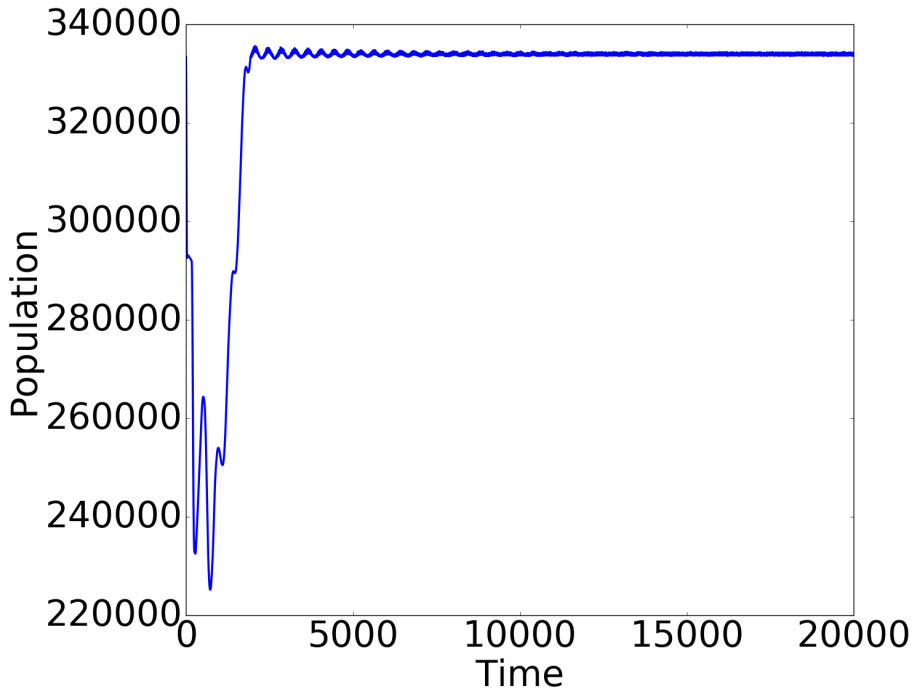

Figure 2.15: Global population evolution for the baseline scenario 1. The rest of the scenarios exhibit a statistically similar behaviour and are therefor not shown.

as figure 2.15 suggests. Looking closely at the portion of figure 2.15 before it reaches equilibrium we notice a damped periodic behaviour. This is an after effect of the initialisation attributed to the female cows being impregnated randomly within an interval ranging from time zero to the maximum pregnancy duration according to a random uniform distribution (see table 2.16). As far as the initial transient is concerned, it is a collective, combined effect of the input farm size distribution, the initial demographic conditions of the animals (age, sex), their initial infectious conditions and the system's tendency to keep its population constant through animal movements and the birth cycles as explained in section 2.2.7.

A quantity that the simulation's observables enable us to study is the various infectious states' tuple (S, I, R, P) of the animals in every farm for every time step. From this quantity we can examine the S, I, R and P infectious states' evolution at two different scales, namely the global-system one and that of the farm. Furthermore, we can easily draw from the output observables the farm PI animal or fraction count distribution along the simulation's farms at any state for any scenario.

Regarding the global evolution of the infectious states in figures 2.16,

2.17 and 2.18 (the latter is merely a magnification of the former around the PI and TI fractions' values) we should make a number of remarks for the interpretation of each scenario separately.

- *Scenario 1 (baseline)*

  After a well-known [Keeling and Whorf, 2005; Murray, 2002; Rohani, 2008] initial epidemic transient representing the outbreak from the initial infectious seeds within the herd-farm level (see the initial conditions in section 2.2.8) and from in-between farms (through movements) the system's infectious state fractions tend to an equilibrium state, with a PI prevalence of around 1.1%. The corresponding PI fraction distribution along all farms in figure 2.18 is the most pronounced of all the scenarios, which is logical as there is no counter measure. Up to the $10{,}000^{\text{th}}$ time step the behaviour of all the scenarios is identical.

- *Scenarios 2, 3*

  Beyond the $10{,}000^{\text{th}}$ time step the R fraction drops significantly and the respective S increases. What happens is that due to the old regulations' effect the PI animals are being removed relatively fast (faster in the new regulation than in the older) and therefore the naive population, i.e. a population of S, is reinstated. When scenario 2 and 3 are compared graphically on the same scale there is no significant difference between them. However, the new regulation's effect in scenario 3 (partly a shorter time between two antigen tests and mostly the probation of a farm upon a PI detection) is more pronounced towards the eradication of PI animals. Taking into account the respective PI population fractions along the different farms in figure 2.18, despite the fact that for scenario 3 we witness a higher PI fraction in some farm than in scenario 2, still the PI fraction distribution is narrower in scenario 3 than in scenario 2 supporting our previous assessment that the new regulation should be more effective than the old one towards the aim of the PI eradication. The higher PI prevalence in the farm distribution of figure 2.18 for scenario 3 is also a result of the Thuringian heterogeneities: there are not as many farms compared to states like Bavaria, but the existing farms consists of huge animal populations. Overall, scenario 3 depicts the current situation in Germany. The time frame between the $10{,}000^{\text{th}}$ day and the $12{,}006^{\text{th}}$ day corresponds roughly to the five and a half years (the half year difference with 2016 refers to a transition period from one mandate to the next) of the old regulation's effect in Germany.

- *Scenario 4*

  Beyond the $10{,}000^{\text{th}}$ and up to the $12{,}373^{\text{d}}$ time step we observe as expected the same behaviour as in scenario 3. After that point a

behaviour similar to that of scenario 1 reappears due to the lift of the intervention strategies. The final PI prevalence nevertheless appears to be slightly less than that of scenario 1, a fact which is reflected in the distribution width of the corresponding scenario of figure 2.18 when compared to the width of the distribution for scenario 1. This could be mainly attributed to the fact that at the point of the simulation where the intervention strategies are lifted the population has settled on a fixed point (see figure 2.15), which is robust to the variations we implemented in the simulation plan (not presented due to minimal, if any, observed changes when compared to figure 2.15). Thus the animals' movements could lead to fewer infections towards the steady state.

- *Scenario 5*

  The behaviour for this scenario is similar to scenario 3 with the essential difference starting from the 12,373$^{\text{d}}$ step where vaccination is added to the new regulation. This action promotes the R population and conversely reduces the S leading the curves to cross for a third time in figure 2.16 before they settle on a steady state. The fact that not all of the animals become immune at the steady state has to do with the interplay between the vaccination and the breeding dynamics, which sustain a non-zero susceptible population. As revealed in figure 2.18 this is one of the scenarios which leads to a PI extinction at the end of the simulation.

- *Scenarios 6, 7*

  In scenarios 6 and 7 the effect of scenario 3 has nearly eradicated the PI animals therefore not exhibiting any dramatic difference from the YCW's implementation from the 12,373$^{\text{th}}$ day onwards, either with a periodicity of a semester (scenario 6 with strategy 5a) or of a year (scenario 7 with strategy 5b). The two scenarios' behaviour is similar to that of 3, with 6 (semesterly YCW testing) leading to a higher naive population reestablishment than 7 (annual YCW testing). This last observation is easier to see in the respective distribution of figure 2.18: the distribution of scenario 6 is narrower than that of scenario 7.

- *Scenarios 8, 9*

  Similarly to scenarios 6 and 7, in scenarios 8 and 9 the effect of scenario 3 has nearly depleted the PI population by the 12,006$^{\text{th}}$ day to see any relevant effect afterwards. However, the inclusion of vaccination leads to a behaviour similar to that of scenario 5 for that last segment of the simulation. The two scenarios, like 5, also lead to a final state PI eradication.

- *Scenario 10*

  In scenario 10 the YCW strategy beyond the 12,006$^{\text{th}}$ day induces some periodicity in the PI population. This is an interesting effect which is attributed to the periodicity of the YCW test. The (declining) peaks' width of the PI population's fraction in figure 2.17 signify the semesterly periodicity of the YCW test, which would remove PI animals generated in the time frame of no testing. This periodicity can also be seen by the declining ripples on the S and R curves in the corresponding plot of figure 2.16. This last effect would be induced by the infectious transmissions of the recurring PI animals. As suggested in figure 2.17, the respective distribution of figure 2.18 indicates that at the final state there is still some non negligent PI occurrence in Thuringia's farms. Although in global population terms this PI prevalence seems to be rather low (less than 0.5%) it is rather alarming that PI animals are relatively broadly distributed along the system's farms, introducing a risk of recurring future infections.

- *Scenario 11*

  Scenario 11 beyond the 12,373$^{\text{d}}$ day is again similar in behaviour to scenario 5 concerning the S and R curves in the corresponding plot of figure 2.16, although less pronounced than scenario 5. Looking closely at the respective plot of figure 2.17 nonetheless we observe a short period where the PI population shoots upwards and is replenished to around the final state without strategy before dropping to minimal levels in the following segment of the simulation. This has to do with the point that was made in the sensitivity analysis section 2.2.8 when comparing the success probabilities of the tests' accuracy and the working probabilities of the vaccination on the PI prevalence, namely that the indiscriminate vaccination scheduling protocol has a slower success rate than that of the ear tag testing. Especially for the peak observed after the 12,373$^{\text{d}}$ day, it is a result of non-targeted vaccination (e.g. vaccination on recovered pregnant cows that are destined to produce a PI will not change the advent of the PI) in conjunction with the scheduling mechanism of the vaccination itself, which is intertwined with the insemination, as the latter needs to be scheduled at least 42 days after the vaccination. To demonstrate the inefficiency of the non-targeted vaccination in one last manner, although the PI fraction has become very low, it is rather extraordinary that after 10,000 days (around 27 years) of the vaccination strategy's effect there is still a relatively (say to that of scenario 6) broad PI fraction distribution along the system's farms.

- *Scenario 12*

Scenario 12 combines the new regulation with indiscriminate vaccination beyond the 12,373$^{\text{d}}$ and up to the 12,738$^{\text{th}}$ day following similar results to scenario 11. However, the post 12,738$^{\text{th}}$ day behaviour, which removes the new regulation's effect, exhibits again a similar, yet lower peak in PI as in scenario 11 before reaching minimal levels of the PI population. This can be attributed to a prolonged declining effect of PI-removed animals induced from the prior enforcement of the new regulation. Otherwise, in terms of the final state of the PI fraction's distribution along farms in figure2.18 the situation is comparable to that of scenario 11 even with slightly broader and higher PI fractions. This demonstrates how unpredictably and inefficiently non-targeted vaccination can affect the PI prevalence of the system: even with a previously combined effect of vaccination with the new regulation, when vaccination is left alone it fails to lead to the eradication of the PI population even in a time-span of 26 years.

- *Scenario 13*

  For scenario 13 the behaviour is similar to scenario 12 up to the 12,738$^{\text{th}}$ day. Beyond that we observe the first peak of the periodical PI increase (roughly extending to a semester again, which is the period of the YCW test) as in scenario 10, but with a smaller value due to the vaccination, which accompanies the YCW strategy at this stage. Henceforth the PI population is led to extinction by the vaccination's effect as can be seen in figure 2.18, underlying once again the importance of testing in the enforced strategy towards PI eradication.

Regarding the local evolution of the S, I, R and P states in specific farms we present some selected results in figures 2.19 to 2.23 concerning the baseline scenario (1), the new regulation (current policy) scenario (3) and one of the extinction scenarios (5) according to figure 2.18. The selection criteria for picking specific farms were driven by spotting the snapshots of the maximum and final global-system state level of the PI prevalence. For those snapshots we then chose the farm with the highest PI animal count (proved to be a single farm in every case) and drew its infectious states' and total population's evolution. For the case of the extinction scenario 5 where at the final state there is no PI animal in any farm we merely chose two farms from the classes with the least and most (figures 2.22 and 2.23 respectively) animal population as given in the Thuringian input farm size distribution.

As seen in figures 2.19 and 2.20 the only noticeable difference for the two farms that exhibit the largest PI animal prevalence at the times of the global maximum of the PI prevalence and at the end of the simulation respectively is their size. Even that feature then follows the exact same trend just at different values. A direct conclusion is that for the given Thuringian farm size distribution the large farms are those that drive the course of the infection as

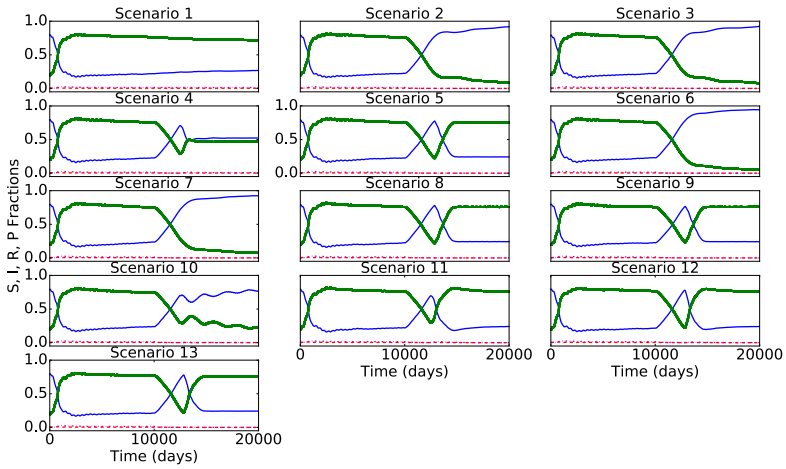

Figure 2.16: Susceptible (solid, blue line), transiently infected (dashed red line), recovered (dotted-dashed, green line) and persistently infected (dashed-dotted, magenta line) fractions of the population for scenarios 1 to 13.

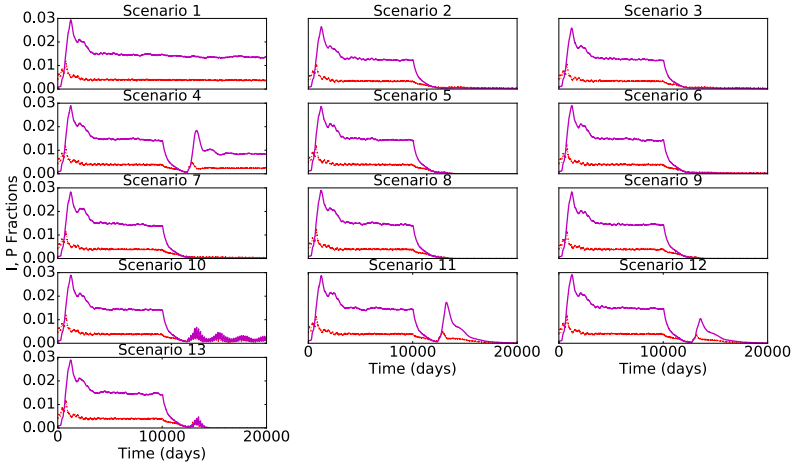

Figure 2.17: Transiently (dashed, red line) and persistently (solid, magenta line) infected population fractions for scenarios 1 to 13. Focus around the TI and PI fractions from figure 2.16.

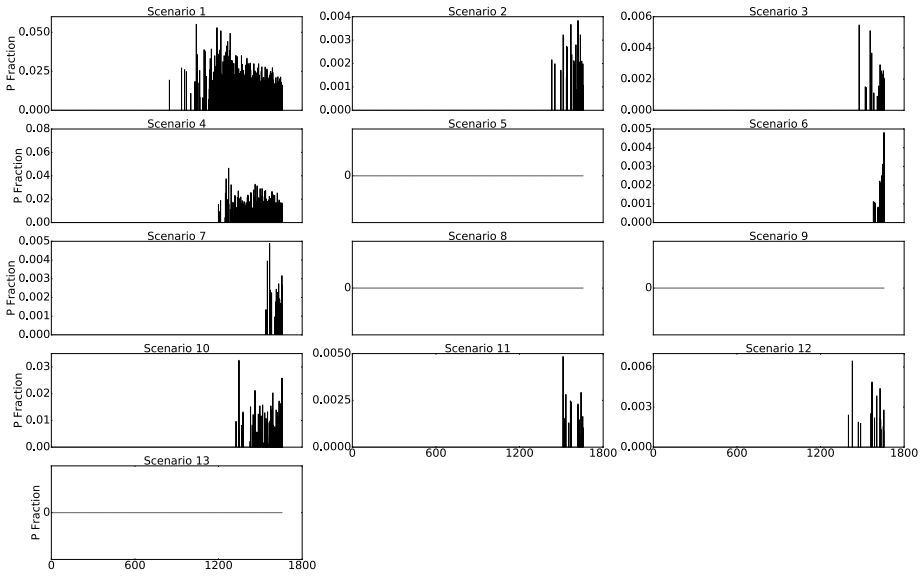

Figure 2.18: P distribution fractions along the system's farms at the final time for scenarios 1 to 13. Eradication is achieved for scenarios 5 (new regulation and vaccination), 8 (vaccination and YCW with a semesterly period), 9 (vaccination and YCW with an annual period) and 13 (new regulation, vaccination and YCW with a semesterly period). See also table 2.23.

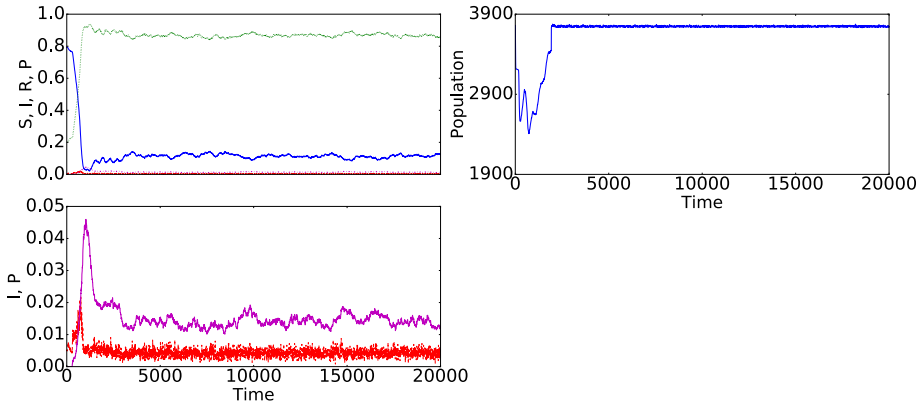

Figure 2.19: Susceptible (solid, blue line), transiently infected (dashed red line), recovered (dotted-dashed, green line) and persistently infected (dashed-dotted, magenta line) fractions of the population for the farm with the maximum PI prevalence at the time of the maximum global PI prevalence in scenario 1-baseline (see upper left plot of figure 2.17) for the upper left plot. To the upper right the farm's population and in the lower row the same time-series as in the upper left plot, but only for the P and I fractions.

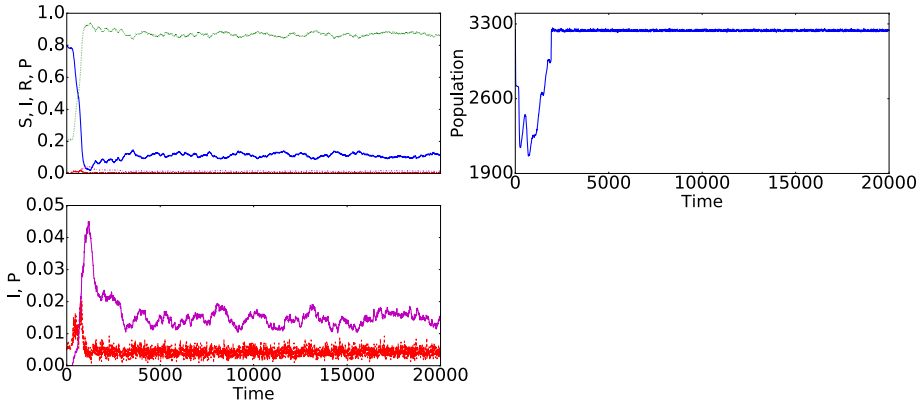

Figure 2.20: Susceptible (solid, blue line), transiently infected (dashed red line), recovered (dotted-dashed, green line) and persistently infected (dashed-dotted, magenta line) fractions of the population for the farm with the maximum PI prevalence at the final time of the simulation in scenario 1-baseline (see upper left plot of figure 2.17) for the upper left plot. To the upper right the farm's population and in the lower row the same time-series as in the upper left plot, but only for the P and I fractions.

they represent a constant supply source of PI animals and, for the baseline scenario, exhibit very similar infectious state dynamics to the corresponding global case in figure 2.16.

In figure 2.21, again the selection criterion at the final state lead to a large farm selection supporting our previous statement of the larger farms driving the course of the infectious states' dynamics. Interestingly though, there is a slight modification (apart from the farm finite-size stochasticity exhibited in the I-P versus time plot) of the farm level dynamics when compared to the system level ones from figure 2.16. When the new regulation's effect takes place the naive population S decreases (with a compensated increase from R) for roughly 1,000 days. This should be attributed to the new regulation's quarantine effect, which inhibits the exit of PI animals from the farm and leads to a chain of infections within the farm. If the quarantine is imposed repeatedly after positive tests for TI animals it then constitutes a plausible explanation for the S-R decrease-increase before the inversion of their trends as the global dynamics of the corresponding plot in figure 2.16 anticipates.

Finally, for the PI extinction scenario 5 of the new regulation augmented by non-targeted vaccination in figures 2.22 and 2.23, as previously mentioned, we selected a small and a large farm to examine their infectious dynamics respectively. Once more, in the case of the small farm dynamics our argument that the small farms do not drive the infection is reinforced, for until the counter measures are applied, with the exception of the initial global infectious transient's time frame, there is no significant contribution to the

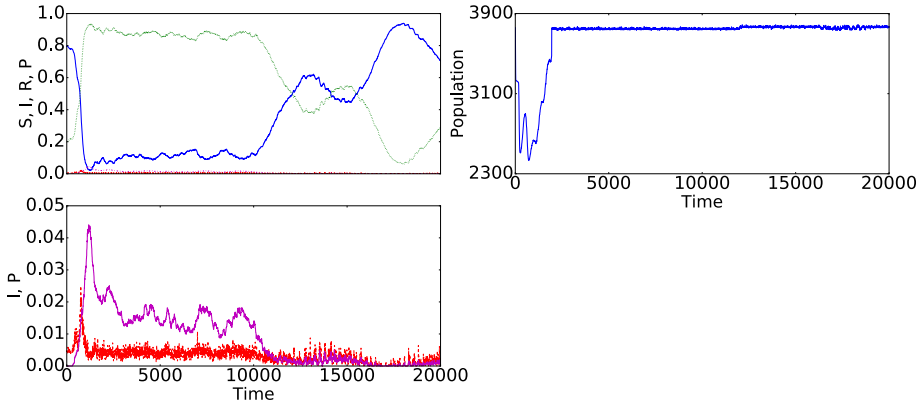

Figure 2.21: Susceptible (solid, blue line), transiently infected (dashed red line), recovered (dotted-dashed, green line) and persistently infected (dashed-dotted, magenta line) fractions of the population for the farm with the maximum PI prevalence at the final time of the simulation in scenario 3-new regulation (see upper right plot of figure 2.17) for the upper left plot. To the upper right the farm's population and in the lower row the same time-series as in the upper left plot, but only for the P and I fractions.

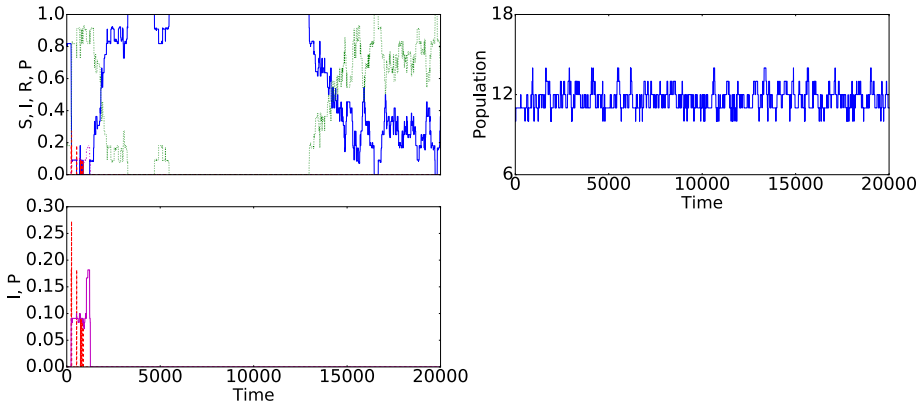

Figure 2.22: Susceptible (solid, blue line), transiently infected (dashed red line), recovered (dotted-dashed, green line) and persistently infected (dashed-dotted, magenta line) fractions of the population for the farm with the maximum PI prevalence at the final time of the simulation in scenario 5-new regulation and vaccination (see upper left plot of figure 2.17) for the upper left plot. To the upper right the farm's population and in the lower row the same time-series as in the upper left plot, but only for the P and I fractions. A specimen of the smallest farm class in the simulation.

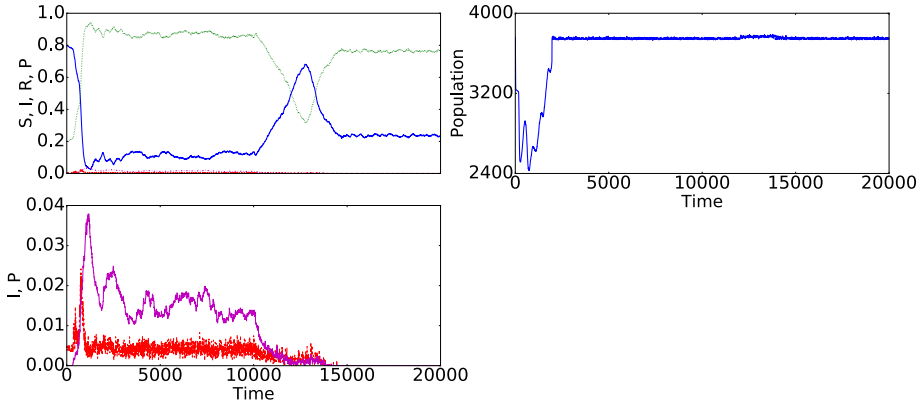

Figure 2.23: Susceptible (solid, blue line), transiently infected (dashed red line), recovered (dotted-dashed, green line) and persistently infected (dashed-dotted, magenta line) fractions of the population for the farm with the maximum PI prevalence at the final time of the simulation in scenario 5-new regulation and vaccination (see upper left plot of figure 2.17) for the upper left plot. To the upper right the farm's population and in the lower row the same time-series as in the upper left plot, but only for the P and I fractions. The biggest farm class in the simulation with its only farm.

global dynamics as exhibited in the corresponding plot of figure 2.16. The latter dynamics are closely followed by those of the large farm of figure 2.23.

To conclude this section, we saw that scenarios 5, 8, 9 and 13 drove the system to a PI eradication indicating that the bio-security measure of surveillance is indispensable to guarantee the success of any mitigation strategy. Additionally, the evidence leads to the conclusion that a critical mass of immunised animals (herd immunity) needs to be achieved before the system is driven to a PI-free state. In the framework so far investigated the herd immunity has been achieved by augmenting the surveillance scheme with vaccination.

2.4.2 Network Scaling

So far all the simulations have been in regard to the cattle farm list size of the state of Thuringia, i.e. around 4,000 farms corresponding to 340,000 animals, out of which we assumed that only 1,657 with a count of 333,350 animals participate regularly in the trading network. Nevertheless, we cannot expect the network structure (heterogeneities) of Thuringia to be representative to that of Germany. Both the connectivity (which farms perform the animal movements) and the weight (how many animals move) distributions are expected to differ substantially. To give an example Thuringia has a much smaller cattle population and less farms than those in Bavaria, which

is still a subnetwork of Germany. Conversely, Thuringia's farms are huge, which is not something typical in Bavaria [Gethmann, 2018].

Ideally, since Thuringia is a subnetwork of Germany, we would like to give as input to the simulation the cattle farm list of Germany, which accounts for around 156,000 farms counting up to more than 12 million animals (see figures 2.5 and 2.6). However, since the market module uses queue containers to match the demands and offers of potential trading partners holding all the information of the simulation until they are met, the relevant cattle movement requirements in memory grow tremendously [Skiena, 1998]. Presently the largest simulations we have been able to run have been with less than 12,000 farms accounting for roughly 1 million animals.

Bearing all the above in mind, we normalised the farm distribution of Germany with regard to the farms and scaled it up in increments of thousands for otherwise identical settings of the simulation for scenario 1 (baseline). The intermediate size (4,000 farms) counted approximately the given of Thuringia both in farms and animals that we used in the simulations. The results for the global fraction of the persistently infected animals at the end of the simulation and at maximum with requirements up to 16 GB in memory can be seen in table 2.24. The larger the system size the more the global PI fraction tends to stabilise to a precision of up to four significant digits. The interpretation is that since the initial conditions, the infection, breeding and network dynamics remain the same, as expected, the prevalence of the persistently infected population fraction at the final state remains nearly constant along the farm increments, provided that the farm number does not become too small. This would constitute a justification for the usage of a scaled down farm size distribution from Germany to the size, in animal population, of Thuringia in the model to draw conclusions for Germany. We could therefore dispense with the non-representative heterogeneities of Thuringia and use those of Germany for the input farm size distribution to draw conclusions for the whole country, provided that we scaled down the farm count of Germany to that of Thuringia.

However, we do need to note that as the system becomes smaller (i.e. by scaling down the farm count of the German farm size distribution), finite-size effects (of the farms) come into play. Thus, although all the above mentioned mechanisms remain the same, due to the dominance of small farms and their sparsity, the infectious and population dynamics are expected to be subject to the fluctuations of the small farms (see e.g. figure 2.22).

2.5 Summary and Outlook

In this chapter we justified on biological, data, policy and agricultural grounds a stochastic, event-driven agent-based model to emulate the current situation of BVD in Germany via within-farm contact mechanisms and through

PI Fraction	Farm No
0.0109	2,000
0.0072	4,000
0.0072	6,000

Table 2.24: PI global fraction at the final state for different values of the total farm count in the system.

animal movement contacts. We furthermore provided a thorough description following a specific protocol (ODD), which included a sensitivity analysis of key parameters identified from expert opinion, the literature and the model's specifics. In addition, we explored a number of mitigation strategies of interest to a cost-benefit analysis for the FLI. The results have demonstrated that the removal of PI animals through testing strategies combined with trading restrictions are more effective than vaccination. Vaccination nevertheless remains an important additional component of any preventing strategy aiming towards the eradication of the massively infectious PI animals, as a means of achieving herd immunity.

As future work, a sensitivity analysis variating the margins of the different pregnancy stages' outcomes for a wide possibility of PI vertical transmissions could aid to further compare with the results of [Ezanno et al., 2007]. Moreover, the hard-coded distribution margins for the time elapsed between a positive test and the animal's possible removal should be further investigated, especially towards the limit of coincidence of the two events as a policy maker result of interest. In addition, as already mentioned in the network scaling section 2.4.2 we would expect finite-size effects to come into play below a certain threshold of scaling down the input farm size distribution of Germany, simply because of the depletion of large farm classes and the dominance of the small ones in the process. Therefore, the limitations of this methodology remain to be explored. In addition, as a next step the code of the simulation should be extended so as to account for the

As far as quarantine strategies are concerned, heuristic approaches such as of [Waniek et al., 2018] could prove useful to explore the possibilities of rewiring contacts meeting certain criteria (e.g. the DICE method standing for 'disconnect internally, connect externally') while keeping certain parts of the network functional, so as to be less obtrusive to the underlying economy. Along the same lines, introducing a measure of robustness to the farm manager and market as in [Schneider et al., 2011] to channel trades and restrictions could quantitatively keep systemically key nodes functional while still providing intervention trade restrictions. Furthermore, the connection strategy of each node (behaviour of farmers) can be modelled in one of the various scoring ways (node ranking, activity, loyalty and differentiation crite-

ria) [Albrecht and Stone, 2017; Gates and Woolhouse, 2015; Gross and Blasius, 2008; Hébert-Dufresne et al., 2016; Shoham and Leyton-Brown, 2008; Wang et al., 2016], which could lead to extensions of the model encompassing these connectivity aspects as well.

Lastly, the code could be adapted to a distributed scheme similar to [Parker, 2007] so as to accommodate the memory requirements of large farm size distributions such as that of Bavaria or of all of Germany. Thus the downscaling methodology, to which we had to base our results and which in turns entails a certain breakdown limit, could be avoided altogether.

CHAPTER 3

BVD Mean Field Model

In this chapter we intend to formulate a mean field model (i.e. having no spatial structure) for the spread of BVD in an animal population. With this deterministic description we aim to compare the infectious dynamics of the agent-based model presented in the previous chapter. Our approach has been meticulous so as to introduce novel aspects, compared to existing models which one could employ to address the same problem [Hethcote, 1994, 2000]. Notwithstanding, the model we will present may provide a baseline model for an analytical approach to mitigation strategies [Pereira and Young, 2015].

We will first logically build on the standard *Susceptible-Infected-Recovered* (SIR) model with demography to include the PI animal production through the effect of *delays* following the biological description of section 2.1.1. After a short treatment on the formulated system's positivity for every time, we will make some basic numerical investigations of the system's stability around its disease-free equilibrium and follow a methodology to estimate the epidemiologically fundamental quantity of the *basic reproduction number*. Finally, we will attempt to interpret our findings up to that point under the scope of the system's numerical integration.

3.1 Introduction

To compare the agent-based model of chapter 2 with an analytical approach we resort to standard work done on deterministic models with *demographics* (i.e. birth-death processes within a population) and spatial heterogeneities within a *metapopulation* context [Allen et al., 2008; Brauer and Castillo-Chavez, 2012; Hethcote, 2000; Murray, 2002; Rohani, 2008]. The former

characteristic refers to a distinction of the population in compartments with mass-action dynamics (anticipated in the reaction scheme (3.4) for the system in question). This means distinguishing different infectious groups within a population and assuming that each group can either interact with the other in pairs (where applicable) to switch to another group or spontaneously reach another one, and in both cases following an exponentially distributed waiting time distribution (Poissonian process) [van Kampen, 2003]. The latter feature (metapopulation) consists of 'populations within populations' exhibiting heterogeneities often termed *patches* in the relevant literature [Allen et al., 2008; Brauer and Castillo-Chavez, 2012]. In particular, the most often employed method to model a metapopulation model is through a network representation where each node contains a portion of the global population with, in general, all the available compartments represented in it. Under this scope the whole network can act as a reaction-diffusion (see [Murray, 2002]) system (reactions concerning the node dynamics and diffusion the migration through the network's connectivity) whose epidemic spread and infectious invasion threshold can be analytically calculated as in [Colizza and Vespignani, 2007; Colizza et al., 2007]. Having obtained this baseline we can then add stochasticity to the infection and the breeding dynamics to improve the level of comparison with the agent-based model [Allen et al., 2008]. Within the scope of this chapter however we shall restrict ourselves to establishing the reaction and demographic segment of the aforementioned analytical programme. That is we shall assume a single population with *mean field theory* contacts (i.e. where the population is assumed to be well-mixed and homogeneous and thus all contacts are equally probable rendering any spatial structure meaningless) and demographics following the German cattle agricultural system's structure and the BVD dynamics' description of chapter 2.

The approach presented in the following is not the first to attempt a deterministic description of BVD. Previous work employed a multi-compartmental system to describe the various PI production pathways through different pregnancy stages [Cherry et al., 1998] and an attempt to calculate fundamental epidemiological quantities (the *basic reproduction number* as shall be defined in section 3.5) [Diekmann et al., 2009, 2013]. It is nevertheless the first to our knowledge which attempts to take into account comprehensively the vertical transmission (i.e. by breeding) dynamics of BVD by incorporating an additional time-scale to that of infections in the system, namely the maturity and birth cycle one. It also avoids the difficulties of high dimensional compartmental systems, such as in [Cherry et al., 1998], by restricting the number of compartments to four, which fundamentally, fully describe the infectious states of BVD following its biological description [Gethmann, 2018; Lanyon et al., 2014; Lindberg, 2003].

3.2 System Formulation

We start with a primitive dynamical system (i.e. whose dependent variables are time-dependent), which is the so-called SIR model with demography and is well established in the literature in [Diekmann et al., 2013; Murray, 2002; Rohani, 2008]

$$\begin{aligned} \dot{S}(t) &= \mu - \Lambda(t)S(t) - \mu S(t) \\ \dot{I}(t) &= \Lambda(t)S(t) - \gamma I(t) - \mu I(t) \\ \dot{R}(t) &= \gamma I(t) - \mu R(t), \end{aligned} \tag{3.1}$$

with S, I and R being the three compartments in which the population has been divided, standing for *susceptible, infected* and *recovered* respectively, $\mu > 0$ a constant rate for births and non disease related deaths (whose inverse is the average lifetime of the population's individuals), $\Lambda(t) = \beta_I I(t)$ the *force of infection* with β_I the infectious transmission rate and γ the rate of recovery (inverse to the average recovery period). Removing the birth-death terms μ from system (3.1) we are left with the standard SIR model established in the seminal work of [Kermack and McKendrick, 1927] and which constitutes the starting point of every well-mixed, homogeneous epidemic model nowadays [Allen et al., 2008; Brauer and Castillo-Chavez, 2012; Hethcote, 2000; Murray, 2002; Rohani, 2008].

System (3.1) however does not capture even crudely the vertical dynamics of BVD described in chapter 2 due at least to births taking place in compartments other than S in reality, and due to the persistently infectious compartment, which is absent from it. As a first attempt to rectify this issue we can introduce an additional persistently infectious compartment P, modify the force of infection as $\Lambda(t) = \beta_I I(t) + \beta_P P(t)$ to take the infectious contributions of the infectious P compartment into account with an infectious transmission rate $\beta_P \gg \beta_I > 0$, and distribute the constant birth term μ from the S compartment of system (3.1) to the S, R and P compartments. However, in this manner we are going to lose the physically necessary disease-free equilibrium point as we can easily see in the form (3.2).

$$\begin{aligned} \dot{S}(t) &= \frac{\mu}{3} - \Lambda(t)S(t) - \mu S(t) \\ \dot{I}(t) &= \Lambda(t)S(t) - \gamma I(t) - \mu I(t) \\ \dot{R}(t) &= \frac{\mu}{3} + \gamma I(t) - \mu R(t) \\ \dot{P}(t) &= \frac{\mu}{3} - \mu P(t) \end{aligned} \tag{3.2}$$

Thus we need to formulate a system starting from (3.1) with the minimal requirements being the modification of the birth and death flows and an extra persistently infectious compartment to start approaching the dynamics described in chapter 2 in a single farm with a well-mixed, homogeneous population (mean field dynamics). To that end we rewrite system (3.3) as

$$\begin{aligned}
\dot{S}(t) &= -\Lambda(t)S(t) + c_S(t) \\
\dot{I}(t) &= \Lambda(t)S(t) - \gamma I(t) + c_I(t) \\
\dot{R}(t) &= \gamma I(t) + c_R(t) \\
\dot{P}(t) &= c_P(t),
\end{aligned} \tag{3.3}$$

which takes into account the persistently infectious animals with compartment P, has as the force of infection the previously modified version $\Lambda(t) = \beta_I I(t) + \beta_P P(t)$ and its birth-death terms $c_i(t)$, i=S, I, R, P are time-dependent. What remains to be done to reach our goal of retrieving a system for BVD with demographics is to determine the $c_i(t)$ terms.

We first start by modelling the BVD transmission and the cattle breeding dynamics that we established in chapter 2 in a horizontal and vertical (i.e. contact and birth based respectively) transmission scheme (3.4) and by illustrating the vertical transmissions in time in figure 3.1. In figure 3.1 we define two time-scales associated with breeding and vertical transmissions; one for the maturity of the animal, which we set as $\mu > 0$ and one for the gestation cycle of the animal, which we set to be $\tau > 0$. Breaking the gestation period τ down into two successive periods τ_1 and τ_2 with $\tau = \tau_1 + \tau_2$ and $\tau_1 < \tau_2$ we can relate the early critical pregnancy period for a PI offspring to enter the P compartment in case of infection of the mother cow with the τ_1 time window. We continue by relating the τ_2 period to correspond to the latter pregnancy period where the offspring undergoes the disease with its mother as an embryo with a developed immune system and is therefore born immune in the R compartment. Thus we have two time-scales in the system: one for the infectious dynamics (in an SIR fashion) and one for the demographics as exhibited in figure 3.1. The time-scale referring to the vertical infections (i.e. those coming from breeding) follows a similar formulation to systems found in [Blyuss and Kyrychko, 2010; Hethcote and van den Driessche, 1995; Sipahi et al., 2007].

We neglect abortions and all other by products of pregnancy considered in the agent-based model and which follow observations, as well as the resting time between cow pregnancies. Furthermore, as the BVD agent-based model was focused on cows as the main proxies of BVD rather than both sexes of cattle, we take only cows into account in the present modelling and thus the dynamics that take place concern only farms with a female population, an approximation which predominantes the structure of a dairy farm.

$$\left\{\begin{array}{ll} S+I & \xrightarrow{\beta_I} I+I \\ & \xrightarrow{\gamma} R+R \\ S+P & \xrightarrow{\beta_P} I+P \\ & \xrightarrow{\gamma} R+P \\ \underbrace{R}_{\text{calf}} & \xrightarrow{\mu} \underbrace{S}_{\text{heifer}} \end{array}\right\} \left\{\begin{array}{ll} S & \xrightarrow{k,\tau} \underbrace{S}_{\text{mother}}+\underbrace{S}_{\text{calf}} \\ \underbrace{I}_{\text{at pregnancy}} & \xrightarrow{k,\gamma,\tau_1,\tau_2,\tau} \left\{\begin{array}{l} \underbrace{R}_{\text{mother}}+\underbrace{R}_{\text{calf}} \\ \underbrace{R}_{\text{mother}}+\underbrace{P}_{\text{calf}} \end{array}\right\} \\ R & \xrightarrow{k,\tau} \underbrace{R}_{\text{mother}}+\underbrace{R}_{\text{calf}} \\ P & \xrightarrow{k,\tau} \underbrace{P}_{\text{mother}}+\underbrace{P}_{\text{calf}} \end{array}\right\} \tag{3.4}$$

Scheme (3.4) exhibits the dynamics that we seek from an individual, reaction perspective, both for horizontal, contact and spontaneous (left block), and for vertical, generative reactions (right block). On the left block we have the standard SIR dynamics, where infections of S individuals take place with a β_I and a β_P infectious rate, depending on the contact conditions with the I or P ones respectively. In turns, infectious individuals I enter the recovered R state spontaneously with a rate γ, whose inverse is the average waiting time in the I state (i.e. the average recovery period). Lastly, in regard to newly arrived individuals in the R state from an R parent (anticipated in the right block), they spontaneously move to the S state after a μ (maturity) waiting time (from now on we shall refer to the maturity period with μ and forget its usage as the birth rate as we saw in systems (3.1) and (3.2)). On the right block we see the vertical, birth dynamics taking place with a rate k. Susceptible individuals throughout a gestation waiting time τ give birth to susceptible ones. Individuals who were infected at some point during the gestation waiting time $\tau = \tau_1 + \tau_2$ recover with a rate γ and produce new individuals whose state depends on the period of τ throughout which their parent was infected. If the parent was infected during the τ_1 period, then the offspring will be in the P state, while if the parent was infected during the τ_2 period, the offspring will be permanently in the R state (see also figure 3.1). Individuals who were in the recovered state R during the gestation time τ produce a temporarily R individual. Finally, individuals who were in the P state during the gestation period τ produce a P offspring.

Following the reasoning of figure 3.1 one way to account for single births at a randomly picked time t is to integrate all the contributor animals over their entire pregnancy period and average the integral with that period. Therefore, for the S compartment such birth contributions would be written as $\frac{1}{\tau}\int_{t-\mu-\tau}^{t-\mu}[S(\theta)+R(\theta)]d\theta$ accounting for the susceptible arrivals from both susceptible and immune cows (through the maturity period μ for the latter case), for the R compartment as $\frac{\tau_2}{\tau^2}\int_{t-\mu-\tau}^{t-\mu} I(\theta)d\theta$ accounting for arrivals from the cows getting infected in the later part of their pregnancy τ_2, as the

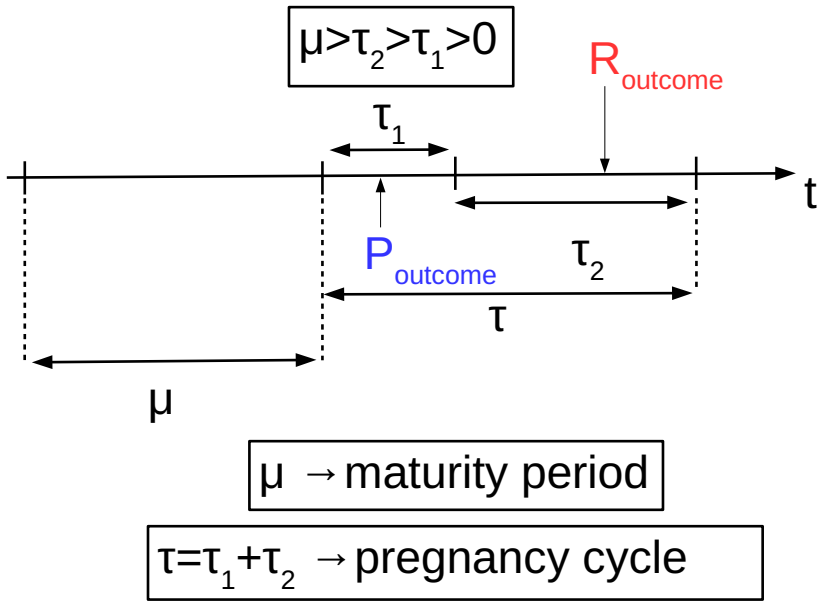

Figure 3.1: Maturity and reproduction cycle of a female animal. With blue we denote the persistently infected to-be-born calves, if the mother is infected in its first stages of the pregnancy (τ_1) and with red the permanently immune to-be-born calves if the mother is infected in the later stages of its pregnancy (τ_2).

τ_2/τ factor implies, and for the P compartment as $\frac{\tau_1}{\tau^2}\int_{t-\mu-\tau}^{t-\mu} I(\theta)+P(\theta)d\theta$ accounting for arrivals from the cows getting infected in the earlier part of their pregnancy τ_1, as the τ_1/τ factor implies, and for the PI cows which reproduce themselves.

We still however need to determine the outflow from the compartments (death). Since we assumed in the BVD agent-based model that the farm attempts to preserve its population constant through trades and we are not going to consider any spatial structure in the analytical model, we define a global control function $D(t)$ such that the total population of the system N is always preserved $N = S(t)+I(t)+R(t)+P(t)$, while retaining the feature of the primitive system (3.1) that the death term should be proportional to the compartment in question.

With all the above in mind system (3.3) becomes

$$\begin{aligned}
\dot{S}(t) &= -\Lambda(t)S(t) + \frac{k}{\tau}\int_{t-\mu-\tau}^{t-\mu}[S(\theta)+R(\theta)]d\theta - D(t)S(t)\\
\dot{I}(t) &= \Lambda(t)S(t) - \gamma I(t) - D(t)I(t)\\
\dot{R}(t) &= \gamma I(t) + \frac{\tau_2}{\tau^2}k\int_{t-\mu-\tau}^{t-\mu} I(\theta)d\theta - D(t)R(t)\\
\dot{P}(t) &= k\int_{t-\mu-\tau}^{t-\mu}\left[\frac{\tau_1}{\tau^2}I(\theta)+P(\theta)\right]d\theta - D(t)P(t)
\end{aligned} \tag{3.5}$$

where $D(t)/k = \frac{\int_{t-\mu-\tau}^{t-\mu} S(\theta)+I(\theta)+R(\theta)d\theta}{\tau N(t)}$ the total births such that $\dot{N}(t) = 0 \quad \forall t$, with $N(t) = \text{const.} = N = S(t)+I(t)+R(t)+P(t)$ for some constant, non disease related birth-death rate $k > 0$. Note that this preservation quality enables us (by knowing the population constant N) to reduce the system's four dependent variables to three. Further, $\mu > 0$ is a constant denoting the average time it takes for calves to reach maturity, τ is the total average gestation period, and $\tau_1 > 0$ and $\tau_2 > 0$ ($\tau = \tau_1 + \tau_2$) are two subperiods of the gestation periods, which correspond to the typically P and R outcomes for the embryo calf ($\tau_1 < \tau_2$) as previously mentioned in scheme (3.4) and following the logic of figure 3.1. Note that the maternal antibody effect featured in the agent-based model of chapter 2 is taken into account by the income of the $R(\theta)$ term in the S compartment with the eventual waning of the protective effect coming through the maturity time shift μ. This is demonstrated as well in the right block of scheme (3.4).

By examining system's (3.5) equilibrium points we quickly realise that there is a trivial endemic equilibrium point where all the population shifts to the P compartment. Although strictly speaking on biological grounds [Gethmann, 2018; Lanyon et al., 2014; Lindberg, 2003] the reproduction of PI animals is non-negligible and possibly in an artificial environment set

to prove the concept an 'all PI' population would be possible, in practice the reported PI population is always a small minority of the total cattle population [Pinior et al., 2017; Ståhl and Alenius, 2012]. Therefore, to make the analytical approach even more biologically plausible altogether we make the assumption that $I(\theta) \gg P(\theta)$ in the integral of the $\dot{P}$ equation of (3.5), so as to make an endemic 'all PI' equilibrium impossible, and the system takes the final form

$$\begin{aligned}
\dot{S}(t) &= -\Lambda(t)S(t) + \frac{k}{\tau}\int_{t-\mu-\tau}^{t-\mu}[S(\theta)+R(\theta)]d\theta - D(t)S(t) \\
\dot{I}(t) &= \Lambda(t)S(t) - \gamma I(t) - D(t)I(t) \\
\dot{R}(t) &= \gamma I(t) + \frac{\tau_2}{\tau^2}k\int_{t-\mu-\tau}^{t-\mu} I(\theta)d\theta - D(t)R(t) \\
\dot{P}(t) &= k\int_{t-\mu-\tau}^{t-\mu}\frac{\tau_1}{\tau^2}I(\theta)d\theta - D(t)P(t)
\end{aligned} \tag{3.6}$$

which is an integro-differential, or a *retarded functional differential*, and autonomous system (i.e. which is invariant to time translations) [Diekmann et al., 1995], defined and continuous in the space $\{[-\mu-\tau, -\mu], \mathbb{R}^+\}$.

In the limit where the maturity and the pregnancy periods vanish, i.e. $\tau \to 0$ and $\mu \to 0$ we retrieve the system (3.7), which is very close to the standard SIR without demography and has an extra constant contribution at its force of infection $\Lambda(t) = \beta_I I(t) + P_0$ ($P_0 = \beta_P P$, since the P compartment remains constant), which takes us back to considering only one time-scale, the one of the horizontal dynamics (i.e. where the infection dynamics take place). The P compartment is uncoupled from the rest of the system and, being constant, does not play a role in the system dynamics other than translating the force of infection by a constant.

$$\begin{cases}
\dot{S}(t) = -\Lambda(t)S(t) \\
\dot{I}(t) = \Lambda(t)S(t) - \gamma I(t) \\
\dot{R}(t) = \gamma I(t) \\
\dot{P}(t) = 0
\end{cases} \tag{3.7}$$

3.3 Positivity of Solutions

Before we proceed to the analysis of system (3.6) and make some brief references to the relevant theory, we present a proof using standard calculus about the sign of its solutions as it evolves in time. This will give physical credibility to the system as negative solutions are meaningless. Regarding that our

analysis will be numerical in the following sections, this result constitutes the only mathematically rigorous one in this chapter.

Assuming that the history functions of $S(t)$, $I(t)$, $R(t)$ and $P(t)$ are all simultaneously non-negative and their sum positive and equal to $N \in \{N \in \mathbb{R} : N > 0\}$ we can prove that the solutions of the equations of system (3.6) are as well simultaneously non-negative for $t > 0$ and that their sum is positive. Symbolically:

$$S(t), \quad I(t), \quad R(t), \quad P(t) > 0 \text{ for } t \in [-\mu - \tau, -\mu) \tag{3.8}$$

where the $[-\mu - \tau, -\mu]$ interval refers to the first pregnancies of the system. Additionally, we assume that the summation of the state variables $S(t)$, $I(t)$, R(t) and $P(t)$ is constant for every given, positive time t. Symbolically

$$S(t) + I(t) + R(t) + P(t) = N > 0 \text{ for } t \in [-\mu - \tau, -\mu) \tag{3.9}$$

where $N \in \{N \in \mathbb{R} : N > 0\}$.

Since the population is a constant N, we need to prove that at the boundaries of $[0, N]^4$ the vector field is directed inwards.

We first normalise the system without loss of generality, i.e. $S^\dagger \equiv \frac{S}{N}$, $I^\dagger \equiv \frac{I}{N}$, $R^\dagger \equiv \frac{R}{N}$ and $P^\dagger \equiv \frac{P}{N}$ for ease and will hence refer to the normalised compartments $S^\dagger, I^\dagger, R^\dagger$ and $P^\dagger$ as S, I, R and P. Therefore the solutions of the system will lie in the interval $[0, 1]$ separately and will all add up to unity $1 = S(t) + I(t) + R(t) + P(t)$.

We start by the $\dot{S}(t)$ equation. Assuming that we are exactly at the left boundary of $[0, 1]$ at the beginning of time (i.e. $S(t) = 0$) we have to prove that $\forall t > 0$, $\dot{S}(t) \,|_{S(t)=0} > 0$. Indeed $\dot{S}(t) \,|_{S(t)=0} = \int_{t-\mu-\tau}^{t-\mu} [S(\theta) + R(\theta)] d\theta > 0$, due to our assumption about the history functions (3.8), which means that the $S(t)$ function monotonically increases with time from its zero value.

The proof continues by examining first the sign of the $\dot{P}(t) \,|_{P(t)=0}$ and then of the $\dot{I}(t) \,|_{I(t)=0}$ and $\dot{R}(t) \,|_{R(t)=0}$ equations in any order. We find that they all have to be positive due to the history functions' assumption (3.8) and the previously established positive signs of their counterparts for $t > 0$. Thus $S(t)$, $I(t)$, $R(t)$ and $P(t)$ are all monotonically increasing with time from their zero values.

We work similarly for the right boundary of $[0, 1]$. In this case $\dot{S}(t) \,|_{S(t)=1} = \int_{t-\mu-\tau}^{t-\mu} [S(\theta) + R(\theta)] d\theta - 1 \leq 0$, again due to the assumptions (3.8) and (3.9) about the history functions. Hence $S(t)$ monotonically decreases with time from unity. Similar argumentation follows to prove that $\dot{I}(t) \,|_{I(t)=1} \leq 0$, $\dot{R}(t) \,|_{R(t)=1} \leq 0$ and $\dot{P}(t) \,|_{P(t)=1} \leq 0$ leading to the conclusion that $I(t)$, $R(t)$ and $P(t)$ all monotonically decrease with time from unity and the vector field points inwards $[0, 1]^4$.

Finally, from the assumption (3.9) and what was just proven for $t > 0$ it follows that

$$S(t) + I(t) + R(t) + P(t) = 1 > 0 \text{ for } t > 0 \tag{3.10}$$

where the result also applies to any $N \in \{N \in \mathbb{R} : N > 0\}$.
Q.E.D.

3.4 Stability Analysis

3.4.1 Rudiments of Delay Differential Equations and Equilibria

In many aspects of direct applicable interest the theory of *ordinary differential equation* (ODE) systems is extended to *delay differential equation* (DDE) systems with some minimal additional requirements [Diekmann et al., 1995; Hale, 1977]. We shall attempt to only describe some points which make the definition of system (3.6) more meaningful and set the stage for the results to be presented.

Most strikingly the difference between ODEs and DDEs appears in the domain (vector space) of definition. Whereas an ODE system is usually defined on a real interval mapped to the real or the complex domain (e.g. $[a, b] \to \mathbb{R}$ for a single equation, which constitutes a finite dimensional vector space) a DDE system has to take into account its delays as well. For instance, for a single-delay DDE with τ as the delay, the domain over which it is defined takes the form $\{[-\tau, 0], \mathbb{R}\} \to \mathbb{R}$ making its vector space infinite dimensional. Moreover and in terms of definition again, any kind of ODE system depends only on *state variables* and not on retarded ones as DDE systems. In other words, in the example of the single-delay DDE that we previously assumed the system is dependent on $t - \tau$ apart from t as independent variables. This intrinsic difference also sets DDE systems apart from ODE ones in that, although both are defined continuously over a certain domain, if the delay τ lies within that domain there will be a discontinuity for the DDE system which will keep following it periodically with a period of exactly that delay τ. This is called *discontinuity propagation* in the DDE theory and is the mechanism that can induce some temporary or permanent periodicity to the system in question [Erneux, 2009]. In the case of system (3.6) we identify this period as the span of the interval $[-\mu - \tau, -\mu]$, that is τ.

However, when treating a differential system as (3.6) at its equilibrium (i.e. when it has become time invariant) both ODE and DDE systems are subject to the same treatment. Furthermore, as far as stability is concerned, DDE systems's behaviour around an equilibrium point is determined by their *eigenvalue spectrum* and the theory pertaining this stability is a natural extension of the ODE theory taking into account the retarded variables and the infinite dimension of the vector space on which the DDE system is defined [Gu et al., 2003].

As far as the equilibria of the system (3.6) at hand are concerned, it is trivial to verify that it has three out of which only one is physically acceptable (disease-free), and two rejected due to extinction and negative population values (3.11). In addition, as we shall see in what is to come, the numerics indicate the existence of at least one equilibrium point as well. Its determination though would have come from the solution of a nonlinear algebraic system, whose form does not seem to be solvable to the extent of our knowledge. What can be done to approximate the (or the more than one) location of the endemic equilibrium in the phase space is to provide an initial position $(S_\infty^0, I_\infty^0, R_\infty^0, P_\infty^0)$ and then use a root finding method, such as *Newton's method* [Burden and Faires, 2005], to approximate the final solution $(S_\infty, I_\infty, R_\infty, P_\infty) = (0, 0, 0, 0)$ of (3.6) at the steady state. We list all the equilibria of (3.6) in (3.11). See also [Kuznetsov, 1995] for equilibria locating methods based on their known stability.

$$\begin{aligned}
&(S_\infty, I_\infty, R_\infty, P_\infty)_1 = (0, 0, 0, 0) \quad \text{(extinction)} \\
&(S_\infty, I_\infty, R_\infty, P_\infty)_2 = (N, 0, 0, 0) \quad \text{(disease-free)} \\
&(S_\infty, I_\infty, R_\infty, P_\infty)_3 = (S, 0, -S, 0) \quad \text{(non-physical)} \\
&(S_\infty, I_\infty, R_\infty, P_\infty)_4 = (g_S, g_I, g_R, g_P) \quad \text{(endemic)},
\end{aligned} \tag{3.11}$$

for some possibly well-behaved (i.e. differentiable) functions $g_i(N, \beta_I, \beta_P, \gamma, k, \tau, \tau_1, \tau_2)$ for $i = S, I, R$ and P separately.

3.4.2 Linearisation Around Equilibria

Since we could not determine the endemic equilibrium, the only physically acceptable equilibrium on which we can focus any linearisation and stability analysis will be the disease-free one.

The most straightforward way to linearise (3.6) is equation-wise, keeping terms of only first order. Furthermore, we approximate the ratio $\frac{1}{x_0+x}$ up to its first order term by expanding it by Taylor around $x = 0$. Thus, $\boxed{\frac{1}{x_0 + x} \approx \frac{1}{x_0} - \frac{x}{x_0^2}}$. We moreover denote all the linear variables with a hat symbol, i.e. $\hat{X} = \hat{S}, \hat{I}, \hat{R}, \hat{P}, \hat{N} = \hat{S} + \hat{I} + \hat{R} + \hat{P}$ and $N_0 = S_0 + I_0 + R_0 + P_0$. This results in

$$
\begin{aligned}
\dot{\hat{S}}(t) =& -\left[\beta_I I_0 S_0 + \beta_P P_0 S_0 + \frac{S_0}{N_0}(S_0 + I_0 + R_0) - S_0 - R_0\right] \\
&- \left(\beta_P P_0 + \beta_I I_0 + \frac{S_0 + I_0 + R_0}{N_0}\right)\hat{S}(t) - \beta_I S_0 \hat{I}(t) \\
&- \beta_P S_0 \hat{P}(t) + \frac{S_0 + I_0 + R_0}{N_0^2} S_0 \hat{N}(t) \\
&+ \frac{k}{\tau}\int_{t-\mu-\tau}^{t-\mu}\left\{\hat{S}(\theta) + \hat{R}(\theta) - \frac{S_0}{N_0}\left[\hat{S}(\theta) + \hat{I}(\theta) + \hat{R}(\theta)\right]\right\} d\theta \\
\dot{\hat{I}}(t) =& \left[\beta_I I_0 S_0 + \beta_P P_0 S_0 - \gamma I_0 - \frac{I_0}{N_0}(S_0 + I_0 + R_0)\right] \\
&+ \left(\beta_P P_0 + \beta_I I_0\right)\hat{S}(t) + \left(\beta_I S_0 - \gamma - \frac{S_0 + I_0 + R_0}{N_0}\right)\hat{I}(t) \\
&+ \beta_P S_0 \hat{P}(t) - \frac{S_0 + I_0 + R_0}{N_0^2} I_0 \hat{N}(t) \\
&- \frac{I_0 k}{\tau N_0}\int_{t-\mu-\tau}^{t-\mu}\left[\hat{S}(\theta) + \hat{I}(\theta) + \hat{R}(\theta)\right] d\theta \\
\dot{\hat{R}}(t) =& \left[\gamma I_0 + \frac{\tau_2}{\tau} I_0 - \frac{R_0}{N_0}(S_0 + I_0 + R_0)\right] + \gamma \hat{I}(t) - \frac{S_0 + I_0 + R_0}{N_0}\hat{R}(t) \\
&- \frac{S_0 + I_0 + R_0}{N_0^2} R_0 \hat{N}(t) + k\int_{t-\mu-\tau}^{t-\mu}\left\{\frac{\tau_2}{\tau^2}\hat{I}(\theta) - \frac{R_0}{\tau N_0}\left(\hat{S}(\theta) + \hat{I}(\theta) + \hat{R}(\theta)\right)\right\} d\theta \\
\dot{\hat{P}}(t) =& \left[\frac{\tau_1}{\tau} I_0 - \frac{P_0}{N_0}(S_0 + I_0 + R_0)\right] - \frac{S_0 + I_0 + R_0}{N_0}\hat{P}(t) - \frac{S_0 + I_0 + R_0}{N_0^2} P_0 \hat{N}(t) \\
&+ k\int_{t-\mu-\tau}^{t-\mu}\frac{\tau_1}{\tau^2}\hat{I}(\theta) - \frac{P_0}{\tau N_0}\left(\hat{S}(\theta) + \hat{I}(\theta) + \hat{R}(\theta)\right) d\theta
\end{aligned}
\tag{3.12}
$$

Substituting the values of the equilibrium disease-free point in the linearised system (3.12) and assuming a linearised population $N = 1$ we obtain a significantly reduced form

$$
\begin{aligned}
\dot{\hat{S}} &= (1 - \beta_I)\hat{I} + \hat{R} + (1 - \beta_P)\hat{P} - \frac{k}{\tau}\int_{t-\mu-\tau}^{t-\mu}\hat{I}(\theta) d\theta \\
\dot{\hat{I}} &= (\beta_I - \gamma - 1)\hat{I} + \beta_P \hat{P} \\
\dot{\hat{R}} &= \gamma \hat{I} - \hat{R} + \frac{\tau_2}{\tau^2} k\int_{t-\mu-\tau}^{t-\mu}\hat{I}(\theta) d\theta \\
\dot{\hat{P}} &= -\hat{P} + \frac{\tau_1}{\tau^2} k\int_{t-\mu-\tau}^{t-\mu}\hat{I}(\theta) d\theta,
\end{aligned}
\tag{3.13}
$$

for which the total population is preserved as it should.

System (3.13) can now serve as the starting point of a stability analysis around the neighbourhood of a totally susceptible population, which is from an epidemiological point of view the most interesting and important. That is because an outbreak occurs exactly from what can be seen mathematically as a perturbation of a susceptible population in favour of the infectious portions (i.e. an infectious source which is at some reference point inserted in the system).

3.4.3 Eigenvalue Identification and Stability

We start examining the stability of system (3.13) by estimating its eigenvalues. To simplify the analysis, we note that only the infectious subsystem of the disease-free linear system (3.13) is significant, as it is the only relevant portion for secondary infections given a certain source in a naive (i.e. totally susceptible) population and therefore for the study of endemic conditions. Another reason according to [Diekmann et al., 2009] is because only *the states of infection*, i.e. those giving rise to new infections, are significant for the calculation of an outbreak. As we shall see in the methodology of section 3.5, the projection on the infectious part of the subsystem suffices to completely describe the conditions for the generation of secondary infections in a completely susceptible population from a single source. Mathematically put, these conditions would be the identification of unstable eigenvectors (those to which positive eigenvalues correspond), if any exist. This coincides with the definition of the *basic reproduction number* R_0 quantity and is equivalent to our first observation. The basic reproduction number R_0 is one of the most important quantities to be calculated from a differential system model providing a threshold condition for an epidemic [Diekmann et al., 2013]. We shall define and treat this quantity more carefully in section 3.5.

The reduced infectious subsystem reads

$$\begin{aligned}\dot{\hat{I}}(t) &= (\beta_I - \gamma - 1)\hat{I}(t) + \beta_P \hat{P}(t) \\ \dot{\hat{P}}(t) &= -\hat{P}(t) + \frac{\tau_1}{\tau^2} k \int_{t-\mu-\tau}^{t-\mu} \hat{I}(\theta) d\theta.\end{aligned} \tag{3.14}$$

To find the eigenvalues of (3.14), we make the ansatz that its solutions are of the form $X(t) = c_x e^{\lambda t}$, where $X(t) = I(t)$ or $P(t)$. Employing this ansatz we retrieve the following system of characteristic equations

$$\begin{aligned}\lambda c_I &= (\beta_I - \gamma - 1)c_I + \beta_P c_P \\ \lambda c_P &= k\frac{\tau_1}{\tau^2}\frac{c_I}{\lambda}\left(e^{-\lambda\mu} - e^{-\lambda(\mu+\tau)}\right) - c_P.\end{aligned} \tag{3.15}$$

To make an assertion about the eigenvalues of system (3.15) in a unified way which spans all of the infectious space we bring it in the form $\mathbf{A}(\lambda)\mathbf{c} = \mathbf{0}$, seen in (3.16), and demand that the determinant of $\mathbf{A}(\lambda)$ be zero, so that it can have linearly independent solutions (equation (3.17))

$$\begin{pmatrix} \beta_I - \gamma - 1 - \lambda & \beta_P \\ k\frac{\tau_1}{\tau}\frac{e^{-\lambda\mu}}{\lambda\tau}(1 - e^{-\lambda\tau}) & -\lambda - 1 \end{pmatrix} \begin{pmatrix} c_I \\ c_P \end{pmatrix} = \begin{pmatrix} 0 \\ 0 \end{pmatrix}. \tag{3.16}$$

From the $\det \mathbf{A}(\lambda) = 0$ relation

$$(\lambda + 1)(\beta_I - \gamma - 1 - \lambda) + \beta_P k\frac{\tau_1}{\tau}\frac{e^{-\lambda\mu}}{\lambda\tau}\left(1 - e^{-\lambda\tau}\right) = 0. \tag{3.17}$$

3.5 The Basic Reproduction Number

In dynamical epidemic systems a fundamental quantity that is seemingly always sought as an epidemic growth indicator is the *basic reproduction number* R_0. It is defined as the ratio of secondary infections in a naive (i.e. completely susceptible) population by a certain seed of infectious arrivals. This of course constitutes no definition and a systematic methodology is required to meaningfully determine it [Diekmann et al., 2013].

In the following we shall apply on the disease-free linearised system (3.13) the formulation outlined in [Diekmann et al., 2009, 2013] based on the so-called *next-generation matrix* (NGM). The main idea behind the NGM is to formulate it so that it takes into account the infectious arrivals of a population demographically, i.e. across generations (hence the name) starting from a naive population (disease-free equilibrium). Once the matrix has been constructed the R_0 quantity is no other than its spectral radius, which is its largest eigenvalue [Boyce and DiPrima, 1997].

The first step would be to note that only the subsystem (3.14) contributes to any infectious arrivals around the disease-free equilibrium point and suffices for that reason to the aim of the NGM analysis. Next, we bring system (3.14) to the form $\dot{\mathbf{x}} = (\mathbf{T} + \mathbf{\Sigma})\mathbf{x}$, where $\mathbf{T}$ is the *transmission* matrix and $\mathbf{\Sigma}$ is the *transition* matrix according to [Diekmann et al., 2009]. The first, $\mathbf{T}$, refers to infectious transmissions, while the latter $\mathbf{\Sigma}$ signifies the demographic arrivals (births-deaths) in the infectious compartments I and P. This distinction is the basis of the NGM formulation.

$$\begin{pmatrix} \dot{\hat{I}} \\ \dot{\hat{P}} \end{pmatrix} = \begin{pmatrix} \beta_I - \gamma - 1 & \beta_P \\ k\frac{\tau_1}{\tau^2}\hat{L} & -1 \end{pmatrix} \begin{pmatrix} \hat{I} \\ \hat{P} \end{pmatrix}, \tag{3.18}$$

where $\hat{L} = \int_{t-\mu-\tau}^{t-\mu} d$ is an operator (i.e. a continuous map acting on a state space to the same space) for the population states.

We now separate the matrix into its $\mathbf{T}$ and $\mathbf{\Sigma}$ components in the sense that we explained:

$$\mathbf{T} = \begin{pmatrix} \beta_I & \beta_P \\ 0 & 0 \end{pmatrix} \text{ and } \mathbf{\Sigma} = \begin{pmatrix} -\gamma - 1 & 0 \\ k\frac{\tau_1}{\tau^2}\hat{L} & -1 \end{pmatrix}.$$

Regarding the components of $\mathbf{\Sigma}$ as the rates of entry into an infectious state, their inverse would equal the average waiting time spent in an infectious state. Furthermore, if an imaginary direction is defined as positive towards the infectious states I and P from the susceptible state S, then the death or the transition to the R state would be defined as negative [Murray, 2002; van Kampen, 2003]. Finally, the product of the average waiting time in an infectious state with the rate of arrival at that state (what the components of the transmission matrix $\mathbf{T}$ represent), defined as the number of susceptible contacts with infectious individuals per unit of time, would result in the newly infected individuals. Following this line of thought and condensing this information into a matrix form, the calculation of the product $-\mathbf{T\Sigma^{-1}}$ retrieves what is in [Diekmann and Heesterbeek, 2000] called the *large domain NGM* $\mathbf{K}_L$. The naming of this matrix already implies some redundancy in many cases, namely that states and arrivals that do not provide any information about the infectious evolution of the system horizontally and vertically are taken into account. The definition of $\mathbf{K}_L$ generally and for the case of (3.18) according to [Diekmann et al., 2009] is exactly the aforementioned product

$$\mathbf{K_L} = -\mathbf{T\Sigma^{-1}} = \begin{pmatrix} \frac{\beta_I}{1+\gamma} + k\frac{\tau_1}{\tau^2}\frac{\beta_P}{1+\gamma}\hat{L} & \beta_P \\ 0 & 0 \end{pmatrix}. \tag{3.19}$$

From that point we would like to reduce $\mathbf{K}_L$ to a matrix $\mathbf{K}$, which would refer only to the arriving and departing infectious states. To that end we define an auxiliary matrix $\mathbf{E}$ consisting of unit column vectors spanning the range of $\mathbf{T}$ (i.e. with as many columns as the corresponding non-zero rows of $\mathbf{T}$), which will serve in the reduction operations of $\mathbf{K}_L$ as we are going to see in a moment. In the case of (3.18), $\mathbf{E}$ is the vector

$$\mathbf{E} = \begin{pmatrix} 1 \\ 0 \end{pmatrix}, \tag{3.20}$$

and from there we define the transformation $\mathbf{K} = \mathbf{E^T K_L E}$ for the calculation of the sought reduced NGM $\mathbf{K}$, whose elements K_{ij} are exactly the

expected number of newly infected individuals at infectious state i from a newly introduced infectious individual at infectious state j. Essentially, with this transformation and the form of $\mathbf{E}$ (remember that it spans the non-zero rows of $\mathbf{T}$ in unit vector columns and thus accounts for transmissions from non-infectious to infectious states) we ascertain that the resulting matrix $\mathbf{K}$ does not contain any redundant information about the propagation of the infectious states of the system at hand. The basic reproduction number is then defined as the spectral radius of $\mathbf{K}$, $\rho(\mathbf{K})$, which simply means the maximum (dominant) eigenvalue of $\mathbf{K}$ [Boyce and DiPrima, 1997; Diekmann et al., 2013]. Of course what we just described is very general and encompasses systems with infectious states that are not themselves infected (e.g. are in an incubation, so-called 'exposed' state). In the case of (3.18) the analysis is considerably simplified as the infectious states I and P have the capacity to generate themselves new infections. This interpretation is reflected in the very simple form that $\mathbf{K}$ assumes in this case, as it is itself a scalar operator (since it contains $\hat{L}$) and therefore coincides with its eigenvalue spectral range $\rho(\mathbf{K})$. Thus, R_0 assumes the form

$$\hat{R_0} = \rho(\mathbf{K}) = \frac{\beta_I}{1+\gamma} + k\frac{\tau_1}{\tau^2}\frac{\beta_P}{1+\gamma}\hat{L}. \tag{3.21}$$

Recalling now that all the methodology we have followed so far concerns the linearised system (3.14), which is in regard to the neighbourhood of the disease-free equilibrium, the only state on which it would be meaningful for $\hat{R_0}$ to act as a proxy of secondary infections from a single source in a naive population would be the constant disease-free one $(S, I, R, P) = (1, 0, 0, 0)$. Then $\hat{R_0}(S, I, R, P)^T = R_0$.

$$\boxed{R_0 = \frac{\beta_I}{1+\gamma} + k\frac{\tau_1}{\tau}\frac{\beta_P}{1+\gamma}}. \tag{3.22}$$

The reason an operator came into play in (3.21) was that in [Diekmann et al., 2009, 2013] only one time-scale was assumed and most importantly the prototype systems presented are ODE rather than functional retarded ones. However, it is interesting to see the conditions under which this methodology suffices to lead to the R_0 calculation in our distributed delay system case assuming that the operator $\hat{R_0}$ acts on the disease-free equilibrium as a hypothetical perturbative factor. A more intricate iterative treatment for the R_0 calculation in distributed delay cases (for the susceptible class) is presented in [Thieme, 2009].

Interestingly and from a consistency viewpoint, we can arrive to the result (3.22) by substituting $\lambda = 0$ in the characteristic equation (3.15) defined in section 3.4.3 and employing the L'Hôpital rule. That is because $\lambda = 0$ is the threshold for the growth or decay of the exponential solutions $X(t) = c_x e^{\lambda t}$ seen in subsection 3.4.3. When $\lambda > 0$ the solutions grow and

the system destabilises (outbreak), while when $\lambda < 0$ the system is stable and an epidemic never takes place.

$$\beta_I - \gamma - 1 + \beta_P k \frac{\tau_1}{\tau} \lim_{\lambda \to 0} \frac{\left[e^{-\lambda\mu}(1 - e^{-\lambda\tau})\right]'}{(\lambda\tau)'} = 0$$

$$\Leftrightarrow 1 = \frac{\beta_I + \beta_P k \tau_1/\tau}{\gamma + 1} \tag{3.23}$$

where with the prime we denote differentiation in respect to λ.

Working inversely, the reasoning of substituting a null eigenvalue $\lambda = 0$ in (3.15) revealed a transcritical bifurcation around the disease-free point, which epidemiologically is reasonable as it suggests an epidemic threshold. An endemic equilibrium may not always exist (e.g. in the SIRS model where the recovered state can return to being susceptible after a well defined time -see [Kyrychko and Blyuss, 2005] for a rigorous example), while the disease-free does.

Comparing the form of (3.22) to that of (3.23) we notice that the latter's right-hand side is identical to that of the former. It follows then that the behaviour of system (3.13) changes qualitatively (bifurcates) in respect to the variation of its parameters for the critical value $R_0 = 1$ exactly because we are looking at the threshold between growth and decay of the exponential solutions for system (3.15). Thus, $R_0 = 1$ is a threshold signifying the appearance of an epidemic equilibrium and thus the conditions under which an epidemic (i.e. $I(t) > I(0)$ for some $t > 0$) can marginally occur. We deduce that the regime $R_0 < 1$ should be that of no outbreak by the interpretation of the parameters coming into (3.23): if the rate of infectious removal γ dominates those of the horizontal β_I and vertical arrivals $\beta_P \frac{\tau_1}{\tau}$, then the infected individuals recover faster than they can transmit their infection and therefore the infectious perturbation vanishes to the disease-free state. Conversely, when $R_0 > 1$ the new infections' rate is greater than their removal one and therefore an epidemic has to occur.

3.6 Numerical Integration

In this section we shall tackle the original system (3.6) and attempt to use the parametric insight gained from the analysis so far. Apart from understanding system (3.6) our goal is to obtain informative solutions on the farm dynamics and possibly on the overall S, I, R and P trends as a baseline comparison to the agent-based model of chapter 2.

The dominant feature that sets numerically DDE systems apart from their ODE counterparts is the fact that initial conditions are not sufficient to provide a solution as in the ODE case. This is attributed to the retarded (delayed) states appearing in DDE systems, which require information of

the system prior to a reference time $t = 0$. In particular for system (3.6) the history of the system lies in the interval $[-\mu - \tau, -\mu)$. Therefore, we will need knowledge of the $S(t)$, $I(t)$, $R(t)$ and $P(t)$ for $t \in [-\mu - \tau, -\mu)$ to numerically integrate (3.6). It is also noteworthy to report that there is a discontinuity at $t = -\mu$, which propagates in periods of τ. This is owed to the open right limit of the interval $[-\mu - \tau, -\mu)$.

Numerical schemes for DDE systems are possible only when their delays are discrete [Erneux, 2009], therefore we introduce auxiliary variables in (3.6)

$$\begin{aligned} Y_1(t) &= \int_{t-\mu-\tau}^{t-\mu} S(\theta)d\theta \\ Y_2(t) &= \int_{t-\mu-\tau}^{t-\mu} I(\theta)d\theta \\ Y_3(t) &= \int_{t-\mu-\tau}^{t-\mu} R(\theta)d\theta, \end{aligned}$$

which will reduce it to from an integro-differential system to a DDE with three more dependent variables. Thus, we are enabled to use a solver from the literature for the now extended, seven variable system

$$\begin{aligned} \dot{S}(t) &= -\Lambda(t)S(t) + \frac{k}{\tau}\left[Y_1(t) + Y_3(t)\right] - k\frac{Y_1(t) + Y_2(t) + Y_3(t)}{S(t) + I(t) + R(t) + P(t)}S(t) \\ \dot{I}(t) &= \Lambda(t)S(t) - \gamma I(t) - k\frac{Y_1(t) + Y_2(t) + Y_3(t)}{S(t) + I(t) + R(t) + P(t)}I(t) \\ \dot{R}(t) &= \gamma I(t) + k\frac{\tau_2}{\tau^2}Y_2(t) - k\frac{Y_1(t) + Y_2(t) + Y_3(t)}{S(t) + I(t) + R(t) + P(t)}R(t) \\ \dot{P}(t) &= k\frac{\tau_1}{\tau^2}Y_2(t) - k\frac{Y_1(t) + Y_2(t) + Y_3(t)}{S(t) + I(t) + R(t) + P(t)}P(t) \\ \dot{Y_1}(t) &= \left[S(t-\mu) - S(t-\mu-\tau)\right] \\ \dot{Y_2}(t) &= \left[I(t-\mu) - I(t-\mu-\tau)\right] \\ \dot{Y_3}(t) &= \left[R(t-\mu) - R(t-\mu-\tau)\right]. \end{aligned} \tag{3.24}$$

Having brought system (3.6) into the form (3.24) we can now employ the *PyDelay* solver for the latter's numerical integration [Flunkert, 2011]. The solver utilises an explicit, i.e. each point on which the integration is calculated is based on previously determined values, Runge-Kutta method [Bogacki and Shampine, 1989] with cubic Hermite polynomials for interpolating

over the given number of points in the interval of integration and an adaptive step size scheme [Burden and Faires, 2005].

Assuming a normalised population and following the biological reasoning of a naive initial population we set the history function of $S(t)$ to be unity over $[-\mu-\tau, 0)$, while we set all the other states to zero on the same interval. At $t = 0$ we allow a discontinuity to take place accounting for a perturbation in the naive population, namely that $S(0) = 0.9$ and $I(t) = 0.1$. The rest of the states remain zero at $t = 0$, except for $Y_1(0) = 1$ to initialise the delayed birth effects in (3.24). We set the total integration time to be equal to eight $\tau+\mu$ periods. This would correspond to two female animals' life cycles in the agent-based model. As far as the system parameters are concerned, we assume the values $(\beta_P, \beta_I, \gamma, k) = (10, 1, 1/14, 1)$ after biological reasoning. In particular, the persistently infectious transmission rate β_P should be much larger than the transiently infected one β_I due to persistently infected animals shedding the virus throughout their lifetime and having larger amounts of it in their bodies than their transiently infected counterparts. In addition, the inverse of the recovery rate $1/\gamma$ should give the average recovery time which coincides with two weeks (fourteen days) and the birth rate is selected to unity since its weight is determined by the weighing population factors found in the expression $D(t)$.

The parameters $\tau = 270$, $\tau_1 = 90$, $\tau_2 = 180$ and $\mu = 550$ correspond to the gestation, first trimester, later gestation stage and maturity period in days respectively. From the rest of the system's parameters we focus on only two parameter variations as of increased importance: firstly on the ratio τ_1/τ encountered in the numerator of the R_0 expression (3.22) in section 3.4.3. This ratio introduces the novelty of vertical persistently infectious transmissions, as we saw in the disease-free linearised system (3.13). It is however also evident from the $\dot{P}$ expression of the original system (3.6). Secondly and more trivially on the β_P transmission rate, as it implicitly reinforces the $\dot{P}$ expression in the original system through the vertical (birth) infectious transmission mechanism and certainly contributes greatly to the force of infection $\Lambda(t)$, as the biology of BVD demands.

Since our analysis focuses on the majority of the initial population being susceptible with the rest being infectious it is reasonable to invoke the linearised result of section 3.5 on the basic reproduction number R_0 to compare with the numerical results. In that respect, both the τ_1/τ and β_P parameters' interplay affect the R_0 non trivially, as they intertwine horizontal and vertical transmission.

Bearing the previous in mind we summarise the different parameter results in figure 3.2. The exact choice of parameters can be found in table 3.1 referencing R_0.

The upper left plot simply demonstrates what we anticipated from the linear analysis for $\tau_1/\tau = 0$: without vertical transmissions of PI animals ($\tau_1 = 0$) the perturbation dies out and the naive population is restored.

The middle left plot exhibits some damped periodicity of period equal to $\mu + \tau$ and settles on an intermediate endemic state where the TI infections dominate the population. It corresponds to the most realistic choice of parameters as explained in section 3.4.3. It is also rather similar, albeit less in periodic damping towards the steady state to the middle right plot where the β_P transmission rate is increased for the otherwise same realistic gestation period parameters' choice. The direct consequence is a dramatic reduction of the S portion due to increased infectiousness and a slight increase of the R portion as a reaction (recovery) to the I dominance. Surprisingly, the P portion is virtually not affected, despite the increased transient infections I which one would expect to increase the infectious portion corresponding to the τ_1/τ term in the $\dot{P}$ equation of (3.6).

The most striking plot however, is the upper right, which both oscillates intensively and settles on a P dominant equilibrium for all the carrying cows' infection shifted to their critical first gestation stage τ_1. If the P portion is high then the infections are on the rise, which explains the pronounced level of I and in turns the recovered curve fluctuation R. The S portion gets virtually depleted, which is something completely counter intuitive to the standard SIR system [Kermack and McKendrick, 1927; Murray, 2002; Rohani, 2008]. In this latter case of the SIR system the epidemic dies out not due to a depletion of the S portion rather because of the choice of the system parameters (infectious transmission and recovery time). The result at hand demonstrates however, that when vertical transmissions are taken into account, then the S population can reach a point of extinction if all the new arrivals (births) enter an infectious compartment (P in our case). In reality though this is highly unlikely as it would imply a gestation period which solely contributes to the P compartment, an implication countering all biological evidence, but which can be artificially induced if all the carrying cows are always infected in their first gestation trimester τ_1. As far as the plots of the lower row in figure 3.2 are concerned, the leftmost exhibits a weakly, damped oscillatory behaviour towards an endemic equilibrium where the S portion dominates. That is due to the decreased effect of the rate β_P, which is brought down to the value of β_I (see table 3.1). The rightmost is virtually identical to the middle left and indicates that the system's infectious dynamics increase only slowly with the decrease of the infectious removal's rate, or said differently, with the increase of the recovery time.

In all the plots of figure 3.2 the basic reproduction number R_0 proves to be an indicator of the severity of the outbreak. For the value less than one, the system's states settle indeed on the disease-free equilibrium as expected according to our analysis in section 3.4.3. For the value greater yet close to one, the system exhibits a weak outbreak and settles on an endemic equilibrium with the S state being dominant. As we keep increasing R_0 the I and, ultimately for the highest value of R_0, the P state becomes dominant with an increasing fluctuation of the intermediate states.

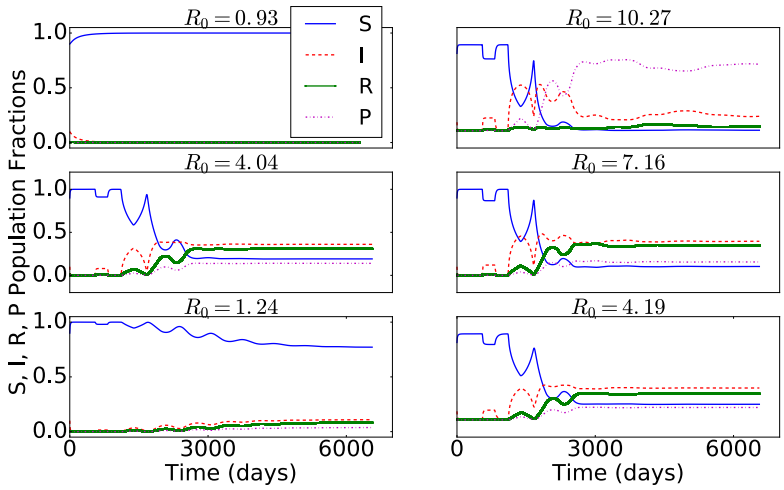

Figure 3.2: Numerical integration for the variation of the parameters of system (3.6) as listed in table 3.1. The S population fraction is represented in solid blue, the I in dashed red, the R in solid green and the P in dashed-dotted magenta. The constant system parameters are $(\beta_I, \mu) = (1, 550)$.

$(\tau_1,\ \tau_2,\ \beta_P,\ \gamma)$	R_0	$(S_0,\ I_0,\ R_0,\ P_0)$
(0, 270, 10, 1/14)	0.93	(1.00, 0.00, 0.00, 0.00)
(90, 180, 10, 1/14)	4.04	(0.19, 0.36, 0.31, 0.14)
(270, 0, 10, 1/14)	10.27	(0.01, 0.17, 0.05, 0.77)
(90, 180, 20, 1/14)	7.16	(0.10, 0.39, 0.35, 0.16)
(90, 180, 1, 1/14)	1.24	(0.77, 0.11, 0.08, 0.04)
(90, 180, 10, 1/30)	4.19	(0.18, 0.37, 0.30, 0.14)

Table 3.1: Parameter variation on the leftmost column and the basic reproduction on the middle for the numerical integration of system (3.6) in figure 3.2. To the rightmost column we list the final states. See the R_0 for the correspondence to each plot.

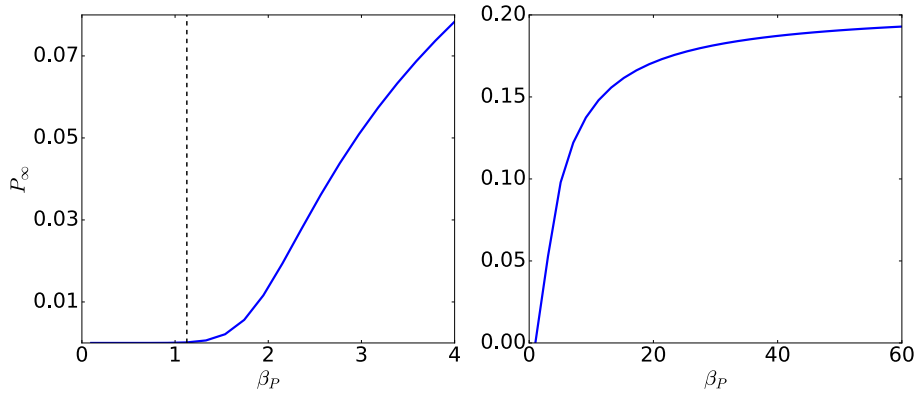

Figure 3.3: Final P_∞ state versus the P transmission rate β_P. The left plot is a magnification of the right to demonstrate the epidemic onset (dashed vertical line). The value of β_P for which $R_0 > 1$ is found to be $\beta_P \approx 1.13$.

Finally, we check the role of the basic reproduction number R_0 as an epidemic threshold quantity in figure 3.3 by examining various final states of the P portion as a function of the P transmission rate β_P. The dashed vertical line on the right plot shows the value of β_P at the onset of the epidemic. Indeed, $R_0 > 1$ in this case according to the formula (3.22) and the numerical value of the epidemic onset is $\beta_P \approx 1.13$. Except for the β_P the system parameters and delays were as in the numerical integration for $R_0 = 4.04$ as seen in table 3.1.

Comparing the plots of figure 3.2 with the baseline scenario 1 for the big (well-mixed) farms of chapter 2 in figures 2.19 and 2.20 we realise that there is no obvious relation between the numerical integration of the mean field system (3.6) and the simulated S, I, R and P states of the agent-based model for the selected values of R_0 in the former case. One major reason where this is attributed to is the lack of spatial structure in the mean field model. Despite the fact that figures 2.19 and 2.20 concern a single farm with a large population, which according to the agent-based model's description, behave in a well-mixed fashion the farm still receives and dispatches animals to other farms-nodes. In that manner, we cannot assert which individuals play which infectious role throughout the evolution of the farm unless we isolate it from the rest of the system. For short periods of time (quarantine period) this isolated behaviour is exhibited in figure 2.21 for the agent-based model. However, the period is short (40 days) and intermittent leading again to wild speculation in the comparison of the agent-based with the mean field case. The same holds for the global states' evolution in the agent-based model because they closely resemble the trends of the well-mixed, large farms. Furthermore, a great range of details in the agent-based model are not captured by the mean field system (3.6). To name a major such feature,

the P contributions to their own class through vertical transmission was neglected from system (3.5) to (3.6) in order to dispense with the endemic 'all PI' equilibrium which we do not observe in practice. Lastly, the role of stochasticity in the agent-based model was not taken into account in the scope of our study.

3.7 Summary and Outlook

In this section we presented a mean field model for the spread of BVD in a population which is required to be held constant. The formulation of the model was built on the standard SIR one with demography, accounting for vertical transmissions by introducing a time-scale for the animal reproduction cycle. We then proceeded to prove the positivity of the solutions for that system and summarised some basic background on the treatment of retarded functional systems. Next, after examining the equilibria of the formulated model, we linearised around its disease-free infectious state and argued on the system's stability based on the resulting eigenvalue growth. As a direct consequence of the stability argumentation, we calculated the basic reproduction number as an epidemiological quantity of fundamental interest for the growth of an epidemic, following the *next generation matrix* formulation, as well as from bifurcation argumentation. Finally, we numerically integrated with the *NumPy* solver the system introducing a number of auxiliary variables and compared the consistency with the basic reproduction number predictions, as well as with some of the agent-based model's results which had structural similarities.

As future points to cover, it is possible that a different set of parameters, for $R_0 > 1$ (outbreak), could lead to an R dominant state for the case of the numerical integration of system (3.6), making the mean field model's evolution better matching to that of a single farm or the global system evolving freely in the agent-based model (scenario 1 of figures 2.16, 2.19 and 2.20). Additionally, delay-induced periodicity is a possibility [Guckenheimer and Holme, 1986; Kuznetsov, 1995] and should be investigated. In particular, the combination of the horizontal transmission parameters β_I and β_P with the vertical transmission coefficient ratio τ_1/τ could lead to recurrent infections related to the birth cycle. Such an effect is hinted through the damped oscillatory behaviour in all the plots of figure 3.2 for which $R_0 > 1$.

Another interesting topic to cover would be the interaction between different strains of BVD. According to laboratory reports, although the worldwide prevalent strains of BVD are at most three [Lindberg, 2003; Pinior et al., 2017; Ståhl and Alenius, 2012], through mutations in a closed environment they can number up to hundreds [Center, 2003]. For such systems there is immense interest in understanding the strain dynamics' interplay for formulating vaccinations, to name an application [Kelling, 2004]. What one

studies in such cases is the indirect effect of strain mutation on the immunological response of the population to different strains. That is because for a certain degree of similarity of the mutated strains portions of the population having recovered from infection pertinent to a specific strain remain immune to other infected portions corresponding to mutated strains (in respect to the reference one) by *cross-immunity* [Gog and Grenfell, 2002; Gog and Swinton, 2002]. To delve into such an analysis we would need to reformulate system (3.6) with as many degrees of freedom as the strains we would like to model. The interaction of the strains on the different infectious states would then be introduced by kernels similar to those reported by [Gog and Grenfell, 2002; Gog and Swinton, 2002; Gomes et al., 2002] and the analysis would follow the line of [Adams and Sasaki, 2009; Bauer et al., 2017; Gao et al., 2007, 2011].

Finally, to truly be able to compare with a model of the level of complexity of the agent-based presented in chapter 2 the incorporation of mitigation strategies such as vaccination in an analytical model for BVD would be necessary. Although this is possible retaining the mean field character of system (3.6) [Wang et al., 2016], the most natural way to include mitigation strategies such as quarantine and vaccination would be to introduce spatial heterogeneities in the model in question. In many cases, this would lead to a network *metapopulation model* for the epidemic spread [Colizza and Vespignani, 2007; Colizza et al., 2007; Lentz et al., 2012] with node dynamics such as of system's (3.6).

CHAPTER 4

BVD Network Risk Analysis

In this chapter we will be focusing on the analysis of some aspects of the German cattle trade network after we have briefly presented the dataset. We do not aim for the analysis to be exhaustive, rather to assess the risk of epidemic spread on the network following mainly works of Steinbach [Steinbach, 2016], Lentz [Lentz, 2013; Lentz et al., 2016] and Valdano [Valdano, 2015]. A lot of the computations are also based on a generic cattle network Python analysis code written in collaboration with Eugenio Valdano, Andreas Koher and Alexandre Darbon. It can be found on GitHub under https://github.com/eugenio-valdano?tab=repositories and is expected to be made publicly available within the following months after the completion of this thesis, along with a publication which has contributed to the analysis of this chapter.

4.1 Datasets

The dataset used to analyse the German cattle trade network was extracted from the HIT database by courtesy of the FLI institute. It consists of quadruple entries of integers of the form (d, u, v, w), where d refers to an ascending time-stamp, u and v refer to unique farm identification numbers and w to the number of animals being moved in each entry (weight). Its time-span ranges from 01.01.2010 to 31.12.2014 and has a daily resolution of cattle movements.

The dataset of the cattle movements was accompanied by a dataset of the unique farm ID entries with a corresponding geographic longitude and latitude, which was randomised within the administrative district (Kreise) of each farm. The reason for this randomisation was to respect the anonymity

of farms within a radius of their administrative district's kilometric span.

4.2 Network Analysis

We will separate our approach into four parts. Firstly, a temporally aggregated static analysis in regard to centrality measures, network components and descriptive statistics [Lentz et al., 2016; Newman, 2010; Valdano, 2015]. Secondly, a spatial concerning the node distribution on a geographical level and Fourier analysis on the geographical data to reveal characteristic cattle movement time-scales and their relative importance, as well as the probability density distributions of the geographic distances covered by the cattle movements [Bajardi et al., 2012; Valdano, 2015; Woolhouse and et al., 2001]. Thirdly, a temporal employing both a trading loyalty measure to pinpoint trade patterns in time [Bajardi et al., 2011; Lentz et al., 2011; Valdano, 2015; Volkova et al., 2010a] as well as node and edge activation time assessments [Lebl et al., 2016; Valdano, 2015]. Finally, a worst-case SI epidemic spread scenario by means of the network's accessibility as applied in [Lentz et al., 2013, 2016].

4.2.1 Static Analysis

Myriads of methods exist for the analysis of static networks [Lentz et al., 2016; Newman, 2010] and it is up to the particularities of the specific study to illuminate which are the most appropriate for the task at hand.

Perhaps the most fundamental quantity that one can calculate directly given a network is its *degree* distribution, which is a distribution of the number of nodes each node of the network is connected to. Mathematically this is best done by means of defining the *adjacency matrix*, i.e. a square binary matrix with a dimension as large as the number of nodes of the network.

$$\mathbf{A}_{ij} = \begin{cases} 1 & \text{if there is a link from i to j} \\ 0 & \text{if there is no link from i to j} \end{cases} \tag{4.1}$$

It follows naturally from the definition of the adjacency matrix whether the network is directed ($\mathbf{A}$ non-symmetric) or undirected ($\mathbf{A}$ symmetric).

Furthermore, if the adjacency matrix has non-binary integer values, then these values represent the *weights* between the respective pairs of nodes, which is an edge attribute. Similarly and extending from the notion of the node degree, a node attribute can be defined measuring the sum of weights resulting from all its connection with all of its neighbours. This is called the *strength* of the node and is discerned to 'out' strength when summing the weights of the edges to which the node is the reference of the connecting pair, and the conversely to 'in' strength when summing the weights of the

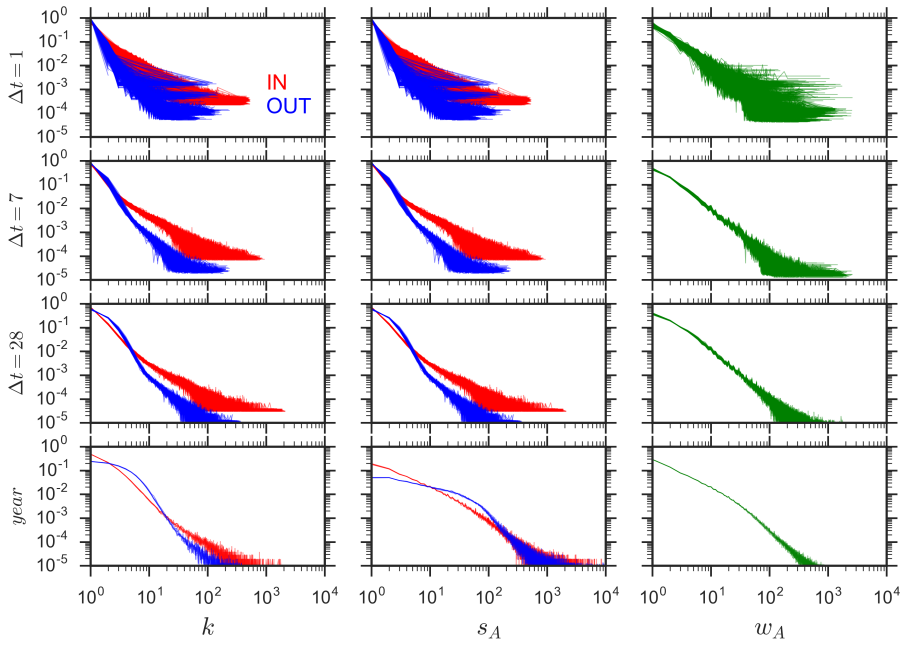

Figure 4.1: The degree (left column k), strength (middle column s_A) and weight (right column w_A) distributions of the German cattle movements' network for different aggregation intervals (daily, weekly, monthly and annually descending in rows from the top). The in and out components (were applicable) are depicted in red and blue respectively. Each plot contains curves drawn from as many sets of points correspond to as many aggregations. For example the subplot to the far lower left contains 2 pairs of 5 curves (5 red 'in' and 5 blue 'out') for the 5 annual aggregations of the dataset.

edges to which the node is the end of the connecting pair [Barrat et al., 2004; Newman, 2010; Valdano, 2015]. Similarly, there is an edge property called *weight* which measures the intensity of interaction between its connecting nodes. Naturally, temporal networks by definition are not *transitive* due to the unique direction of time (i.e. if i is connected to j at time t_1 and j is connected to k at time t_2 then i is not necessarily connected to k in both times). Nevertheless, we can extract temporal aggregations from such networks in which any sense of temporal directionality is omitted.

Another fundamental way to summarise basic statistics of the network is on annual temporal aggregation levels and on a complete temporal aggregation as shown in tables 4.1, 4.2 and 4.3. The quantities counted or measured in those tables per aggregated year and per the total aggregated time-span of the dataset make reference to the total amount of animals moved, to the total batches, i.e. groups of animals moved per trade event, the total edges, i.e.

the number of recorded trade partners and the number of nodes (farms) in table 4.1. Further, for the same aggregations, they refer to the average batch size, i.e. average number of animals traded per event, weight with reference to animals, i.e. average number of animals per pair of trading partners, and batches, i.e. average number of trading events per pair of trading partners, separately in table 4.2. Moreover, for the same aggregations, they include the average degree per node and the average strength with respect to animals, i.e. average number of traded animals per node, and batches, i.e. average number of trade events per node, separately in table 4.3.

Year	Animals	Batches	Edges	Nodes
2010	13,420,268	3,166,372	755,163	183,486
2011	13,287,493	3,131,322	725,167	176,955
2012	13,251,071	3,083,943	701,942	170,324
2013	13,202,637	3,009,917	688,413	165,123
2014	13,636,593	3,025,296	686,728	161,285
TOTAL	66,798,062	15,416,850	1,822,373	209,336

Table 4.1: German trade network statistics according to the HI-Tier database for the period 2010–2014 and each year separately. Animal, batch, edge and node count.

Year	Av Batch Sz	Av Weight (Animals)	Av Weight (Batches)
2010	4.2	17.8	4.2
2011	4.2	18.3	4.3
2012	4.3	18.9	4.4
2013	4.4	19.2	4.4
2014	4.5	19.9	4.4
TOTAL	4.3	36.7	8.5

Table 4.2: German trade network statistics according to the HIT database for the period 2010–2014 and each year separately. Average batch size count, average weight for animals' and average weight for batches' count.

Furthermore, one can statically investigate the component composition of a real-world network as in [Steinbach, 2016] and [Lentz et al., 2016]. This analysis includes among others the determination of connectivity clusters (subsets of nodes) called *components*, with implications for spreading processes on the whole aggregated network. For a real world network, such as the German cattle movements, one can follow a rigorous treatment to define a *giant* component, as a connected component (i.e. one for which all nodes are connected through an arbitrary number of intermediate links) of a relative non-zero size to the rest of the network [Dorogovtsev et al., 2001;

Year	Av degree	Av Str (ANIMALS)	Av Str (BATCHES)
2010	4.1	73.1	17.2
2011	4.1	75.1	17.7
2012	4.1	77.8	18.1
2013	4.2	80.1	18.2
2014	4.3	84.5	18.8
TOTAL	8.7	319.1	73.6

Table 4.3: German trade network statistics according to the HIT database for the period 2010–2014 and each year separately. Average degree count, average strength of animals' and of batches' count.

Newman, 2010].

Following Letz et al. [Lentz et al., 2016] we can define a subset of nodes of the network for which a *path* exists among all pairs of nodes in it, (in the network terminology we say that the network is connected in this case) where by path we mean a connection between any two nodes of the network traversing an arbitrary number of intermediate nodes. In the literature, when directionality is neglected, this subset is called the *giant weakly connected component* (GWCC). Conversely, if that subset of the network is directed the component is called the *giant strongly connected component* (GSCC). Similarly, we can define giant components of nodes which can reach to or be reached from the GSCC, but are not part of the GSCC themselves. These are called the *giant in and out components* -GIC and GOC- respectively [Dorogovtsev et al., 2001; Lentz et al., 2016; Nicosia et al., 2012]. Moreover, nodes reachable from the GIC or that reach the GOC, but are not part of the GSCC are called tendrils [Nicosia et al., 2012]. Finally, there are also nodes that are part of the GWCC with no access to the GOC. These are called *EXT* [Lentz et al., 2016]. It should be evident by now that the tendrils and the external nodes are by definition of lower strategical importance in controlling a spreading process on a connected network.

Once one has defined one of the aforementioned giant components, and particularly the GSCC, one can calculate the range, average shortest path length and the diameter. The *length* of a path is simply the number of nodes traversed to reach one node from another and the *shortest path length* is the minimal such length available on the network. The *diameter* of a network is simply its maximum shortest path length, while the *range* of a specific node is the number of nodes it can reach through a path of an arbitrary length. This latter quantity is naturally of most interest for infections (and generally for spreading processes) as it is a vulnerability indicator of the network given a certain source of infection (spread) [Lentz et al., 2016; Newman, 2010].

In her master's thesis Steinbach made all the relevant network compo-

nent calculations of the aggregated German cattle trade network, as well as the calculations for the range distribution of the network, and the diameter and average shortest path length of the GSCC, which are all vulnerability indicators on an aggregated level [Steinbach, 2016]. We summarise the main results of our findings which agree with her work in tables 4.4 and 4.5.

Components	Nodes	Edges
GWCC	209,155	1,822,268
GSCC	145,704	1,439,603
GIC	45,126	6,905
GOC	15,274	4,707
EXT,TEN	3,232	371,158

Table 4.4: Components' enumerated elements.

Network Quantity	Value
Average shortest path length (GSCC)	4
Max. range (GSCC)	160,977
Max. range (GIC)	161,002
Diameter	17

Table 4.5: Static vulnerability indicators.

According to these calculations the edges or trades of the GIC and GOC are rather limited compared to those of the GWCC and GSCC, and are mostly directed to and from the GSCC respectively. Similarly, seeing (table 4.5) that the GSCC has access to around 77% of the network within an average of 4 steps elevates it to a crucial hub for the spread of an infection. In addition, the GIC is implicitly of great importance to the spread, as it gives input (i.e. is inwardly connected) to the GSCC while having access to 77% of the network's nodes (table 4.5). Together, the GSCC and GIC constitute around 91% of the network's nodes bringing them to the forefront of a targeted control scheme (e.g. node removal).

4.2.2 Temporal Analysis

So far we have ignored the temporal aspect of the German cattle trade network. In works such as [Grindrod et al., 2011; Konschake et al., 2013] however it is stressed that quantities calculated for an evolving network may vary wildly compared to their aggregated counterparts.

As in the static case, the approaches that one can follow to exhibit the importance of the temporal aspect of a network on an infectious spread are manifold [Holme, 2015; Kostakos, 2009; Lentz et al., 2016; Nicosia et al., 2012]. Here we shall focus on two examples of such a temporal analysis,

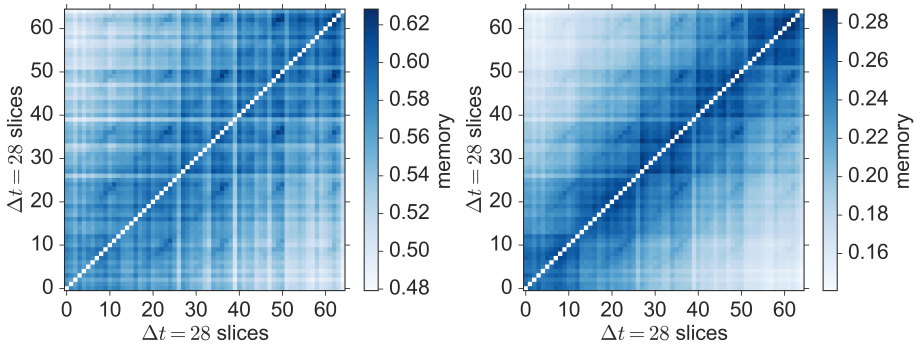

Figure 4.2: The monthly memory heat maps for the German cattle trade network. Both the horizontal and vertical axes represent time in months. By $\Delta t = 28$ slices we mean that we assume 28 consecutive day aggregations as a month. Nodes' case on the left and edges' case on the right.

which illustrate the effect of temporal evolution on the epidemic dynamics, namely the memory of the network and its activation time distributions.

With the quantity of *memory* we essentially calculate the *Jaccard index*, which is a statistical index measuring the similarity of two sets of objects. In our case these objects are defined to be two arbitrary snapshots of the network, i.e. two configurations of the network's nodes and edges for two discrete time steps t and t' [Skiena, 2017; Valdano et al., 2015b].

$$J^{t,t'} = \frac{\left|\mathcal{S}^t \cap \mathcal{S}^{t'}\right|}{\left|\mathcal{S}^t \cup \mathcal{S}^{t'}\right|}, \tag{4.2}$$

with $\mathcal{S}^t$ being a snapshot of the network at time t, i.e. a set of the network's nodes or edges at that time. It is directly evident that the Jaccard index takes values in [0,1], with the left and right extrema representing total dissimilarity and absolute identification respectively.

We observe symmetrical patches of dissimilarity of consecutive months, approximately at annual intervals, when measuring the memory for both the nodes and the edges of the network. This means that the time-aggregated network in question differs strongly from all other observation windows, i.e. the set of common nodes or edges (left and right plot respectively) is small compared to all the unions with the rest of the time-aggregated networks. We further observe dark, diagonal stripes that correspond to a time shift of about 12 to 24 months, meaning that we observe similar trade patterns after about one year. This might reflect external factors differentiating the network's activity such as the demands around Christmas time or the end of the year. Note that along the diagonal we do not perform the calculation for clarity of the presentation, as the memory value is always equal to unity.

Regarding the activation time distributions, we measure the probabilities

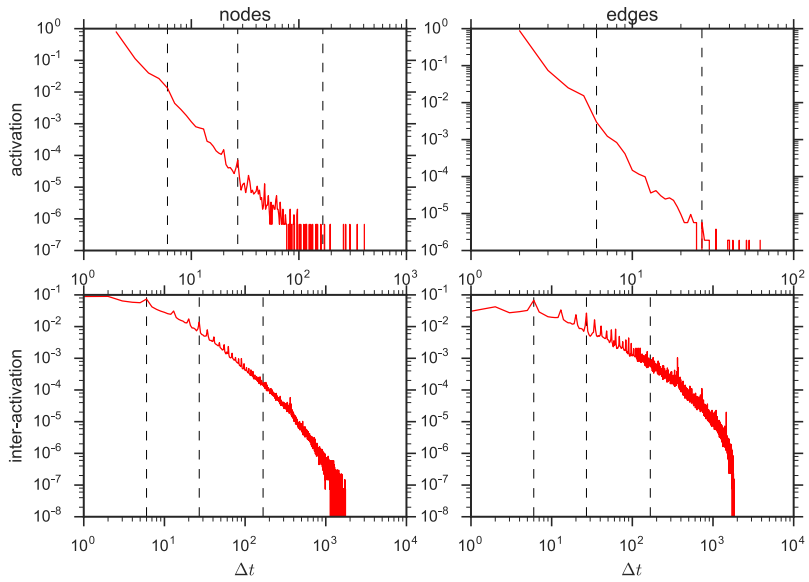

Figure 4.3: Activation (top row) and inter-activation (lower row) time distributions for the nodes (left column) and the edges (right column) of the cattle trade network of Germany on a log-log scale. The dashed vertical lines correspond to a week, month and semester. Note that for the inter-activation distributions the calculations assume that $\Delta t = 1$ as the minimal duration of inactivity of a node or an edge, while for the activation distributions $\Delta t = 2$ as the the minimal duration of a node or an edge's activity.

of randomly selected nodes or edges in the network being continually active or inactive (inter-activation time). The relevant plots are shown in figure 4.3.

The inter-activation and activation distributions of figure 4.3 on the other hand enable us to detect the natural time-scales which are most probably active or not throughout the dataset. The inter-activation plot spans virtually the whole dataset's duration, indicating the farms and trading partners (nodes and edges) that rarely trade at the tail of the distribution. Conversely, the activation diagram indicates that trading partners barely trade continually for more than 70 days and farms only seldom for up to 400 days in the dataset. Especially in the inter-activation diagram the declining peaks refer to time-scales which are of higher inactivity than the trend would otherwise indicate, of which the most prominent belong to weekly, monthly and semesterly pauses of the farms trading (node case) or of trading partners trading (edge case) [Valdano, 2015]. The results of figure 4.3 are in good agreement with similar produced in [Steinbach, 2016].

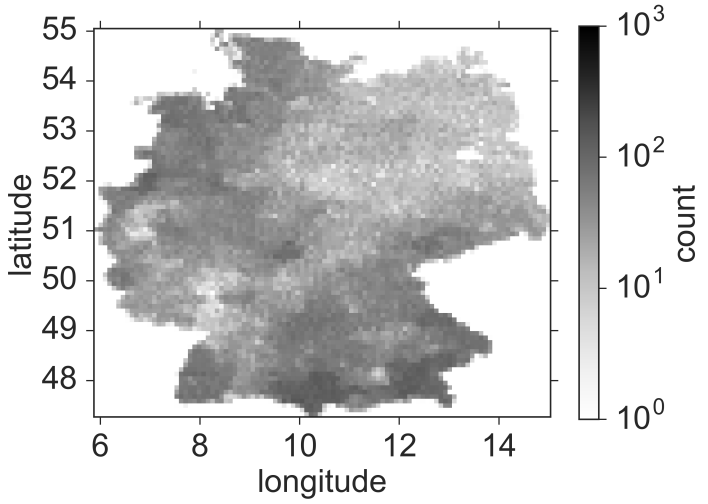

Figure 4.4: Farm count distribution in Germany in bins of 10×10 km^2.

This piece of information could be used to estimate the final outbreak activity with an underlying SIR process as done in [Lebl et al., 2016] and for different infective transmission rates as in both [Lebl et al., 2016] and [Steinbach, 2016].

4.2.3 Spatial Analysis

Although the analysis of a network is generally uncoupled from analysing a physical (geographical) space (the latter case of networks is called *embedded*, while the former *topological* [Skiena, 1998]), since the nodes of the German cattle trade network refer to geographical locations it is insightful to map some of the analysis on a geographical level. To that end, we present the distribution of the nodes on a map of Germany and draw a connection of the network's connectivity to characteristic time-scales of animal movements. We further investigate the distance distributions corresponding to monthly and annual aggregations of the network as a likelihood proxy for long-range disease transmissions.

The first result is a direct representation of the nodes' distribution on Germany's administrative borders as seen in figure 4.4. For illustrative purposes we partitioned the map into bins of 10×10 km^2, where the darker colours of the grayscale imply a higher farm count. With such a representation it is directly evident which regions of the country are more dense in farms.

Having an overview of the farms' distribution in Germany it is important to understand if there are specific time-frames of movement activity and how intense these are. The most intuitive option would be to check for divisions

of time of a calendar nature. We therefore search for the dominant activity of movements in intervals of half a week, a week, a month, 2, 3 and 4 months, a semester, and 1 and 2 years as shown in the colour code of figure 4.5. By dominant activity we mean revealing the nodes that trade more intensely on the aforementioned time-scales. The methodology we follow to that end consists of several steps.

First, we isolate the trade of the dataset within the geographic bins of figure 4.4. Next, we draw a histogram of all the real *discrete Fourier transform* (DFT) amplitudes on the weight sequence $\{\mathbf{x_n}\}$ of N elements from the given edgelist, as displayed in equation (4.3) within each geographic bin. Essentially the weights of the sequence refer to the 'in' and 'out' number of traded animals in time and in respect to a node. We apply the DFT using the real *fast Fourier transform* [Hamming, 1980]. Next, we keep the squares of the DFT transform (the power spectrum) and rank those which fall within a ± 0.1 tolerance interval centered around the previously mentioned time-scales. Thus, to each time-scale corresponds a maximum amplitude from the filtered ones. We call the lower ranked amplitudes *harmonics* due to the reminiscent parallels this methodology draws to a ranking of frequencies which are submultiples of a fundamental. However, this is not the case and let the naming not be misleading towards the lower ranked frequencies being submultiples of the dominant in our methodology.

$$X_k = \sum_{n=0}^{N-1} x_n \cdot \exp\left(-\frac{2\pi i}{N} kn\right) \tag{4.3}$$

These lower frequencies are shifted towards longer time-scales as can be seen in figures 4.6-4.8 (2^{nd}, 3^{d} and 6^{th} harmonics). For the 2^{nd} and 3^{d} harmonic we can already observe in figures 4.6 and 4.7 that the south of Germany exhibits already more intense movements at time-scales longer than the order of the corresponding harmonic. That is attributed to the practice of moving cattle to higher altitudes in time-frames of 4 months to semesters for the benefits that the Alpine climate has to offer to the cattle's well-being.

The last result of the spatial analysis is the distance probability density functions of the trading events in monthly and annual aggregation intervals as presented in the top and bottom row of figure 4.9 respectively, in the weighted and unweighted case (left and right column respectively). Not surprisingly, the weighted cases of any of the two aggregation partitions pronounces the granulation of the distribution since the weights' inclusion make the events more heterogeneous on the time-space plane.

The immediate conclusion of the plots from figure 4.9 is that the vast majority of cattle trading took place in distances less than 700 km, with smaller distances being ever more favourable for the dataset's time-span. Finally, the fact that virtually no single trading event from node to node

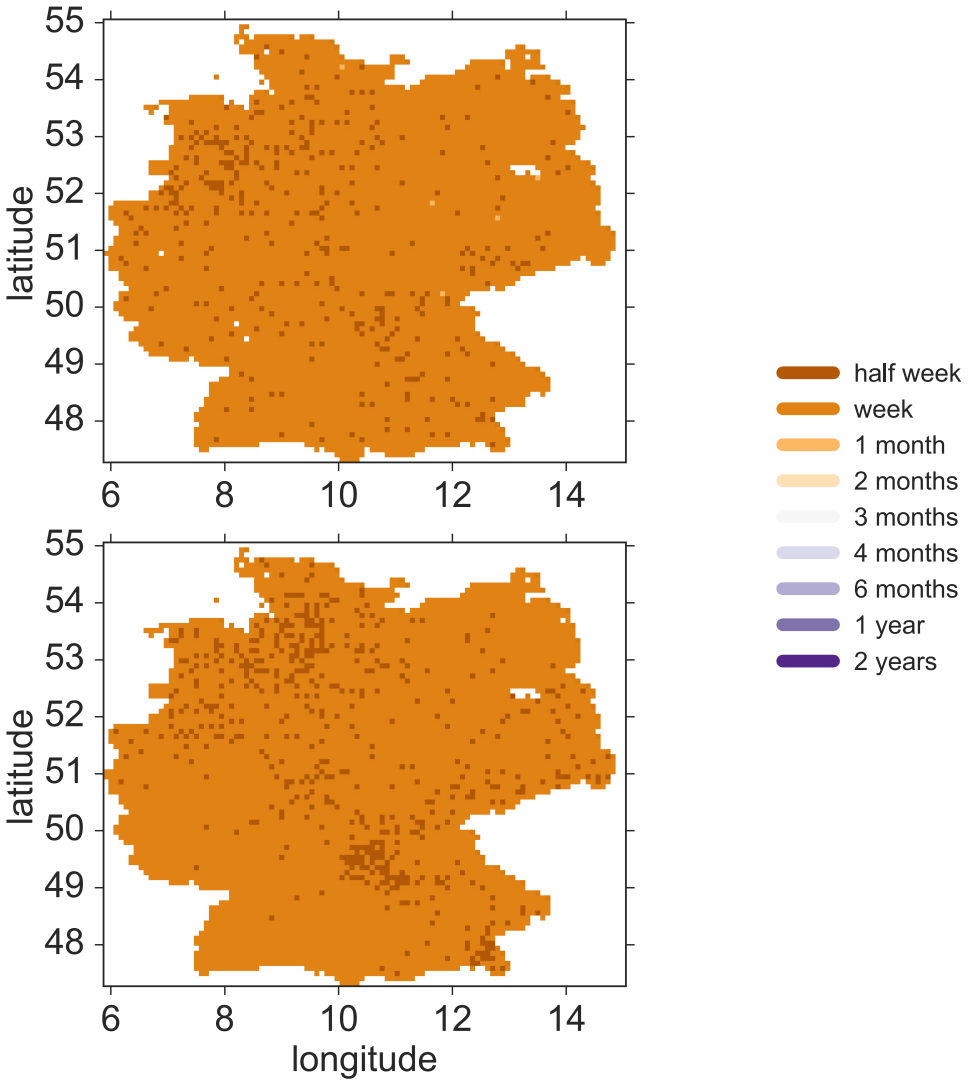

Figure 4.5: Characteristic dominant time-scales of animal movements in bins of 10×10 km^2. The upper figure concerns incoming activity to the node distribution, while the lower the outward.

Figure 4.6: Characteristic second time-scales' harmonics of animal movements in bins of 10×10 km^2. The upper figure concerns incoming activity to the node distribution, while the lower the outward.

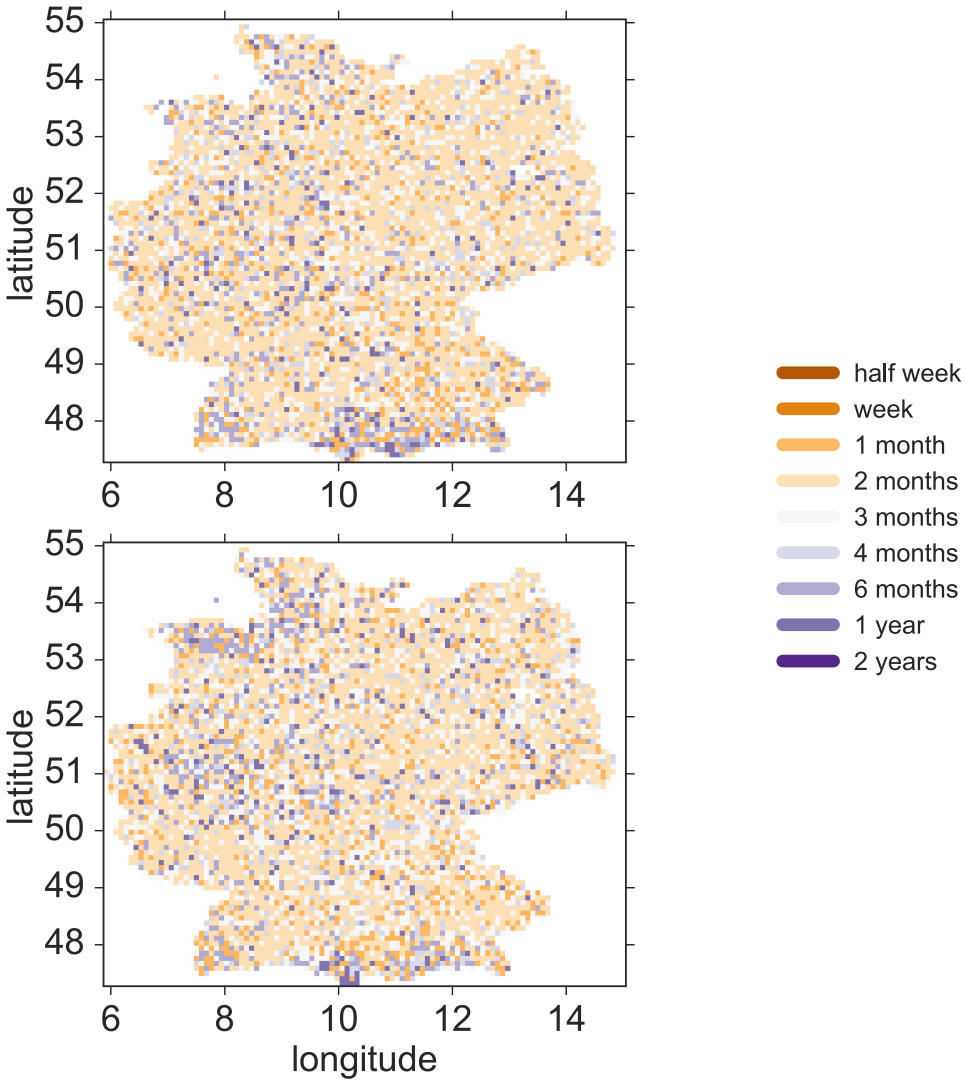

Figure 4.7: Characteristic third time-scales' harmonics of animal movements in bins of 10×10 km^2. The upper figure concerns incoming activity to the node distribution, while the lower the outward.

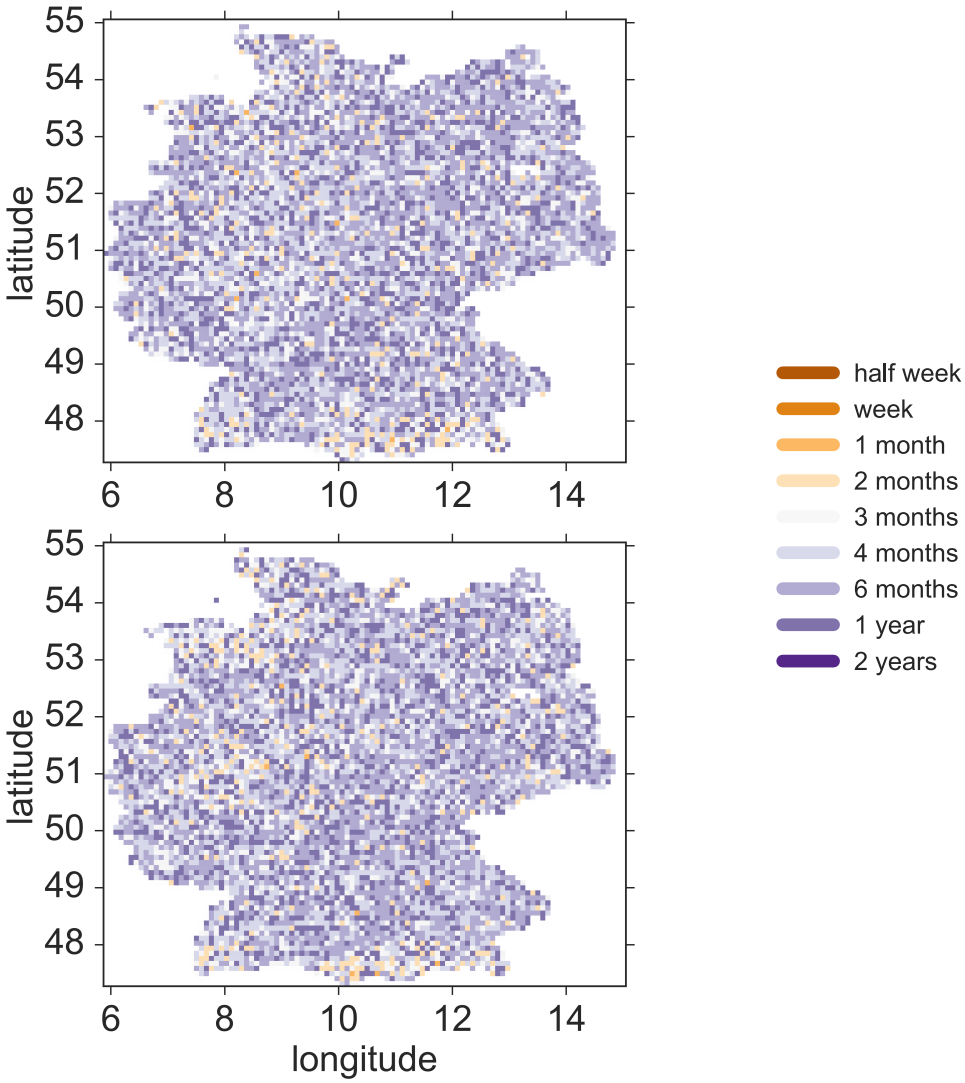

Figure 4.8: Characteristic sixth time-scales' harmonics of animal movements in bins of 10×10 km^2. The upper figure concerns incoming activity to the node distribution, while the lower the outward.

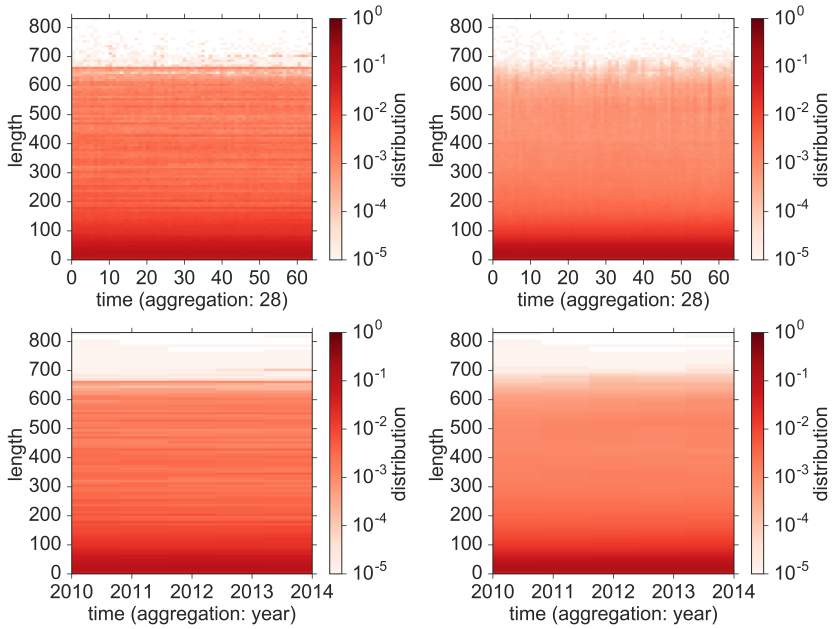

Figure 4.9: Monthly (top row) and annually (bottom row) aggregated distance probability density functions of the German cattle trade network's trading events throughout the dataset's timespan. Both the weighted (left column) and the unweighted cases (right column) are included.

surpassed 800 km is consistent with the fact of the dataset's representation of domestic trades in Germany. Such trades could not exceed the maximum distance of the space (the country's) available!

4.2.4 Network Accessibility

The concept of accessibility is not new and is well understood for static networks of N nodes through the definition of the (static) accessibility matrix (4.4) as a function of the adjacency matrix that we defined in section 4.2.1 **A** [Grindrod et al., 2011; Holme, 2005; Lentz et al., 2016; Travençolo and Costa, 2008]. The maximum order of the accessibility matrix (4.4) gives information about the number of visits to a certain node. However, in the work of [Lentz et al., 2013] this accessibility matrix was defined for temporally evolving networks with T time steps, corresponding to a causal series of T snapshots of the network's adjacency matrices $\{A_1, A_2 \dots A_T\}$, as presented in equation (4.5). The main idea behind the form of equation (4.5) in contrast to equation (4.4) is that given the causal nature of an evolving network and the potential loss of causal paths in a sequence of snapshots of that network, the number of time-steps (in the static accessibility counterpart we refer to *path length* instead of time-steps) needed for any node to

reach another can only be revealed from the accessibility matrix if there is some sort of memory term. This memory term is introduced by the identity matrix in (4.5), which accounts for waiting times between the activation of node pairs (i.e. the disappearance of edges due to the network's evolution).

$$\mathcal{P}_{stat} = \sum_{n=1}^{N} (\mathbf{A}^n) \tag{4.4}$$

$$\mathcal{P}_{temp} = \prod_{t=1}^{T} (\mathbf{A}_t + \mathbf{I}) \tag{4.5}$$

One of the great strengths that the accessibility matrix of a temporal network offers for the study of spreading processes is that it allows the calculation of the *path density* $\rho(\mathcal{P}_{temp})$ of the network

$$\rho(\mathcal{P}_{temp}) = \frac{\text{nnz}(P)}{N^2} \tag{4.6}$$

where the $1/N^2$ is a normalisation factor for the size $N \times N$ of the adjacency matrix and the $\text{nnz}(P)$ refers to the number of nonzero elements of P. The path density assumes values within $[0, 1]$ and expresses (under the frequentist scope) the probability that a randomly chosen pair of nodes (potentially the same node twice) is connected through a time-respecting path of maximum lentgth t, given as $F_n = P(l \leq t) = \rho(\mathcal{P}_{temp})$ [Lentz, 2013; Lentz et al., 2013]. As a direct result we can estimate the outreach of a worst-case directed spreading process. In the case of an epidemic spread that is equivalent to the maximum outreach of an infected source node entering the evolving network at $t = 0$ while the other nodes are all susceptible and remain infected after they have been infected.

Lastly, knowing the path density of the temporal network we can numerically calculate its shortest path duration probability distribution by its numerical derivative $\text{SPD} = F_n - F_{n-1}$ for all the times corresponding to the evolving network's adjacency matrix sequence $\{A_1, A_2 \dots A_T\}$ [Lentz et al., 2016; Steinbach, 2016]. The maximum value of this probability density distribution corresponds to the most likely shortest path duration, i.e. the time it most probably takes the outbreak to reach its peak.

In figure 4.10 we present the path density of the German cattle trade network for times between 0 and 1865 (the five years of the dataset counted in days from 01.01.2010 to 31.12.2014) on the right axis and the corresponding shortest path densities, assuming that the network is directed, on the left axis. We observe that in the directed network case the most probable peak of the spread given a source at $t = 0$ occurs at 84 days, a result which also agrees with that of [Steinbach, 2016]. Strikingly, as noted in [Steinbach, 2016], this epidemic peak at 84 days does not correspond to a characteristic time-scale of the cattle chain of production as was the case in the swine trade

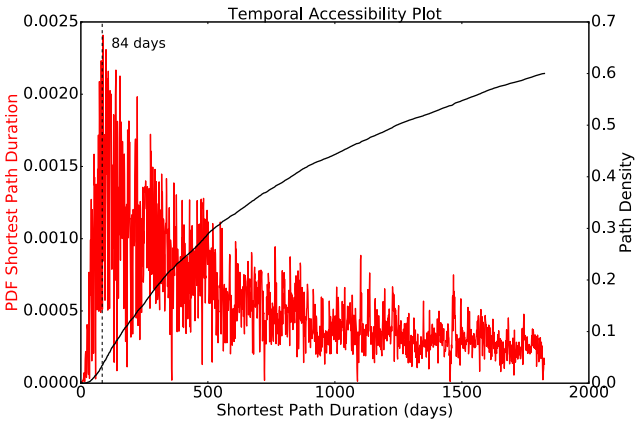

Figure 4.10: Probability density function (PDF) of the shortest path duration assuming a directed network. The peak is observed at 84 days (vertical, black, dashed line). The black, solid line represents the path density (integral of the PDF) of the network

network shown in the work of [Lentz, 2013; Lentz et al., 2016]. The outbreak in the cattle trade network case must be therefore attributed to a supply and demand dictated structure of the network.

For the generation of figure 4.10 we employed the code of Hartmut Lentz [Lentz et al., 2013] adapted to our needs. The original code can be found on the GitHub repository https://github.com/hartmutlentz/TemporalNetworkAccessibility.

4.3 Summary and Outlook

We outlined a short programme for the risk analysis of an infection spread on the given network of the German cattle trade. The analysis contained static, temporal, spatial and network accessibility components, all of which we deem to be complementary for the purpose of an epidemic risk assessment.

As further work, the computationally intensive problem of the temporal GSCCs calculation is worth investigating as presented in [Nicosia et al., 2012, 2013]. Furthermore, there is ongoing work and possibilities of estimating the vulnerability of the evolving network mentioned in this chapter from a viewpoint of a block-adjacency matrix containing the temporal component and with an underlying SIS process as presented in [Taylor et al., 2012; Valdano, 2015; Valdano et al., 2015a, 2018]. Moreover, a robustness analysis can elicit the vulnerability of specific nodes of the network as demonstrated in [Holme

et al., 2002; Lentz, 2013] and [Steinbach, 2016]. Regarding precise outbreak predictions employing a variable activation time see [Lebl et al., 2016]. For targeted network rewiring strategies leading to epidemic extinction see the Hamiltonian formulation of [Hindes and Schwartz, 2016; Schwartz et al., 2011] with an underlying SIR process and furthermore [Holme, 2013] for a component and synthetic network investigation to the extinction end, also employing an SIR process. Moreover, since the network structure of the German cattle trade is heterogeneous from an aggregated perspective (as in it can be partitioned to constituent components as we saw in section 4.2.1) a basic reproduction number can be defined for each one of its constituent components as instructed in [Diekmann et al., 1990]. Then, as shown in [Volkova et al., 2010b], the weight distributions of the components can provide a means to calculate the variation of the basic reproduction number for each one of them.

Furthermore, the movements between different production types can have an effect on the epidemic spread as exhibited in [Iotti et al., 2017; Koeppel et al., 2018; Lindström et al., 2010]. Therefore a classification of farm types and the partitioning of the network edgelists accordingly can serve towards more accurate network analysis taking the subtlety of the farm types into account. In addition, regarding the centrality analysis of the static, aggregated network, if the farm type classification is made, then it would also be important to measure the degree of *assortativity* for a certain node, i.e. its tendency to connect to those with similar behaviour, where the similarity in behaviour can be in class, activity, flow, etc. as in [Lentz et al., 2011, 2012, 2016; Rocha et al., 2010; Woolhouse and et al., 2001].

Lastly, visualisations resulting from the static and temporal network analysis such as that of figure 4.11 can be furthered to reflect more sophisticated work similar to that of [McGrath et al., 2018].

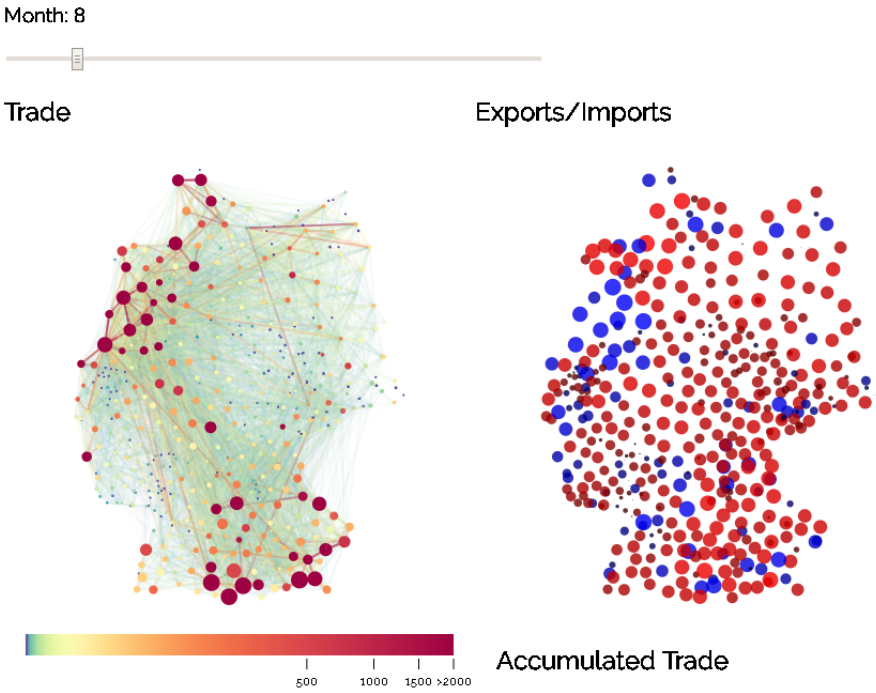

Figure 4.11: Excerpt of trades and node in and out fluxes (right side in blue and red colours respectively) for month 8 out of the 60 from the German cattle trade network datset. The coloured nodes of the figure to the left represent what we defined as strength in the static analysis. The animation whose this graph is a snapshot of was generated with the work of Lukas Kikuchi (DAAD student).

APPENDIX A

Abbreviations

BVD Bovine Viral Diarrhea

DDE Delay Differential Equation

DFT Discrete Fourier Transform

FLI Friedrich-Loeffler Institute

FN False Negative

FP False Positive

HIT Herkunftssicherungs und Informationssystem für Tiere

I Transiently Infected

GIC Giant in Component

GOC Giant out Component

GSCC Giant Strongly Connected Component

GWCC Giant Weakly Connected Component

NGM Next-Generation Matrix

ODE Ordinary Differential Equation

ODD Overview, Design concepts and Details

P Persistently Infected

PI Persistently Infected

R Recovered

S Susceptible

TI Transiently Infected

TN True Negative

TP True Positive

YCW Young Calf Window

List of Tables

List of Figures

Bibliography

B. Adams and A. Sasaki. Antigenic distance and cross-immunity, invasibility and coexistence of pathogen strains in an epidemiological model with discrete antigenic space. *Theor. Popul. Biol.*, 76(3):157–167, 2009.

S. V. Albrecht and P. Stone. Autonomous agents modelling other agents: A comprehensive survey and open problems. *Artif. Intell.*, 258:66–95, 2017.

L. J. S. Allen, F. Brauer, P. Van den Driessche, and J. Wu. *Mathematical epidemiology*, volume 1945. Springer, 2008.

R. H. Anderson and R. M. May. *Infectious diseases of humans: dynamics and control.* Oxford Univ. Press, Oxford and New York, 1992.

P. Bajardi, A. Barrat, F. Natale, L. Savini, and V. Colizza. Dynamical patterns of cattle trade movements. *PLOS ONE*, 6:e19869, 2011.

P. Bajardi, A. Barrat, L. Savini, and V. Colizza. Optimizing surveillance for livestock disease spreading through animal movements. *J. Royal Soc. Interface*, 9(76):2814–2825, 2012.

A. Barrat, M. Barthélemy, R. Pastor-Satorras, and A. Vespignani. The architecture of complex weighted networks. *Proc. Natl. Acad. Sci. U.S.A.*, 101(11):3747–3752, 2004. doi: 10.1073/pnas.0400087101.

L. Bauer, J. Bassett, P. Hövel, Y. N. Kyrychko, and K. B. Blyuss. Chimera states in multi-strain epidemic models with temporary immunity. *Chaos*, 27(11):114317, 2017. doi: 10.1063/1.5008386.

L. Bioglio, M. Génois, C. L. Vestergaard, C. Poletto, A. Barrat, and V. Colizza. Recalibrating disease parameters for increasing realism in modeling epidemics in closed settings. *BMC Infect. Dis.*, 16(1):676, 2016.

K. R Bisset, J. Chen, X. Feng, V. S. Kumar, and M. V. Marathe. Epifast: a fast algorithm for large scale realistic epidemic simulations on distributed memory systems. In *Proceedings of the 23rd international conference on Supercomputing*, pages 430–439. ACM, 2009.

P. Blunk. Containment strategies in networks of livestock trade. Master's thesis, TU Berlin, 2017.

K. B. Blyuss and Y. N. Kyrychko. Stability and bifurcations in an epidemic model with varying immunity period. *Bull. Math. Biol.*, 72(2):490–505, 2010.

P. Bogacki and L. F. Shampine. A 3(2) pair of Runge - Kutta formulas. *Appl. Math. Lett.*, 2(4):321–325, 1989. ISSN 0893-9659. doi: doi:10.1016/0893-9659(89)90079-7.

W. E. Boyce and R. C. DiPrima. *Elementary Differential Equations and Boundary Value Problems*. Wiley, New York, 1997.

F. Brauer and C. Castillo-Chavez. *Mathematical models in population biology and epidemiology*, volume 40. Springer, 2012.

F. Brülisauer, F. I. Lewis, A. G. Ganser, I. J. McKendrick, and G. J. Gunn. The prevalence of bovine viral diarrhoea virus infection in beef suckler herds in Scotland. *Vet. J.*, 186(2):226–231, 2010.

R. L. Burden and J. D. Faires. *Numerical analysis*. Thomson Brooks/Cole, 2005.

D. S. Burke, J. M. Epstein, D. A. T. Cummings, J. I. Parker, K. C. Cline, R. M. Singa, and S. Chakravarty. Individual-based computational modeling of smallpox epidemic control strategies. *Acad. Emerg. Medic.*, 13(11):1142–1149, 2006.

Novartis Knowledge Center. The fundamentals of BVD. Technical report, Novartis, 2003.

B. R. Cherry, M. J. Reeves, and G. Smith. Evaluation of bovine viral diarrhea virus control using a mathematical model of infection dynamics. *Prev. Vet. Med.*, 33(1-4):91–108, 1998.

V. Colizza and A. Vespignani. Invasion threshold in heterogeneous metapopulation networks. *Phys. Rev. Lett.*, 99:148701, 2007.

V. Colizza, R. Pastor-Satorras, and A. Vespignani. Reaction-diffusion processes and metapopulation models in heterogeneous networks. *Nat. Phys.*, 3:276, 2007.

F. J. Conraths and J. Gethmann. Epidemiologische Untersuchungen in Tierpopulationen. Technical report, FLI, Greifswald - Insel Riems, August 2015.

A. Courcoul and P. Ezanno. Modelling the spread of bovine viral diarrhoea virus (bvdv) in a managed metapopulation of cattle herds. *Vet. Microbiol.*, 142(1-2):119–128, 2010.

A. Damman, A. F. Viet, S. Arnoux, M. C. Guerrier-Chatellet, E. Petit, and P. Ezanno. Modelling the spread of bovine viral diarrhea virus (BVDV) in a beef cattle herd and its impact on herd productivity. *Vet. Res.*, 46 (1):12, 2015.

O. Diekmann and J. A. P. Heesterbeek. *Mathematical epidemiology of infectious diseases: model building, analysis and interpretation*, volume 5. John Wiley & Sons, 2000.

O. Diekmann, J. A. P. Heesterbeek, and J. A. J. Metz. On the definition and the computation of the basic reproduction ratio R_0 in models for infectious diseases in heterogeneous populations. *J. Math. Biol.*, 28(4): 365–382, 1990.

O. Diekmann, S. A. van Gils, S. M. Verduyn Lunel, and H. O. Walther. *Delay Equations*. Springer-Verlag, New York, 1995.

O. Diekmann, J. A. P. Heesterbeek, and M. G. Roberts. The construction of next-generation matrices for compartmental epidemic models. *J. Royal Soc. Interface*, page rsif200903, 2009. doi: 10.1098/rsif.2009.0386.

O. Diekmann, H. Heesterbeek, and T. Britton. *Mathematical Tools for Understanding Infectious Disease Dynamics*. Princeton University Press, Princeton, New Jersey, USA, 2013.

S. N. Dorogovtsev, J. F. F. Mendes, and A. N. Samukhin. Giant strongly connected component of directed networks. *Phys. Rev. E*, 64:025101, July 2001. doi: 10.1103/physreve.64.025101.

K. T. D. Eames. Networks and epidemic models. *Journal of The Royal Society Interface*, 2(4):295–307, 2005. ISSN 1742-5689. doi: 10.1098/rsif.2005.0051.

L. Elveback, E. Ackerman, L. Gatewood, and J. P. Fox. Stochastic two-agent epidemic simulation models for a community of families. *Am. J. Epidem.*, 93(4):267–280, 1971.

J. M. Epstein. *Generative social science: Studies in agent-based computational modeling*. Princeton University Press, 2006.

T. Erneux. *Applied delay differential equations*. Springer, 2009.

P. Ezanno, C. Fourichon, A. F. Viet, and H. Seegers. Sensitivity analysis to identify key-parameters in modelling the spread of bovine viral diarrhoea virus in a dairy herd. *Prev. Vet. Med.*, 80(1):49–64, 2007.

G. Fishman. *Discrete-event simulation: modeling, programming, and analysis*. Springer Science & Business Media, 2013.

V. Flunkert. Pydelay: A simulation package. In *Delay-Coupled Complex Systems*, pages 165–178. Springer, 2011.

M. Galassi et al. *GNU Scientific Library Reference Manual (3rd Ed.), ISBN 0954612078*, 2018. http://www.gnu.org/software/gsl/.

A. Ganesh, L. Massoulié, and D. Towsley. The effect of network topology on the spread of epidemics. In *INFOCOM 2005. 24th Annual Joint Conference of the IEEE Computer and Communications Societies. Proceedings IEEE*, volume 2, pages 1455–1466. IEEE, 2005.

S. Gao, Z. Teng, J. J. Nieto, and A. Torres. Analysis of an SIR epidemic model with pulse vaccination and distributed time delay. *Biomed. Res. Int.*, 2007:64870, 2007.

S. Gao, Y. Liu, J. J. Nieto, and H. Andrade. Seasonality and mixed vaccination strategy in an epidemic model with vertical transmission. *Math. Comput. Simul.*, 81(9):1855–1868, 2011.

M. C. Gates and M. E. J. Woolhouse. Controlling infectious disease through the targeted manipulation of contact network structure. *Epidemics*, 12: 11–19, 2015.

J. Gethmann. Programm zur Simulation der BVD-Sanierung. Personally prepared doc file, 2015.

J. Gethmann. Personal communication with Dr. J. Gethmann, from the Friedrich-Loeffler Institute, 2018.

J. Gethmann, T. Homeier, M. Holsteg, H. Schirrmeier, M. Saßerath, B. Hoffmann, M. Beer, and F. J. Conraths. BVD-2 outbreak leads to high losses in cattle farms in Western Germany. *Heliyon*, 1(1):e00019, 2015.

D. T. Gillespie. A general method for numerically simulating the stochastic time evolution of coupled chemical reactions". *J. Comput. Phys.*, 22:403, 1976.

J. R. Gog and B. T. Grenfell. Dynamics and selection of many-strain pathogens. *Proc. Natl. Acad. Sci. USA*, 99(26):17209–17214, 2002.

J. R. Gog and J. Swinton. A status-based approach to multiple strain dynamics. *J. Math. Biol.*, 44(2):169–184, February 2002.

M. G. M. Gomes, G. F. Medley, and D. J. Nokes. On the determinants of population structure in antigenically diverse pathogens. *Proc. R. Soc. Lond. [Biol.]*, 269(1488):227–233, 2002.

D. M. Green, I. Z. Kiss, and R. R. Kao. Modelling the initial spread of foot-and-mouth disease through animal movements. *Proc. R. Soc. B*, 273 (1602):2729–2735, 2006.

I. Greiser-Wilke, B. Grummer, and V. Moennig. Bovine viral diarrhoea eradication and control programmes in europe. *Biologicals*, 31(2):113–118, 2003.

V. Grimm, U. Berger, D. L. DeAngelis, J. G. Polhill, J. Giske, and S. F. Railsback. The ODD protocol: a review and first update. *Ecol. Model.*, 221(23):2760–2768, 2010.

P. Grindrod, M. C. Parsons, D. J. Higham, and E. Estrada. Communicability across evolving networks. *Phys. Rev. E*, 83:046120, April 2011. doi: 10.1103/physreve.83.046120.

T. Gross and B. Blasius. Adaptive coevolutionary networks: a review. *J. R. Soc. Interface*, 5(20):259–271, 2008. doi: 10.1098/rsif.2007.1229.

K. Gu, V. L. Kharitonov, and J. Chen. *Stability of Time-Delay Systems*. Birkhauser Boston, 2003.

J. Guckenheimer and P. Holme. *Nonlinear Oscillations, Dynamical Systems, and Bifurcations of Vector Fields*. Springer, Berlin, 1986.

J. K. Hale. *Theory of functional differential equations*. Springer, New York, 1977.

R. Hamming. *Coding and Information Theory*. Prentice Hall, Englewood Cliffs, 1980.

L. Hébert-Dufresne, J. A Grochow, and A. Allard. Multi-scale structure and topological anomaly detection via a new network statistic: The onion decomposition. *Sci. Rep.*, 6:31708, 2016.

H. W Hethcote. A thousand and one epidemic models. In *Front. Math. Biol.*, pages 504–515. Springer, 1994.

H. W. Hethcote. The mathematics of infectious diseases. *SIAM review*, 42 (4):599–653, 2000.

H. W. Hethcote and P. van den Driessche. An sis epidemic model with variable population size and a delay. *J. Math. Biol.*, 34(2):177–194, 1995. ISSN 1432-1416. doi: 10.1007/bf00178772.

J. Hindes and I. B. Schwartz. Epidemic extinction and control in heterogeneous networks. *Phys. Rev. Lett.*, 117(2):028302, 2016.

A. Höfig. *Untersuchungen zu epidemiologisch relevanten Einflussfaktoren auf die Bekämpfung der Bovinen Virusdiarrhoe (BVD) in Thüringer Rinderherden mit BVD-Infektionen im Rahmen der verpflichtenden BVDV-Bekämpfung in Deutschland im Jahr 2011-Ermittlung von Risikofaktoren und Ansätzen für die Rechtssetzung*. PhD thesis, Universität Leipzig, 2014.

P. Holme. Network reachability of real-world contact sequences. *Phys. Rev. E*, 71:046119, April 2005. doi: 10.1103/physreve.71.046119.

P. Holme. Extinction times of epidemic outbreaks in networks. *PloS one*, 8 (12):e84429, 2013.

P. Holme. Modern temporal network theory: a colloquium. *Eur. Phys. J. B*, 88(9):1–30, 2015.

P. Holme and J. Saramäki. Temporal networks. *Phys. Rep.*, 519:97–125, March 2012. ISSN 03701573. doi: 10.1016/j.physrep.2012.03.001.

P. Holme, B. J. Kim, C. N. Yoon, and S. K. Han. Attack vulnerability of complex networks. *Phys. Rev. E*, 65(5):056109, 2002.

P. Hoscheit, S. Geeraert, G. Beaunée, H. Monod, C. A. Gilligan, J. A. N. Filipe, E. Vergu, and M. Moslonka-Lefebvre. Dynamical network models for cattle trade: towards economy-based epidemic risk assessment. *Journal of Complex Networks*, page cnw026, 2016.

H. Houe. Epidemiological features and economical importance of bovine virus diarrhoea virus (BVDV) infections. *Vet. Microbiol.*, 64(2-3):89–107, 1999.

B. Iotti, E. Valdano, L. Savini, L. Candeloro, A. Giovannini, S. Rosati, V. Colizza, and M. Giacobini. Farm productive realities and the dynamics of bovine viral diarrhea (bvd) transmission. *bioRxiv*, page 230045, 2017.

Fredrik Johansson et al. *mpmath: a Python library for arbitrary-precision floating-point arithmetic (version 0.18)*, December 2013. `http://mpmath.org/`.

C. D. Keeling and T. P. Whorf. The implications of network structure for epidemic dynamics. *Theoretical population biology*, 2005.

C. L. Kelling. Evolution of bovine viral diarrhea virus vaccines. *Vet Clinics*, 20(1):115–129, 2004.

W. O. Kermack and A. G. McKendrick. A contribution to the mathematical theory of epidemics. *Proc. R. Soc. A*, 115(772):700–721, 1927.

I. Z. Kiss, J. C. Miller, and P. L. Simon. *Mathematics of Epidemics on Networks*. Springer Int. Publ., 2017.

L. Koeppel, T. Siems, M. Fischer, and H. H. K. Lentz. Automatic classification of farms and traders in the pig production chain. *Prev. Vet. Med.*, 150:86–92, 2018.

M. Konschake, H. H. K. Lentz, F. J. Conraths, P. Hövel, and T. Selhorst. On the robustness of in- and out-components in a temporal network. *PLoS ONE*, 8(2):e55223, 2013. doi: 10.1371/journal.pone.0055223.

V. Kostakos. Temporal graphs. *Physica A*, 388(6):1007–1023, 2009.

K. Krishnamoorthy. *Handbook of statistical distributions with applications*. Chapman and Hall/CRC, 2006.

Y. A. Kuznetsov. *Elements of Applied Bifurcation Theory*. Springer, New York, 1995.

Y. N. Kyrychko and K. B. Blyuss. Global properties of a delayed SIR model with temporary immunity and nonlinear incidence rate. *Nonlin. Anal. RWA*, 6(3):495–507, 2005.

S. R. Lanyon, F. I. Hill, M. P. Reichel, and J. Brownlie. Bovine viral diarrhoea: pathogenesis and diagnosis. *Vet. J.*, 199(2):201–209, 2014.

K. Lebl, H. H. K. Lentz, B. Pinior, and T. Selhorst. Impact of network activity on the spread of infectious diseases through the German pig trade network. *Frontiers in Veterinary Science*, 3:48, 2016.

H. H. K. Lentz. *Paths for epidemics in static and temporal networks*. PhD thesis, Humboldt-Universität zu Berlin, 2013.

H. H. K. Lentz, M. Konschake, K. Teske, M. Kasper, B. Rother, R. Carmanns, B. Petersen, F. J. Conraths, and T. Selhorst. Trade communities and their spatial patterns in the german pork production network. *Preventive Veterinary Medicine*, 98(2-3):176–181, 2011. ISSN 0167-5877. doi: 10.1016/j.prevetmed.2010.10.011.

H. H. K. Lentz, T. Selhorst, and I. Sokolov. Spread of infectious diseases in directed and modular metapopulation networks. *Phys. Rev. E*, 85:066111, June 2012. doi: 10.1103/physreve.85.066111.

H. H. K. Lentz, T. Selhorst, and I. Sokolov. Unfolding accessibility provides a macroscopic approach to temporal networks. *Phys. Rev. Lett.*, 110:118701, March 2013. doi: 10.1103/physrevlett.110.118701.

H. H. K. Lentz, A. Koher, P. Hövel, J. Gethmann, T. Selhorst, and F. J. Conraths. Livestock disease spread through animal movements: a static and temporal network analysis of pig trade in Germany. *PLoS ONE*, 11 (5):e0155196, May 2016. doi: 10.1371/journal.pone.0155196.

A. L. E. Lindberg. Bovine viral diarrhoea virus infections and its control. a review. *Veterinary Quarterly*, 25(1):1–16, 2003. doi: 10.1080/01652176.2003.9695140. PMID: 12670010.

A. L. E. Lindberg and S. Alenius. Principles for eradication of bovine viral diarrhoea virus (BVDV) infections in cattle populations. *Vet. Microbiol.*, 64(2-3):197–222, 1999.

T. Lindström, S. A. Sisson, S. Stenberg Lewerin, and U. Wennergren. Estimating animal movement contacts between holdings of different production types. *Prev. Vet. Med.*, 95(1-2):23–31, 2010.

C. M. Macal and M. J. North. Tutorial on agent-based modelling and simulation. *Journal of simulation*, 4(3):151–162, 2010.

T. Marschik, W. Obritzhauser, P. Wagner, V. Richter, M. Mayerhofer, C. Egger-Danner, A. Käsbohrer, and B. Pinior. A cost-benefit analysis and the potential trade effects of the bovine viral diarrhoea eradication programme in Styria, Austria. *The Vet. J.*, 231:19–29, 2018.

G. McGrath, J. A Tratalos, and S. J. More. A visual representation of cattle movement in Ireland during 2016. *Irish Vet. J.*, 71(1):18, 2018.

Federal Ministry of Food and Agriculture. Verordnung zum Schutz der Rinder vor einer Infektion mit dem Bovinen Virusdiarrhoe-Virus, 2008.

Federal Ministry of Food and Agriculture. Zweite Verordnung zur Änderung der BVDV-Verordnung, 2016.

J. D. Murray. *Mathematical Biology: I. An Introduction*. Interdisciplinary Applied Mathematics. Springer, 2002.

F. Natale, A. Giovannini, L. Savini, D. Palma, L. Possenti, G. Fiorea, and P. Calistri. Network analysis of italian cattle trade patterns and evaluation of risks for potential disease spread. *Preventive Veterinary Medicine*, 92 (4):341–350, 2009.

M. E. J. Newman. *Networks: an introduction*. Oxford University Press, Inc., New York, 2010.

V. Nicosia, J. Tang, M. Musolesi, G. Russo, C. Mascolo, and V. Latora. Components in time-varying graphs. *Chaos*, 22(2):023101, 2012. doi: 10.1063/1.3697996.

V. Nicosia, J. Tang, C. Mascolo, M. Musolesi, G. Russo, and V. Latora. Graph metrics for temporal networks. In P. Holme and J. Saramäki, editors, *Temporal Networks*, Understanding Complex Systems. Springer Berlin Heidelberg, 2013. ISBN 978-3-642-36460-0. doi: 10.1007/978-3-642-36461-7_2.

A. Ortiz-Pelaez, D. U. Pfeiffer, R. J. Soares-Magalhaes, and F. J. Guitian. Use of social network analysis to characterize the pattern of animal movements in the initial phases of the 2001 foot and mouth disease (fmd) epidemic in the uk. *Prev. Vet. Med.*, 76(1):40–55, 2006.

J. Parker. A flexible, large-scale, distributed agent based epidemic model. In *Simulation Conference, 2007 Winter*, pages 1543–1547. IEEE, 2007.

R. Pastor-Satorras and A. Vespignani. Epidemic Spreading in Scale-Free Networks. *Phys. Rev. Lett.*, 86:3200–3203, 2001. doi: 10.1103/physrevlett.86.3200.

T. Pereira and L. S. Young. Control of epidemics on complex networks: Effectiveness of delayed isolation. *Phys. Rev. E*, 92(2):022822, 2015.

B. Pinior, C. L. Firth, V. Richter, K. Lebl, M. Trauffler, M. Dzieciol, S. E. Hutter, J. Burgstaller, W. Obritzhauser, P. Winter, et al. A systematic review of financial and economic assessments of bovine viral diarrhea virus (BVDV) prevention and mitigation activities worldwide. *Prev. Vet. Med.*, 137:77–92, 2017.

E. B. Postnikov and I. M. Sokolov. Continuum description of a contact infection spread in a sir model. *Math. biosci.*, 208(1):205–215, 2007.

L. E. C. Rocha, F. Liljeros, and P. Holme. Information dynamics shape the sexual networks of internet-mediated prostitution. *PNAS*, 107(13): 5706–5711, March 2010.

S. P. Rodning, M. D. Givens, M. S. D. Marley, Y. Zhang, K. P. Riddell, P. K. Galik, T. L. Hathcock, J. A. Gard, J. W. Prevatt, and W. F. Owsley. Reproductive and economic impact following controlled introduction of cattle persistently infected with bovine viral diarrhea virus into a naive group of heifers. *Theriogenology*, 78(7):1508–1516, 2012.

P. Rohani. *Modeling infectious diseases in humans and animals*. Princeton University Press, Princeton, 2008.

L. M. Sander, C. P. Warren, I. Sokolov, C. P. Simon, and J. Koopman. Percolation on heterogeneous networks as a model for epidemics. *Math. Biosci.*, 180(1-2):293–305, 2002.

I. M. G. A. Santman-Berends, M. H. Mars, L. Van Duijn, and G. van Schaik. Evaluation of the epidemiological and economic consequences of control scenarios for bovine viral diarrhea virus in dairy herds. *J. Dairy Sci.*, 98 (11):7699–7716, 2015.

S. Sarrazin, J. Dewulf, E. Mathijs, J. Laureyns, L. Mostin, and A. B. Cay. Virulence comparison and quantification of horizontal bovine viral diarrhoea virus transmission following experimental infection in calves. *Vet. J.*, 202(2):244–249, 2014.

C. M. Schneider, A. A. Moreira, J. S. Andrade, S. Havlin, and H. J. Herrmann. Mitigation of malicious attacks on networks. *Proc. Natl. Acad. Sci.*, 108(10):3838–3841, 2011.

I. B. Schwartz, E. Forgoston, S. Bianco, and L. B. Shaw. Converging towards the optimal path to extinction. *J. Royal Soc. Interface*, 8:1699, 2011.

Y. Shoham and K. Leyton-Brown. *Multiagent systems: Algorithmic, game-theoretic, and logical foundations*. Cambridge University Press, 2008.

R. Sipahi, F. M. Atay, and S. I. Niculescu. Stability of traffic flow behavior with distributed delays modeling the memory effects of the drivers. *SIAM Jour. App. Math.*, 68(3):738–759, 2007.

S. S. Skiena. *The algorithm design manual: Text*, volume 1. Springer, 1998.

S. S. Skiena. *The Data Science Design Manual*. Springer, 2017.

J. T. Sørensen, C. Enevoldsen, and H. Houe. A stochastic model for simulation of the economic consequences of bovine virus diarrhoea virus infection in a dairy herd. *Prev. Vet. Med.*, 23(3-4):215–227, 1995.

K. Ståhl and S. Alenius. BVDV control and eradication in Europe – an update. *Jpn. J. Vet. Res.*, 60:S31–S39, 2012.

I. Steinbach. Agent-based modeling of epidemics in networks of livestock trade. Master's thesis, TU Berlin, 2016.

S. H. Strogatz. *Nonlinear Dynamics and Chaos*. Westview Press, Cambridge, MA, 1994.

X. Sun, Y. Liu, Y. Wang, P. Li, A. Guo, Z. Jia, X. Wang, H. Zhang, J. Zhang, Y. Yu, et al. The patterns and risks for disease spreading of cattle movement in china. *Agric. Sci.*, 2013, 2013.

M. Taylor, T. J. Taylor, and I. Z. Kiss. Epidemic threshold and control in a dynamic network. *Phys. Rev. E*, 85(1):016103, 2012.

H. R. Thieme. Spectral bound and reproduction number for infinite-dimensional population structure and time heterogeneity. *SIAM J. Appl. Math.*, 70(1):188–211, 2009.

B. Thomann, A. Tschopp, I. Magouras, M. Meylan, G. Schüpbach-Regula, and B. Häsler. Economic evaluation of the eradication program for bovine viral diarrhea in the Swiss dairy sector. *Prev. Vet. Med.*, 145:1–6, 2017.

H. H. Thulke, M. Lange, J. A. Tratalos, T. A. Clegg, G. McGrath, L. O'Grady, P. O'Sullivan, M. L. Doherty, D. A. Graham, and S. J. More. Eradicating bvd, reviewing irish programme data and model predictions to support prospective decision making. *Prev. Vet. Med.*, 150:151, 2017.

M. R. Tinsley, F. I. Lewis, and F. Brülisauer. Network modeling of BVD transmission. *Vet. Res.*, 43(1), 2012. doi: 10.1186/1297-9716-43-11.

J. A. Tratalos, D. A. Graham, and S. J. More. Patterns of calving and young stock movement in ireland and their implications for BVD serosurveillance. *Prev. Vet. Med.*, 142:30–38, 2017.

B. A. N. Travençolo and L. d. F. Costa. Accessibility in complex networks. *Phys. Lett. A*, 373(1):89–95, 2008.

E. Valdano. *Analyse quantitative de la vulnérabilité des réseaux temporels aux maladies infectieuses*. PhD thesis, UPMC, Sorbonne Universités, 2015.

E. Valdano, L. Ferreri, C. Poletto, and V. Colizza. Analytical computation of the epidemic threshold on temporal networks. *Phys. Rev. X*, 5:021005, 2015a.

E. Valdano, C. Poletto, A. Giovannini, D. Palma, L. Savini, and V. Colizza. Predicting epidemic risk from past temporal contact data. *PLOS Comput. Biol.*, 11:e1004152, 2015b.

E. Valdano, M. R. Fiorentin, C. Poletto, and V. Colizza. Epidemic Threshold in Continuous-Time Evolving Networks. *Phys. Rev. Lett.*, 120(6):068302, November 2018.

W. Van den Broeck, C. Gioannini, B. Goncalves, M. Quaggiotto, V. Colizza, and A. Vespignani. The GLEaMviz computational tool, a publicly available software to explore realistic epidemic spreading scenarios at the global scale. *BMC Infect. Dis.*, 11(1):37, 2011. doi: 10.1186/1471-2334-11-37.

N. G. van Kampen. *Stochastic Processes in Physics and Chemistry*. North-Holland, Amsterdam, 2003.

C. L. Vestergaard and M. Génois. Temporal Gillespie Algorithm: Fast Simulation of Contagion Processes on Time-Varying Networks. *PLOS Comput. Biol.*, 11(10):e1004579, 2015. doi: 10.1371/journal.pcbi.1004579.

A. F. Viet, C. Fourichon, H. Seegers, C. Jacob, and C. Guihenneuc-Jouyaux. A model of the spread of the bovine viral-diarrhoea virus within a dairy herd. *Prev. Vet. Med.*, 63(3):211–236, 2004.

A. F. Viet, C. Fourichon, and H. Seegers. Review and critical discussion of assumptions and modelling options to study the spread of the bovine viral diarrhoea virus (BVDV) within a cattle herd. *Epidemiol. Infect.*, 135(05): 706–721, 2007.

V. V. Volkova, R. Howey, N. J. Savill, and M. E. J. Woolhouse. Sheep movement networks and the transmission of infectious diseases. *PLOS ONE*, 5(6):e11185, 2010a.

V. V. Volkova, R. Howey, N. J. Savill, and M. E. J. Woolhouse. Potential for transmission of infections in networks of cattle farms. *Epidemics*, 2(3): 116–122, 2010b.

Z. Wang, C. T. Bauch, S. Bhattacharyya, A. d'Onofrio, P. Manfredi, M. Perc, N. Perra, M. Salathé, and D. Zhao. Statistical physics of vaccination. *Phys. Rep.*, 664:1–113, 2016. ISSN "0370-1573". doi: "http://dx.doi.org/10.1016/j.physrep.2016.10.006".

M. Waniek, T. P. Michalak, M. J. Wooldridge, and T. Rahwan. Hiding individuals and communities in a social network. *Nature Hum. Beh.*, page 1, 2018.

K. Wernike, J. Gethmann, H. Schirrmeier, R. Schröder, F. J. Conraths, and M. Beer. Six years (2011–2016) of mandatory nationwide bovine viral diarrhea control in Germany – a success story. *Pathogens*, 6(4):50, 2017.

S. Widgren, S. Engblom, P. Bauer, J. Frössling, U. Emanuelson, and A. Lindberg. Data-driven network modelling of disease transmission using complete population movement data: spread of vtec o157 in swedish cattle. *Veterinary Research*, 47(1):81, 2016.

M. E. J. Woolhouse and et al. Dynamics of the 2001 UK foot and mouth epidemic: Stochastic dispersal in a heterogeneous landscape. *Science*, 294: 813, 2001.